European Conference on Permafrost

18-22 June, 2023, Puigcerdà

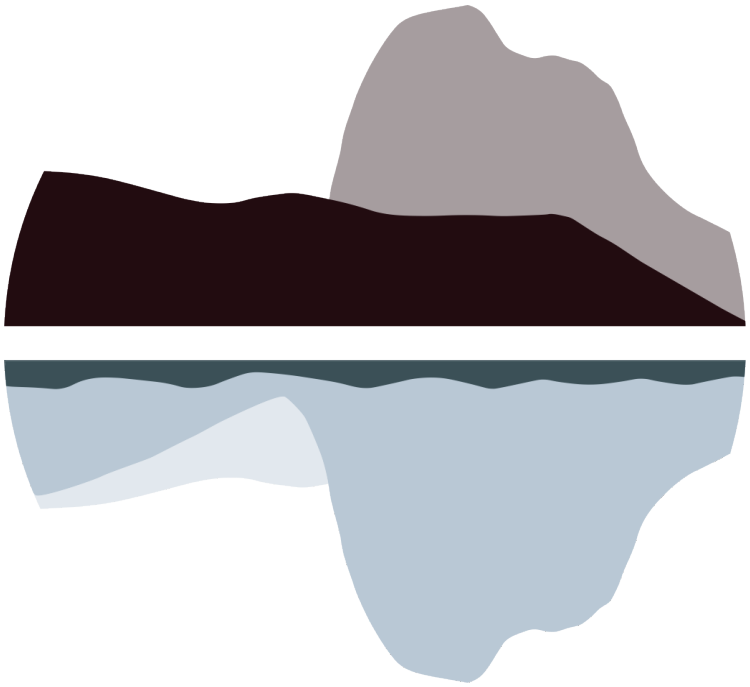

Excursions book

Editors

Julia Garcia-Oteyza Ciria
Josep Bonsoms
Marc Oliva

European Conference on Permafrost

Excursions book

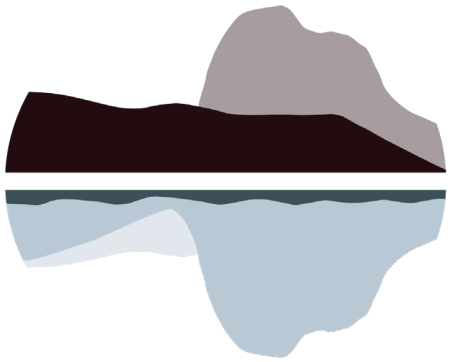

EUCOP6 PUIGCERDÀ
18-22 JUNE 2023

DOI: 10.52381/EUCOP6.excursionsbook.1

European Conference on Permafrost

Excursions book

EUCOP6 PUIGCERDÀ
18-22 JUNE 2023

Sponsors

UNIVERSITAT DE BARCELONA

Ajuntament de Puigcerdà

Diputació de Girona

IDAPA
Institut per al Desenvolupament i la Promoció de l'Alt Pirineu i Aran
Institut entath Desvolopament e era Promocion deth Naut Pirenèu e Aran

IPA

FGC TURISME

VALL DE NÚRIA RIPOLLÈS

LaMolina CERDANYA BERGUEDÀ RIPOLLÈS

CADÍ Des de 1915

beadedstream

INDEX

LOCAL EXCURSIONS

EUROPEAN CONFERENCE ON PERMAFROST
19-23 JUNE, 2023, PUIGCERDÀ

LOCAL EXCURSIONS

1 Field trip to:

Puigpedrós - Perafita mountains, Cerdanya

de Andrés, N.[1], Palacios, D. [1], Fernández-Fernández, J.M. [1], Oliva, M. [2]

[1]Universidad Complutense de Madrid
[2]Universitat de Barcelona

EUROPEAN CONFERENCE ON PERMAFROST

19-23 JUNE, 2023, PUIGCERDÀ

Puigpedrós - Perafita mountains, Cerdanya

de Andrés, N.[1], Palacios, D. [1], Fernández-Fernández, J.M. [1], Oliva, M. [2]

[1]Universidad Complutense de Madrid
[2]Universitat de Barcelona

INTRODUCTION

The trip visits some of the main glacial cirques in the southeasten Pyrenees, in the Cerdanya region (Catalonia). This region forms a depression located between the central Pyrenean axis (the so-called Axial Zone) and the outer mountain ranges (Pre-Pyrenees). The depression is crossed by the river Segre between the towns of La Seu d'Urgell (west) and Puigcerdà (east), right on the border with France. To the north of the Segre River, there are the massifs, namely Tossa Plana de Lles (2,904 m) to the west and Puigpedrós (2,914 m) to the east, which form part of the Axial Zone, composed of Palaeozoic rocks, mainly metamorphic and plutonic. To the south of La Cerdanya we find the Cadí-Moixeró pre-Pyrenean ranges, composed of Mesozoic and Cenozoic rocks, mainly limestones, sandstones and conglomerates.

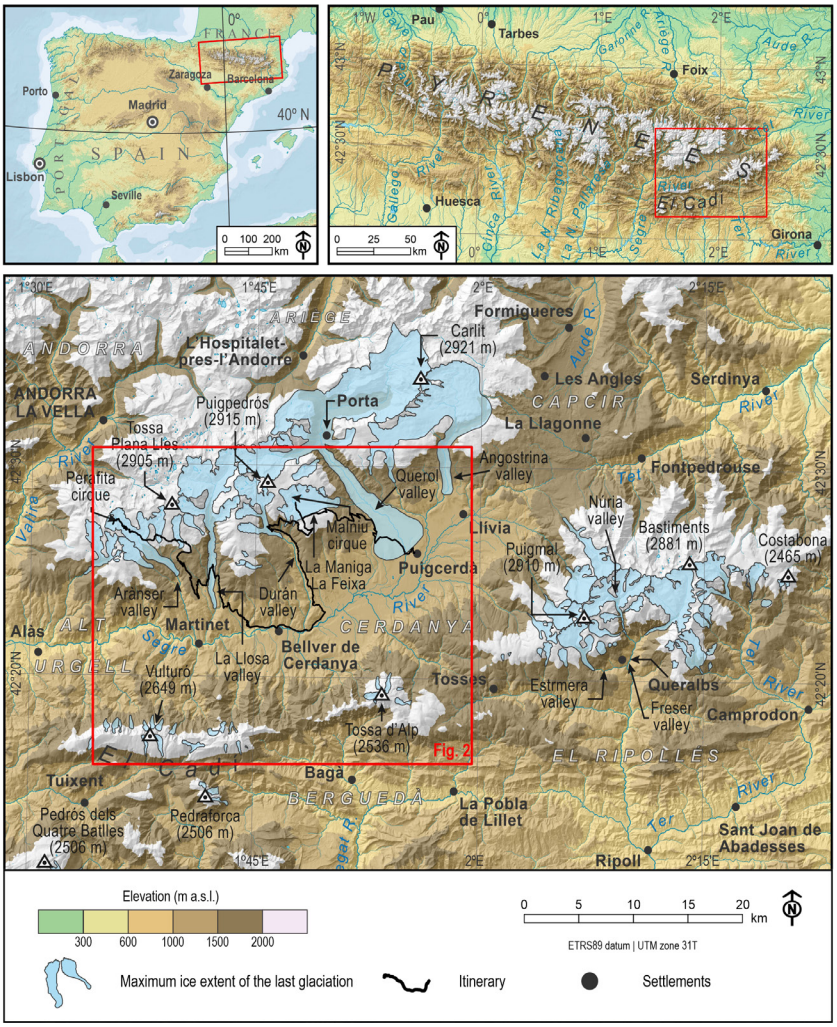

Figure 1. Maximum ice extent of the last glaciation in Cerdanya area and location of figures in this field guide. Adapted from Salvador-Franch et al. (2021).

The geographic characteristics of these mountains and their geomorphological evolution have been recently described in the book "Iberia, Land of Glaciers" (Oliva et al. (Eds.), 2021), specifically in the chapter dedicated to the Eastern Pyrenees (Salvador-Franch et al., 2021). In this guide, we will refer to the information provided in this book and the publications cited therein.

The trip will focus on the cirques located on the southern slopes of the northern massifs of La Cerdanya. The Puigpedrós massif is bounded to the east by the Querol River, which descends from the Carlit massif at 2,921 m (in France), and connects with the Segre River near Puigcerdà. To the west, it is bounded by the Duran Valley, with important glacial cirques at its head. The summits of Puigpedrós are flattened, as they correspond to the remnants of ancient erosion surfaces, and steep tectonic steps on its slopes alternate with several staggered erosion surfaces at different elevations. Six glacial cirques are carved out in the northern slope of the flat summit plateau up, with vertical walls and very flat bottoms. The Tossa Plana de Lles massif stretches from the Llosa Valley in the east, the head of which lies between the Andorran mountains and the Aransèr Valley in the west, which borders the Andorran administrative border. The configuration of the relief in this massif is similar to that of Puigpedrós, also with flattened

summits and numerous cirques on its southern slope. The most outstanding one is the cirque of La Pera, located at the head of the Aränser, under the Pic de Perafita (2,752 m).
Tectonic dynamics in Cerdanya are characterized by active processes resulting from extensional features due to the post-orogenic uplift of the mountain range, and trans-tensional due to the opening of the Valencia Trench, with a still important influence at present in the network of Segre River dynamics. The climate of these mountains is marked by a Mediterranean influence, but with a high degree of continentality. The average annual air temperature ranges between 1 and 3 °C at 2,500 to 2,900 m, with an annual rainfall accounting for 700 to 1,200 mm between altitudes of 1,000 and 2,000 m. Ca. 25% to 35% of precipitation occurs in the form of snow at 2,000 m. The vegetation in the mountain belt from 900 to 1,600/1,800 m is composed of oak (Quercus gr. Fagineae, Q. pubescens, and Quercus ilex) and the Scots pine (Pinus sylvestris). The subalpine level (1,600/1,800 to 2,200/2,300 m) is dominated by the black pine (Pinus uncinata) and the forest at 2,200/2,300 m is gradually replaced by mountain scrub (Juniperus nana and Rhododendron ferrugineum) and grasslands (Festuca supina, F. pseudoeskia, etc.).
To understand the geomorphological evolution of the Puigpedrós and the Tossa Plana de Lles massifs, it is important to consider the intensity of the dense tectonic network that has fractured and altered the Paleozoic rocks. This network has been exploited by intense weathering throughout the Quaternary, which has formed a deep weathering mantle in the crystalline rocks, deeper in areas affected by faults. Due to the low altitude of these mountains, Quaternary glaciers were concentrated in the highest cirques but with limited extent, much smaller compared to the Central or Northern Pyrenees. Only below the summits above 2,900 m altitude, extensive glaciers developed, with ice masses descending from coalescent cirques and formed valley glaciers of 3-10 km in length. The interfluves and lower summits were not glaciated as shown by the presence of the thick (chemical) weathering mantle. On the contrary, the valleys that hosted glaciers dragged this mantle, which allowed the formation of large moraine deposits in relation to the limited size of the glaciers that built them. In many glacial cirques, however, remnants of the weathering mantle were preserved on the tops of their walls and in the channels that follow the fracture lines. This explains why, after the deglaciation of the cirques or during their deglaciation process, paraglacial processes on the slopes were so that intense and produce so much debris. This may be the origin of the abundant rock glaciers found in most of these cirques.
The highest peaks were also covered by glaciers; however, other culminating do not show evidence of glacial erosion. On the contrary, their broad flat surfaces show often include patterned ground features. It is not clear whether these- surfaces were glaciated and the gentle slopes prevented glacial erosion or whether, on the contrary, they were not covered by ice masses and the low temperatures prevailing during the periods of maximum glacial extent - of more than 10 °C lower than today in the Pyrenees - were the cause of the formation of these meter-sized sorted circles. The only moraines formed during glaciations prior to the last glacial cycle correspond to the frontal moraines of the Querol Valley, located around the town of Puigcerdà. In the Puigpedrós and the Tossa Plana de Lles massifs, the maximum glacial extent coincided with the Last Glacial Maximum (LGM; 29-19 ka) as they were dated through Cosmic-Ray Exposure (CRE) dating at around 24 to 19 ka - except for some glacial boulders, found in front of large moraine formations of the LGM, with ages between 35-50 ka (Delmas, 2015) -. After the LGM, there is evidence of rapid glacial retreat, interrupted only by small glacier advances or standstills dated at 16-15 ka. Most likely, the glaciers disappeared from most of the cirques at the beginning of the Bølling-Allerød (BA) interstadial, as CRE dating of polished rock surfaces revealed. In some cirques, rock glaciers formed at that time, whose fronts stabilized almost immediately, while their roots remained active until the middle of the Holocene. Only some north-facing cirques under higher peaks (around 2,900 m), hosted glaciers during the Younger Dryas. The Cadí-Moixeró Pre-Pyrenees massif, composed of Mesozoic and Cenozoic rocks, will not be visited during this trip, but its northern face can be observed during the route. In this slope, there are 19 glacial cirques of a very small size (1 to 1.5 km long), embedded in old torrential headwaters. Small glaciers left frontal moraines at 1-3 km from the headwaters, at minimum altitudes of 1,600 m. The southern slope includes only three glacial cirques, but they are the largest as the slope is less pronounced that the very steep northern walls.

THE ROUTE

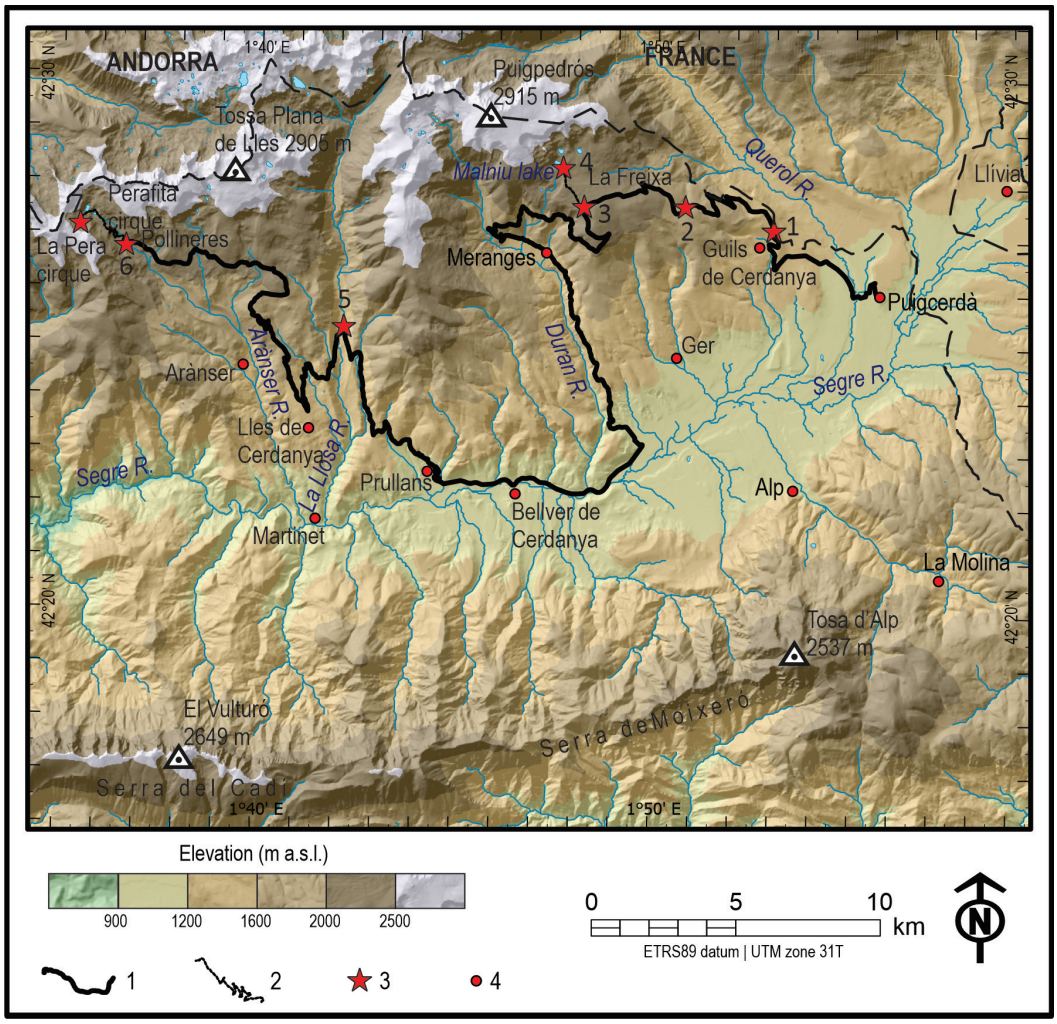

Figure 2. Itinerary map and overview. Key of symbols 1: road route; 2: walking route; 3: stopping points (labels 1 to 7 locate the sequence); 4: settlements (main towns).

1 Guils de Cerdanya: Moraine complex from several glaciations distributed across the Puigcerdà surroundings

The aim of this stop is to observe the Querol frontal moraine system, close to Puigcerdà town, east of Guils de Cerdanya village, with the large lateral and frontal moraines of the Querol Valley, the most relevant in the southern slope of the eastern Pyrenees. A former glacier descended from the Carlit Peak (2,921 m) and ended in the plains near the town of Puigcerdà, at least during the last three or four glaciations. This complex will be covered and explained in detail in the trip to Têt - Angoustrine – Querol - Col de Puymorens, but we will stop here to enjoy the excellent view of this exceptional moraine landscape, despite substantial human disturbance in the area. The description of the complex here follows the summaries given in Delmas et al. (2022) and Calvet et al. (2022).

The innermost moraine system dates back to the LGM, with an average CRE age between 24 and 25 ka; it is divided into several ridges that show evidence of the frequent pulsations of the LGM. Although the outermost ridges of this system can be from the MIS 2, 3 or 4. A second moraine system, possibly originated during MIS 6, is located ahead of the younger moraines mentioned above. It forms an important crest just below Guils de Cerdanya and is clearly visible on the hill (Puig San Martín 1,302 m) located just south of the town of Saneja. The existence of several moraine boulders in these old moraines, with a similar degree of alteration and topographically related to fluvioglacial terraces covered with ancient soils like those studied in the Ariège Valley (nearby valley) suggests that it may have developed during the Marine Isotope Stage (MIS) 6 as the latest.

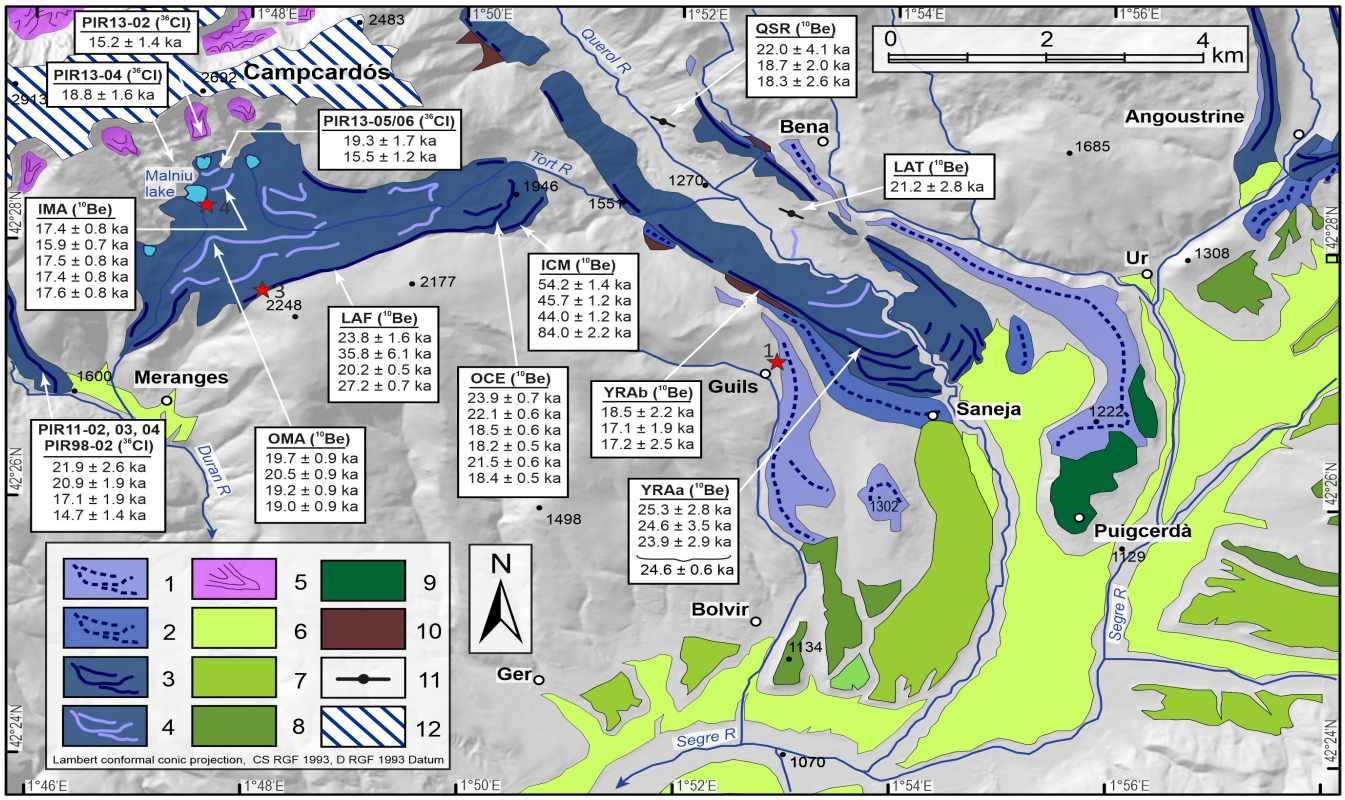

Figure 3. Glacial deposits in the Querol River basin with the existing dates. Key of symbols– 1- Pre-Eemian moraines (MIS 8–10). 2- Pre-Eemian moraines (MIS 6). 3- LLGM moraines. 4- Post-LLGM moraines. 5- Rock glaciers. 6- Glaciofluvial terraces (generation T1) connected to the Late Pleistocene moraines. 7- Glaciofluvial terraces (generation T2) connected to pre-Eemian moraines. 8- Intermediate glaciofluvial terraces (generation T3). 9- Uppermost (and oldest) glaciofluvial terraces (Puigcerdà outwash plain). 10- Late Pleistocene ice-marginal glaciolacustrine deposits. 11. Ice-polished bedrock step. 12. Low-gradient pre-Quaternary erosion surfaces). The red stars locate the point of the route stops and the associated number indicates their sequence. Spot elevations in metres above the sea level. Adapted from Delmas et al. (2022) and Calvet et al. (2022).

This moraine connects with the intermediate fluvioglacial terraces (T2), which are clearly visible to the south of Saneja and to the east of Puig de San Martín. The terrace is currently occupied by a golf club, at 1,120 m elevation. At a slightly lower altitude, around 1110 m, are the terraces (T 1) that link up with the LGM moraines, located to the north of the town of Puigcerdà.

Just to the east of Guils de Cerdanya village, we can observe the outer lateral moraine and connects with the fluvial terraces (T3), in the vicinity of Bolvir. This terrace can be clearly seen southeast of Bolvir, where a plateau remains, occupied by the Corona housing development, at an altitude of 1140 m. These moraines have the same degree of alteration and the soils yielded a similar age to that of the moraines that end near the town of Puigcerdà. Therefore, these moraines are superimposed on older terraces (T4) occupied by the centre of the town, which could be originated at the MIS 10-12. A second moraine ridge, possibly of MIS 6 age, is interposed between the previous moraines and the town of Puigcerdà. These moraines are located just below Guils de Cerdanya and are clearly visible on the hill (Puig Sant Martí, 1,302 m) located just to the south of Saneja village. These moraines link up with the intermediate fluvioglacial terraces (T2), which are clearly visible to the south of Saneja and to the east of Puig de Sant Martí. The terrace is located below T3, to the east, and is occupied by a golf club, at 1120 m altitude. At a slightly lower altitude, around 1,110 m, we find the terraces (T1) that link up with the LGM moraines, located to the north of the town of Puigcerdà. As has been explained, the only features dated in the entire complex are the innermost moraines and their corresponding terraces (T1), originated during the LGM. The correlation between the terraces T2, T3, and T4 and the Stadial MIS 6, MIS 8 and MIS 10-12, respectively, are based on ages obtained in similar relative chronostratigraphic positions in the central and eastern Pyrenees (synthesis in Delmas et al., 2022 and Calvet et al., 2022).

Figure 4. Querol valley, upstream of Puigcerdà, to the north, with lateral and frontal moraines of at least three glacial cycles and their corresponding fluvioglacial terraces. To the left, the Puigpedrós (2914 m) massif and its southern glacial cirques.

2 Guills-Fontanera Nordic ski resort: Lateral Moraines of Querol valley and frontal moraine complex from La Feixa-Malniu glacial cirques.

At this stop, we can observe the contrast between the landforms generated by large glaciers and the landforms left by more marginal one, located on lower peaks and on the southern slope. In the first case, the glaciers generated in the highest peaks of the eastern Pyrenees, whereas in the Carlit (2,928 m) large ice caps developed. From these ice caps, outlet glaciers descended the Querol Valley during periods of large glacial expansion, which reached the current location of Puigcerdà, as it was seen in the previous stop. Lateral moraines can be seen in the slopes below the stop, towards the east, parallel to the Querol River, which are currently being eroded. Some of the outermost ridges of these moraines are considered to date back from an earlier glaciation due to the high degree of surface weathering of their boulders. The main ridges of these lateral moraines have been attributed to the LGM. Parallel lateral moraines can be clearly observed on the opposite slope of the Querol valley, as well as the deep incisions caused by post-glacial erosive dynamics.

In contrast to these large lateral moraines existing in the Querol Valley, we can see to north of the stop the front of a large moraine complex descending from the group of seven glacial cirques on the eastern slope of Puigpedrós Peak (2914 m). The small glaciers of these cirques converge on a very flat surface, which corresponds to the Plana de La Màniga-La Feixa. From here, a former glacier was fed by all the small cirques, resulting in a single ice mass that descended mainly towards the east but did not reach the lateral moraines of the Querol Valley. Another small tongue descended towards the west, covering one slope of the Durán Valley. The low intensity of glacial erosion in these cirques implied that important remnant of the weathering mantle have been preserved on their walls. For this reason, despite the small size of these glaciers, their debris load was very significant. In fact, the moraines that cover the La Feixa plateau are considered to result from the collapse of a debris-covered glacier.

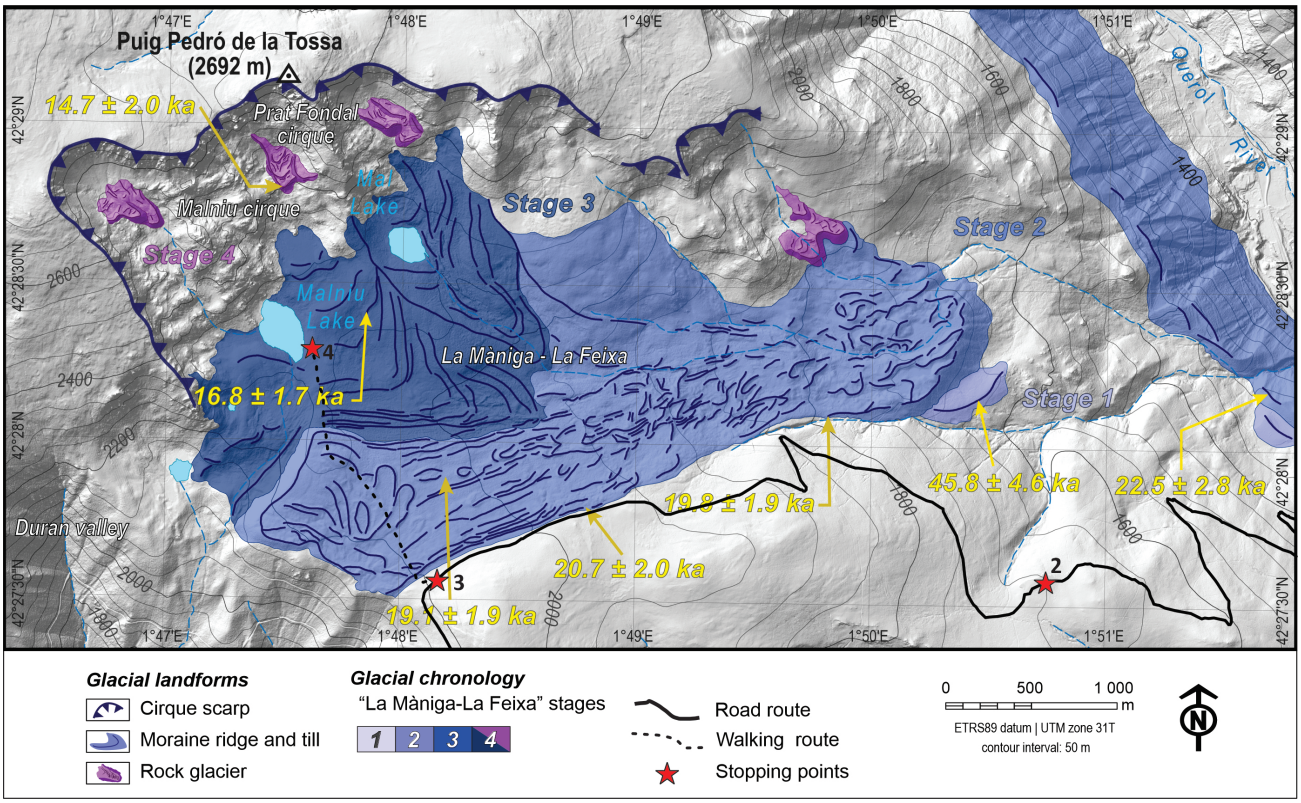

Figure 5. Distribution of glacial and periglacial landforms in La Màniga-La Feixa complex with associated surface exposure dates according to Oliva et al. (2019). Adapted from Salvador-Franch et al. (2021).

From stop 2 we can see the huge 100 m high front of the moraine complex, where the boulders were transported by the glaciers along 3 km from the cirque walls. CRE dating of the outermost boulders of the moraine complex showed ages falling within the LGM. However, beyond this front, there are some aligned glacial boulders defining a small arc that reported exposure ages between 40 and 50 ka; this is the only place (at least in this sector) where it is proven that the maximum advance of ice during the last glaciation occurred prior to the LGM. Above the main moraine complex, in the easternmost cirque, small rock glaciers can be seen within the cirques, showing that the end of deglaciation culminated in the formation of these periglacial landforms.

Figure 6. In the foreground, Saneja village under the hill of Puig de St. Martí (1302 m), with the moraine formed probably during MIS 6: in the foreground, the northern slope of the Pre-Pyrenean massifs, from left to right of the Tosa d'Alp (2,536 m), Moixeró-Cadí (2,648 m)

Between the La Màniga-La Feixa morainic complex and the lateral moraines of the Querol Valley, the slopes have not been affected by glaciers and therefore conserve relief features characteristic of the deep chemical weathering of the crystalline rocks, with abundant tors and alteration basins. To the south, on the other side of the Cerdanya depression, the Pre-Pyrenean mountains can be seen, amongst them the Tosa d'Alp (2,536 m), to the west, and the Cadí-Moixeró massifs (2,648 m) to the east. In the Tosa d'Alp there are glacial cirques approximately 1.5 km long in its western, northern, and eastern slopes. The largest cirque, facing the north-northeast, is 1,800 m long and left some moraines. This entire glacial cirque has been heavily damaged by the Masella ski resort.

3 Plana de La Màniga-La Feixa: the limits of glacial expansion and the contrast between glaciated and non-glaciated areas

Stop 3 is in front of the frontal-lateral moraines of the La Màniga-La Feixa complex. To the north, the peak of Puig Pedró de la Tossa (2692 m) can be seen, located on the eastern slope of the Puigpedrós peak (2913 m). Both peaks are joined by a flattened summit surface that corresponds to the remnants of an old erosion surface, uplifted by tectonic dynamics. This summit surface lacks erosive glacial landforms but, on the contrary, preserves important areas occupied by periglacial patterned ground. It remains unclear whether this area was covered by glaciers with very limited erosion capacity, or it remained ice-free, under the influence of intense periglacial processes.

Below this summit sector, on the edge of a tectonic step, the seven glacial cirques that fed the Plana de La Màniga-La Feixa glacier can be observed. Right at the top of the walls, it is clearly visible the cut on the deep weathering mantle, where the crystalline and metamorphic rocks are intensely sandblasted. This alteration level has supplied large volumes of debris deposited onto the surface of the former glaciers, leading to the formation a large debris-covered glacier on the Plana. This glacier encountered an obstacle in its southward advance in the Bosc del Gili hill (2,248 m), which protrudes only 50 m above the Plana. The obstacle was sufficient to create a glacial diffluence, where part of the glacier turned westwards and plunged over the lateral slopes of the Durán Valley. The other sector of the glacier turned eastwards and advanced towards the east, hanging over the Querol Valley, as it was seen in the previous stop. The stop is therefore located at the point of diffluence between the two main glacial flow lines.

Figure 7. In the background, the Puigpedrós (2914 m) massif and its southern glacial cirques. Below the cirques, in the forest, the moraine complex of La Màniga-La Feixa. In the foreground, in the forest-free plains, the area not affected by glaciers of the La Màniga-La Feixa.

The moraine of the debris-covered glacier is formed by a set of ridges parallel to the main flow of the former glacier. CRE dating yielded ages between 20 and 27 ka for the boulders of the outermost ridge, demonstrating a glacial advance during the LGM. The following inner ridges show somewhat lower exposure ages, between 19 and 20 ka, representative of the occurrence of the pulsations at the end of the LGM.

Towards the central part of the glacial moraine system, parallel ridges tend to disappear and adopt a hummocky topography; we interpret this as the progressive disintegration of the glacier, with a period of dead ice followed by its slow chaotic melting across the Plana. Collapse depressions are frequent in these sectors, and some of them are occupied by small lagoons and peatlands. Further inland, towards the peaks, there is a core of concentric moraine ridges overlapping the outermost ones, where CRE dating yielded younger ages, between 16 and 17 ka.

The ages allow us to infer that these moraines correspond to glacial advances related to the Heinrich-1 Stadial. Behind, already at the base of the upper cirques, polished rock outcrops have been dated to 16 ka. Further up, under the walls of the small cirques, small rock glaciers are present, some of whose fronts have been dated, yielding ages that evidence their definitive stabilization at the beginning of the B-A Interstadial at ca. 14-15 ka. Thus, the moraine and rock glacier complex of La Màniga-La Feixa preserves the entire history of the culmination of the last glacial cycle and the deglaciation. In these cirques there is no evidence of glacier inception during the Younger Dryas, probably due to their low altitude and southern orientation, although moraines of this age have been found in the highest cirques on the northern slopes of these peaks.

In this stop we can observe the contrast in the landscape between the sectors dominated by glacial erosion and sedimentation and those that were not affected by glaciers, such as the southern area of the Plana de La Màniga-La Feixa. These latter are dominated by the sandy alterites soils, and the alternation of (chemical) weathering depressions where water accumulates in the subsoil, and rock outcrops forming tors and other physical weathering landforms. It is precisely in the depressions with a deeper water table that freeze-thaw processes easily form periglacial microforms in the soils, such as earth hummocks, solifluction sheets and lobes, turf-banked terraces, etc. Remarkably, extensive earth hummocks persist on the southern side of the plateau (non-glaciated during the last glacial cycle), being one of the most impressive active periglacial features in the Eastern Pyrenees. The area is under a seasonal frost regime, with negative ground temperatures from November to April/May; this fact, together with intense snow drift in this flat environment, favour intense cryoturbation dynamicsand the development of these periglacial features. In recent decades, a rise in the timberline has been observed, with the black pine reaching 2,300-2,350 m a.s.l. This increase may have multiple origins. Firstly, due to the reforestation in some sectors of this mountain range, especially on the steeper slopes. It is also due to the decrease in summer grazing, as livestock tends to stay more in the lowlands. At present, grazing is limited to the flat areas with well-developed soils, such as the Plana de La Màniga-La Feixa. Nevertheless, natural causes are also important, with a steady decline in the permanence of snow on the ground, especially during the spring season, more evident since the late 1970s. This decline is a major issue in many of the region's ski resorts, which are increasingly producing artificial snow.

Figure 8. Active earth hummocks field on the non-glaciated southern side of the plateau of the La Màniga-La Feixa.

4 Malniu Lake: a route through the labyrinth of moraine ridges from the LGM to the last moraines of Hienrich Stadial-1 at the base of the cirques. 45 min hiking.

re La Màniga-La Feixa moraine complex along the diffluence between the western sector (towards the Durán Valley) and the eastern sector (towards the Querol Valley). In the first sector of the route, the path ascends from 2,200 m, where La Feixa is located, to 2,265 m, the highest elevation of the complex. This sector of the route crosses the LGM moraine system, dated from the beginning of the period (around 27 ka) to the onset of deglaciation (19 ka). The route crosses the enti From this high point, the path descends to the Malniu Lake (2,255 m) an overdeepened depression probably associated to the last glacial advance (Heirinch-1 stadial). The path keeps crossing several moraine ridges younger that the previous ones (between 16 and 17 ka) that dam the lake's waters.

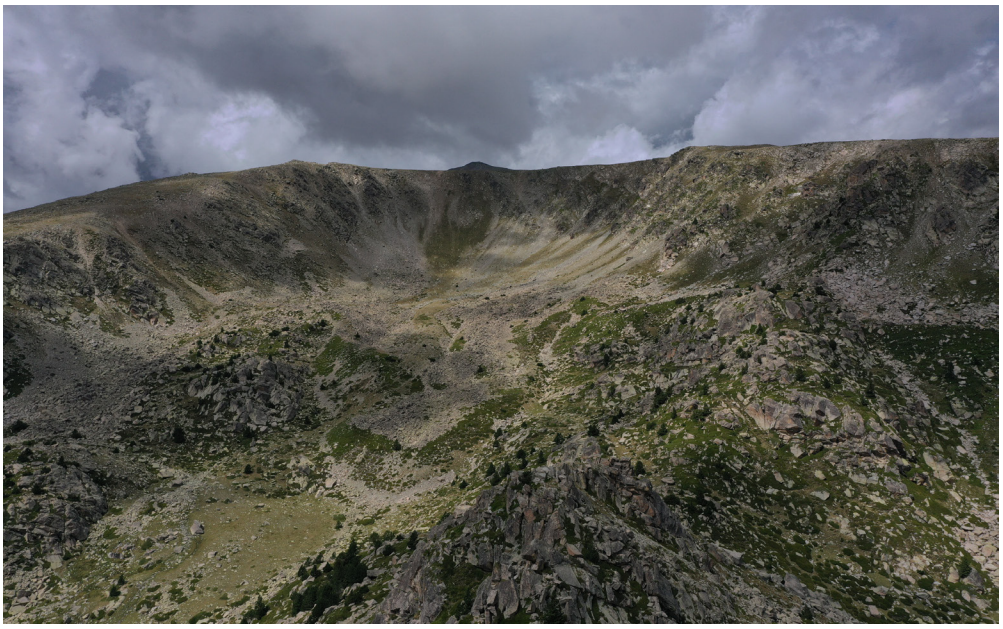

Figure 9. Rock glacier in the cirque of Clot de Malniu, above the lake of Malniu, with possible origin in the B-A interstadial

Above the lake, there are some glacially polished rocky outcrops and some higher moraines, with ages around 16 ka, which also retain the waters of seasonal lagoons. In the easternmost cirque of Malniu Lake, above the polished rocky outcrops, the front of a small rock glacier can be seen. This rock glacier has its roots at an altitude of 2,550 m and ends at 2,400 m with a length of ca. 400 m. Its front has also been dated and revealed a stabilisation age between 14 and 15 ka. Rock glaciers of similar dimensions extend over most of the cirque bottoms and are associated with the significant vertical development of the walls. Their origin has been related to the last phases of deglaciation, as their fronts have yielded the same age at the beginning of the B-A interstadial. The origin of these rock glaciers can lead to an interesting discussion about their relationship with both cold crises (which enhance the role of permafrost in their formation) or warm crises (which promote the deglaciation of the cirque walls and trigger paraglacial processes). These processes are particularly intense given the weakness of the weathering mantle observed in the culminating sectors of these walls. This weathering mantle explains the huge volume of debris distributed between the moraines maze as well as the enormous size of most of their boulders. However, it may also explain how these debris covered the small glaciers during the beginning of the interstadial. This must have allowed their evolution into rock glaciers with a certain flow capacity, although the stabilization of their fronts occurred shortly after their formation. Another alternative hypothesis of rock glaciers being formed during the Older Dryas cold crisis is also plausible. Unfortunately, the high range of uncertainty provided by CRE dating complicates the interpretation. However, according to other palaeoclimatic proxies, the impact of this stadial in the region was very limited as it was short and characterized by cold and arid conditions.

Unfortunately, the route does not include a visit to the northern slopes of these massifs, whose landscape is very different from that of the southern ones. These northern cirques are not very accessible and require long walks to observe them, which has not favoured geomorphological research yet. In the north, the cirques fed relict rock glaciers of much greater size and complexity, including overlapped lobes of various generations, with their lengths often exceeding 1 km.

Moreover, they are not only present at the bottom of the cirques, as in the south, but are also frequent at the foot of rock fall talus, on slopes or walls at various locations. Moreover, their fronts can descend to 2,000 m. These northern rock glaciers have no chronology of their formation and development is yet available, but logically their origin is likely to be more complex than in the case of the southern ones, probably more related to a cryogenic origin than to the gradual transformation of retreating glaciers. The route does not reach the summit surfaces, although their observation poses very interesting problems at the transition between glacial and periglacial domains. As it was mentioned above, the flat summits preserve a deep weathering mantle. Rocky outcrops are scarce and lack polished surfaces. They look more like ancient tors. On the other hand, inherited periglacial landforms are numerous. In some sectors, there are remnants of large, sorted circles, stone stripes, blockfields, block streams, nivation hollows and cryoplanation

terraces. All these features, which may be related to the existence of permafrost, are currently inactive. The visit to these summit surfaces could bring an interesting discussion about their origin, whether they were actually covered by glaciers or the action of the wind drifting prevented snow accumulation on the summits. The age of these ancient periglacial formations related to the existence of permafrost can also be discussed. They may have formed during the LGM, the coldest phase of the last glacial cycle, thanks to the absence of glaciers on these summits. These landforms may have also been formed prior to last glaciation and glaciers did not erase them due to their low erosion capacity, given the low slope and high altitude; this fact, together with a thin ice mass, could have favoured the development of cold-based glaciers. Another possibility would be that they were formed just following the glacial retreat after the LGM, and that the glaciers were replaced by intense periglacial conditions under a permafrost regime - this may have happened during the Heinrich-1 Stadial, one of the coldest phases of the last glacial cycle, as shown by other palaeoclimatic records in the Pyrenees. At present, periglacial landforms are related to seasonal frost, such as earth hummocks, ploughing boulders, turf-banked terraces, solifluction sheets and lobes, small nivation niches, etc. These landforms are either active nowadays or show recent activity, and they are always related to the existence of fine materials in the soil, derived from the subaerial disintegration of the weathering mantle.

Figure 10. Network of periglacial polygons on the flattened peaks of Calmquerdós.

5 La Llosa glacial valley: LGM lateral moraines, topographically constrained by a single moraine ridge and with their fronts completely eroded. Lunch.

The route continues along the Duran Valley, where a former alpine glacier descended from the western slope of Puigpedrós Peak, leaving lateral moraines dating back to the LGM. Back to the Segre Valley, the trip will continue towards the Llosa Valley where Stop 5 will take place and we will have lunch. The Llosa Valley follows a major fault line that crosses the entire Pyrenees from north to south and separates the Puigpedrós massif to the east from the Tossa Plana de Lles (2,904 m) to the west. The head of the valley is already in Andorra, and it is surrounded by peaks up to 2,700-2,800 m. An important glacier filled the entire headwaters and was connected by a col to the east with glaciers that descended towards the Querol Valley, going all the way around the Puigpedrós massif to the north. The elevation of the lateral moraine remnants indicate that the glacier exceeded 400 m of ice thickness. It descended along 12 km through the Llosa Valley to an altitude of 1,200 m and was one of the longest glaciers in the south-eastern Pyrenees. The minimum altitude of the Llosa glaciers was very similar to that reached by the Querol glaciers in Puigcerdà.

However, the moraine landscape is very different. Here we do not find the succession of moraine ridges that can be seen in Puigcerdà, nor on the La Màniga-La Feixa plain, but instead we have a polygenic moraine ridge. In the case of La Llosa, the palaeoglacier flowed inside the valley in its frontal sector and did not extend over the surrounding plains, as it occurred in the Duran Valley, Querol or Aránser Valley, as we will see in the next stop.

The ice flow was constrained by the narrow and vertical valley walls. The consequence is that, firstly, there is a tendency to form a single moraine ridge, polygenic, where the sediments from all the numerous LGM pulses must have accumulated. On the other hand, the intense erosion of the river has dismantled and erased the frontal moraines. This completely limits the opportunities of successfully applying CRE dating to the moraine boulders. The geomorphological setting in the terminal area of the Llosa valley is similar to that of the Duran and Aránser valleys, and consequently, the dating results in the three valleys are also similar. The oldest ages, corresponding to the last pulses of the LGM (20-21 ka), were obtained from the boulders of the most stable moraine ridges, located still far from the central sector. The boulders closer to the frontal terminal sector gave younger ages, probably due to greater denudation compatible with the fact that moraines that should have marked the maximum advance of the glacier may have completely disappeared due to erosion. In the case of La Llosa, there are no dates of more recent moraine formations, as they have not been found. A rocky outcrop with a polished surface at 1,700 m gave an exposure age reporting deglaciation as early as the beginning of the B-A interstadial. Throughout the route, the Cadí-Moixeró Pre-Pyrenean massif (2,648 m), can be seen to the south. This is the front of the thrust mantle of the southern Pyrenees, where the Mesozoic and Cenozoic strata, mainly limestone and sandstone, have been displaced southwards by the uplift of the Axial Pyrenees during the Alpine orogeny. This tectonic structure gives rise, as in the rest of the Pre-Pyrenees, to dissymmetrical mountain ranges, with a very steep northern front - as it can be seen from the entire route - and a gentler southern slope. In the case of Cadí-Moixeró, the steep slopes of its northern slope have preserved a more natural vegetation, with oak groves of Q. ruber and beech (Fagus sylvatica) and black pine (Pinus uncinata), which explained its designation as Natural Park.

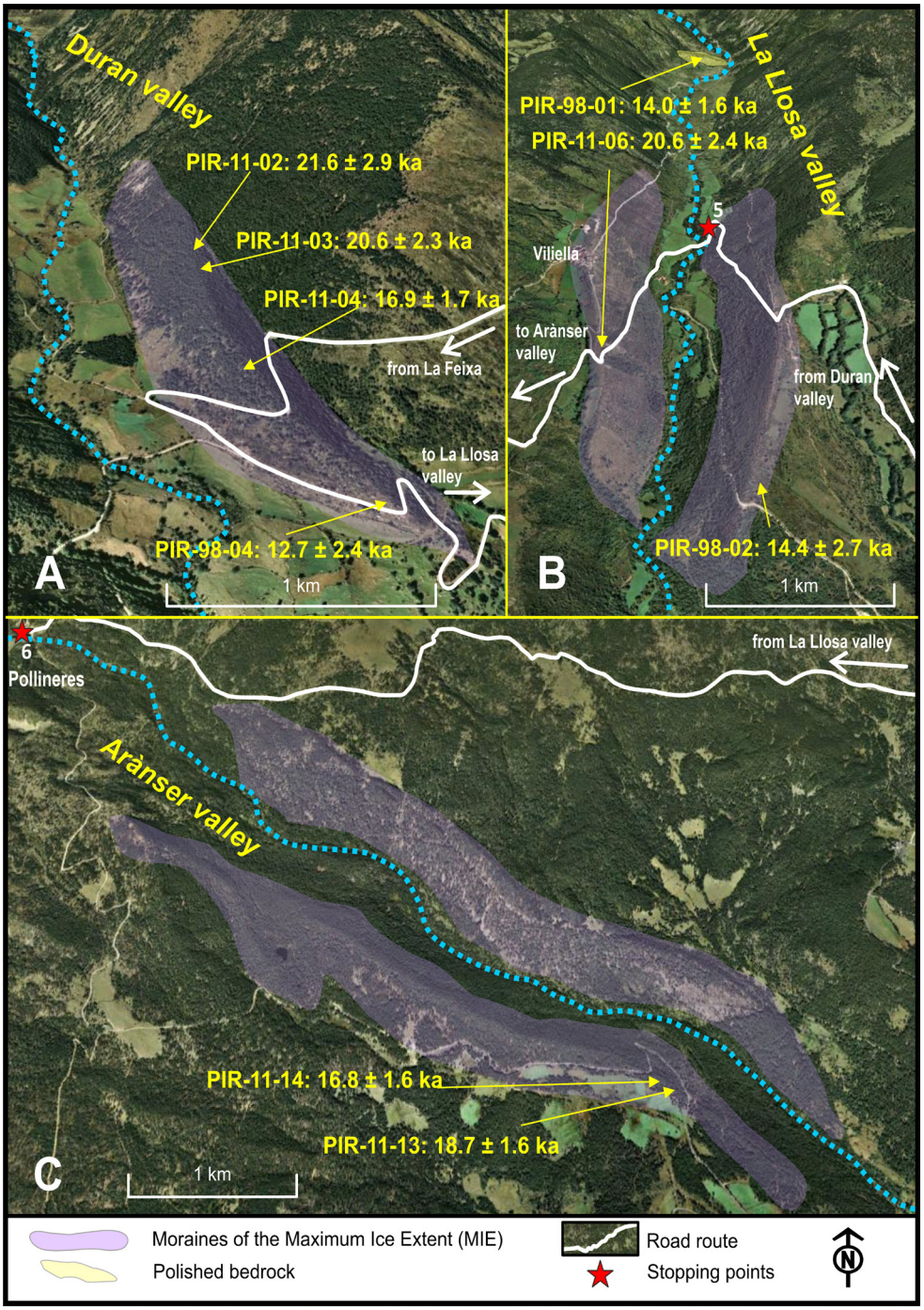

Figure 11. Oblique Google Earth views of the maximum ice extent moraines of the Duran (A), La Llosa (B) and Aránser valleys. Adapted from Andrés et al. (2018) and Oliva et al. (2019).

Here, lower incoming solar radiation allowed the formation of numerous small glaciers at the headwaters of ancient ravines (where 19 glacial cirques developed), with glaciers between 1 and 3 km long descending to elevations down to 1,600 m. In this massif, no rock glaciers developed. On the southern slope, despite the glaciers were longer, favoured by gentle slopes, only 3 well-developed glacial cirques formed, with a strong dissymmetrical character, as their accumulation areas were located on the eastern slopes of the cirques, in the lee of the prevailing westerly winds, and significantly favoured by the snow blowing over the broad and flat summits.

6 7

Pollineres and La Pera Cirque: The headwaters of the Aràn ser Valley, glacial landforms and visit to the rock glaciers of Claror.
30 min hiking.

The route continues to the massif of the Tossa Plana de Lles through the dense forest that starts at the nordic ski resort of Lles. On this southern slope of this massif, there are several small glacial cirques, with moraines frequently cut by the road. The most important of these is found in the La Pera Cirque, Aràn ser Valley. The lateral moraines of the Aràn ser Valley, located below the resort (1,750 m) can be seen from the road. No frontal moraines are found in the area. CRE dating of these lateral moraines gave similar ages to those of the Llosa and Duran valleys, with the same interpretation challenges mentioned in the previous stop. The bus route ends at Les Pollineres, at an altitude of 2,200 m. The car parking is just below a small rock glacier front, 350 m long on granitic rocks. This front has been dated, showing stabilisation at the beginning of the B-A interstadial. We will walk to the cirque through a series of polished rocky steps, with abundant erratic boulders deposited on them. Under the east-facing wall, new talus-derived rock glaciers and protalus lobes of about 300 m in length and steep fronts developed. The forest track ends at La Pera lakes.

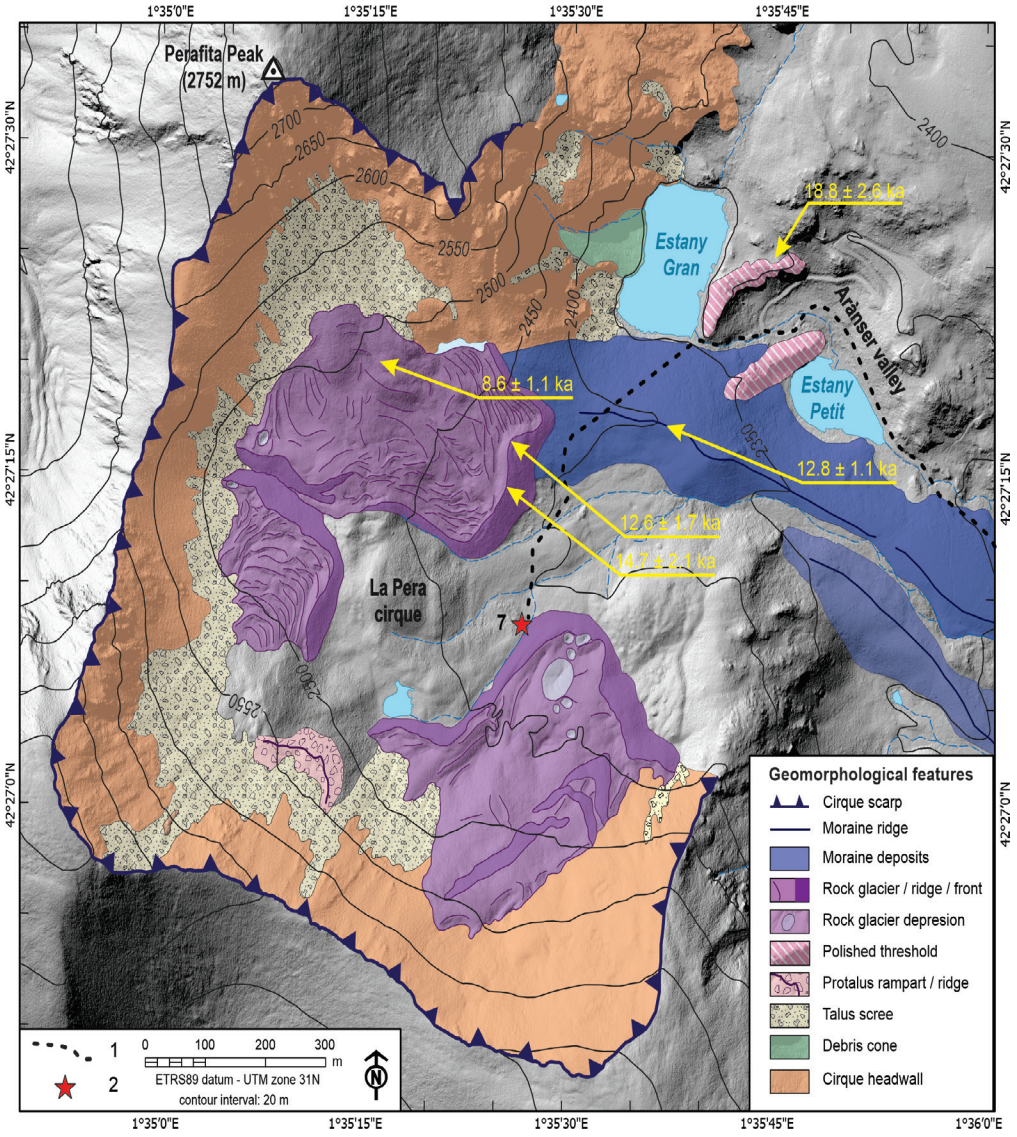

Figure 12. Distribution of glacial and periglacial landforms in La Pera cirque with associated CRE dates). Symbols key 1: walking route; 2: stop point. Adapted from Andrés et al. (2018) and Oliva et al. (2019).

Figure 13. Rock Glacier dominating the eastern wall, above the parking at Les Pollineres (2,200 m).

La Pera cirque lies below the Perafita Peak (2,752 m) and is favoured by its easterly orientation, at the leeward of the prevailing westerly winds, with some mountain ridges with slopes even facing north. It is therefore a basin that was very prone to glacial accumulation. On the other hand, the walls are very vertical and show the presence of rocks deeply affected by chemical weathering in their upper sectors. The cirque shows a great variety of glacial and periglacial landforms, many of which have been dated; however, the 36Cl age updates gave a very high range of uncertainty, sometimes exceeding 2 ka, which makes it difficult to frame the ages of the landforms within the rapid succession of stadial and interstadial cycles of the last deglaciation. In any case, the chronological sequence is in good agreement with cronostratigraphical arrangement and sorts the landforms from the oldest (to the west) to the most recent (to the east).

In the lower, easternmost part of the cirque there are a series of glacially polished rock steps. Their dating yielded the oldest ages of the cirque, with an uncertain age ranging from 20 to 16 ka, although the chronological sequence and the geomorphological setting indicate that the most recent age corresponds to the deglaciation time at this site. The eastern part of the cirque is enclosed by a moraine, which also dams a lake. A single boulder of this moraine gave an exposure age between 11.7 and 13.9 ka; however, as it is a single block, this age should be taken with caution, especially with such a high age uncertainty. The route climbs up the moraine and enters the western sector of La Pera cirque, known as the Claror. This sector is exposed only to the west and is enclosed by steep walls facing south, east and north. From all of them there areblocky landforms of different characteristics. Many of them correspond to well-developed rock glaciers, with numerous transverse arches,

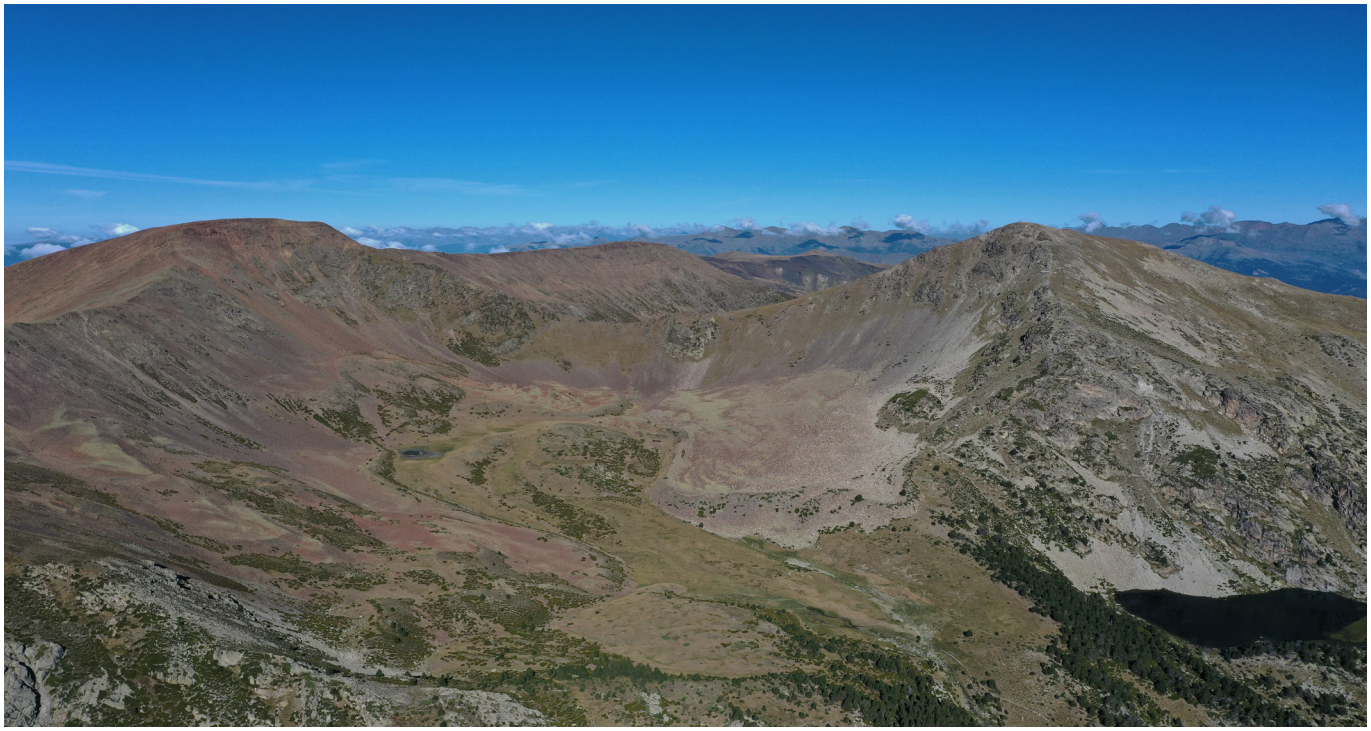

Figure 14. On the right, the Perafita Peak (2,752 m) above of the La Pera lake. On the central and left sectors, The Claror area, the western sector of the La Pera cirque, with several rock glacier formations.

and several generations overlapping each other. This is the case of those located under the eastern wall. Others have a transitional morphology between rock glaciers with some sectors characterized by lobed arches, and former debris-covered glaciers, with a thin debris mantle and where longitudinal ridges predominate, such as those descending from the southern wall of Perafita Peak. Other formations look more like the frontal moraines of very small glaciers, such as those located near to the base of the northern wall. Finally, others are halfway between talus-derived and protalus rampart, such as those found on the northern wall. Obviously, it should be borne in mind that these landforms are dependent on the characteristics of the different lithology of these cirque walls, which are slates and schists, very different from the previous sectors visited, composed of granites.

Figure 15. Overhead vision of a rock glacier on the eastern wall of Claror area, in la Pera Cirque.

Figure 16. Northern face of la Tossa Plana massif, covered by rock glaciers of great entity and complexity, which show a more varied evolution related to the presence of permafrost than those visited on the south face.

In this case we will not visit the northern slope of these peaks. On this slope, as in the case of Puigpedrós, the northern cirques are occupied by complex and diverse generations of rock glaciers, also abundant at the foot of the talus and with a much greater size than those on this southern slope. The observation of this wide range of blocky formations in the Claror sector can give rise to an interesting discussion on their origin and, on the sometimes-blurred boundaries, between glacial and periglacial domains. The discussion can be extended to include the factors that condition the origin of these formations, such as the different lithology (the greater or lesser presence of fines and the availability of materials), the aspect, the vertical development of the walls and, of course, the palaeoclimatic conditions and the subsequent elevation of the lowest permafrost elevation during their active flow period. The only one of these formations that has been dated is the one on the southern slope, whose front gave ages between 15 and 11 ka. A boulder from the highest sector of the rock glacier at its root yielded an age between 9 and 7 ka, which suggest that it remained active during the first half of the Holocene. This situation may lead to an interesting discussion on how to date inactive and fossil rock glaciers and the significance of the results.

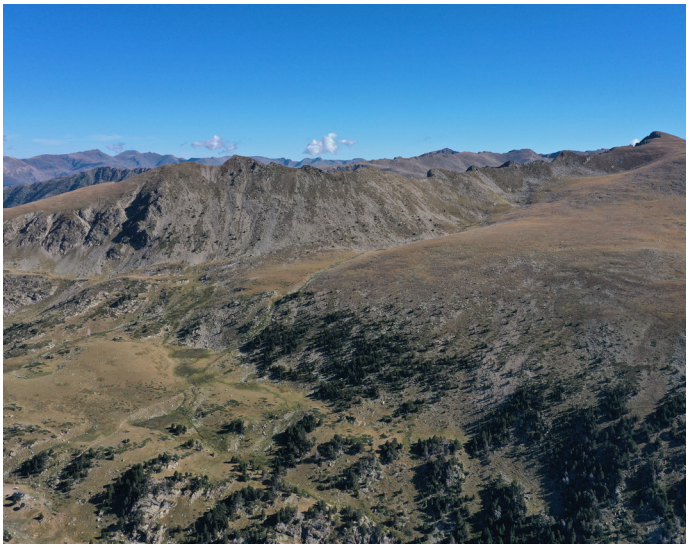

Figure 17. Summit surfaces of the western sector of the Tossa Plana massif, east of Perafita Peak, where the weathering mantle affected by periglacial processes (patterned ground) is preserved.

In fact, the ages can be interpreted as the final collapse of the formation and disappearance of the inner ice core, or the end of its flow, although the ice could remain with no flow much longer, even thousands of years, as has been detected in other regions.

CONCLUSIONS

The route crosses two massifs that serve as an example of the characteristic landscape of the south-eastern Pyrenees. The Mediterranean climate-influence defines landscapes in the Eastern Pyrenees that are significantly different than those of the Central (greater continentality,igher altitude) and Western Pyrenees (higher rainfall, lower elevation). In this sector, erosive glacial landforms predominate only on the highest peaks above 2,900 m, especially on the northern slopes. This is where ice caps formed, which give rise to longer valley glaciers, such as those of Querol and La Llosa. The moraine formations that they left behind depend on the topography of the glacier's frontal sector. Only in open and flat sectors multiple moraine ridges corresponding to two or three glacial cycles can be observed, such as in Puigcerdà, or moraines formed during several advances of the last cycle, prior to the LGM, such as in La Màniga-La Feixa plain. But with these exceptions, most of the glacial landforms that show the maximum ice expansion developed within the LGM. In most of the valleys, there is evidence of a glacial advance during the Heirinch-1 Stadial. To date, evidence confirms that glaciers disappeared at the onset of the B-A interstadial, although in most of the southern cirques these glaciers evolved into rock glaciers (glacier-derived origin).

The complexity of glacial and periglacial evolution is much greater on the northern slopes of the highest peaks. It is noteworthy to remember that on these slopes the complexity of the origin of rock glaciers is much greater. At the same time, their relationship with the existence of talus slopes affected by permafrost is much more frequent (cryogenic origin). Moreover, the impact of the Younger Dryas and, probably, the Holocene cold crises, must have had a much greater impact on the evolution of these rock glaciers.

The most interesting thing about the periglacial landscape of these southern mountains is that the existence of periglacial landforms is closely related to the existence of previous features derived from the survival of the weathering mantle, where it was not eroded by subsequent glaciers. In fact, rock glaciers formed in these areas where the cirque walls provided a large debris supply; the remnants of the weathering mantle is only preserved in the summit surfaces. Rock glaciers are absent on highly polished walls intensely eroded by glaciers or in massifs characterized by other lithologies, such as the Cadí-Moixeró massif. Patterned ground features (i.e. meter-sized sorted circles), earth hummocks and solifluction landforms are mainly present on flat or gently sloping surfaces, where the weathering mantle is preserved and where fine sediments allow the formation of these active seasonal frost formations.

There are still many questions to be answered about periglacial dynamics in these mountains, such as the origin, evolution and age of rock glaciers and patterned ground features in the summit areas, as well as the intensity and characteristics of present-day periglacial processes.

REFERENCES

- Andrés, N., Gómez-Ortiz, A., Fernández-Fernández, J. M., Tanarro, L. M., Salvador-Franch, F., Oliva, M., Palacios, D. (2018). Timing of deglaciation and rock glacier origin in the southeastern Pyrenees: a review and new data. Boreas, 47(4), 1050-1071.
- Calvet, M., Delmas, M., Gunnell, Y., & Laumonier, B. (2022). Geology and Landscapes of the Eastern Pyrenees: A Field Guide with Excursions. Springer Nature.
- Delmas, M., Gunnell, Y., Calvet, M., Reixach, T., Oliva, M. (2022) The Pyrenees: glacial landforms from the Last Glacial Maximum. In: Palacios, D., Hughes, P.D., García-Ruiz, J.M., Andrés, N. (Eds.). European Glacial Landscapes: Maximum Extent of Glaciations. Elsevier, 461-472.
- Oliva, M., Palacios, D., Fernández-Fernández, J. M., Rodríguez-Rodríguez, L., García-Ruiz, J. M., Andrés, N., ... Hughes, P. D. (2019). Late Quaternary glacial phases in the Iberian Peninsula. Earth-science reviews, 192, 564-600.
- Oliva, M., Palacios, D., Fernández-Fernández, J. M. Eds. (2021). Iberia, Land of Glaciers: How The Mountains Were Shaped By Glaciers. Elsevier.
- Salvador-Franch, F., Andrés, N., Gómez-Ortiz, A., Palacios, D. (2021) The glaciers of the Southeastern Pyrenees. In: Oliva, M., Palacios, D., Fernández-Fernández, J. M. (Eds.). Iberia, Land of Glaciers: How The Mountains Were Shaped By Glaciers. Elsevier, 61-85.

2 Field trip to:

Têt - Angoustrine – Querol - Col de Puymorens

Magali Delmas[1], Théo Reixach[1], Régis Braucher[2], Marc Oliva[3], Yanni Gunnell[4], Marc Calvet[1]

[1]Université de Perpignan Via Domitia
[2]Aix-Marseille Université
[3]Universitat de Barcelona,
[4]Université de Lyon

EUROPEAN CONFERENCE ON PERMAFROST

19-23 JUNE, 2023, PUIGCERDÀ

Têt - Angoustrine – Querol - Col de Puymorens

Magali Delmas[1], Théo Reixach[1], Régis Braucher[2], Marc Oliva[3], Yanni Gunnell[4], Marc Calvet[1]

[1]Université de Perpignan Via Domitia
[2]Aix-Marseille Université
[3]Universitat de Barcelona,
[4]Université de Lyon

INTRODUCTION

Pleistocene glaciations in the Pyrenees

Despite their southerly latitude, the Pyrenees were glaciated at every stage of the Pleistocene. The Pyrenean icefield typically extended uninterrupted for 250 km from the Capcir Basin in the east to Pic d'Orhy in the west (Fig. 1). The spatial distribution of glaciers is now well established and has been synthesised and updated repeatedly over time (Penck, 1883, 1894; Taillefer, 1957, 1967, 1969; Hérail et al., 1987; Martí Bono and García Ruiz, 1994; Calvet, 2004, with detailed references therein; Barrère et al., 2009; Calvet et al., 2011; Delmas et al., 2022a, b, c; Delmas et al., 2023a, b, c).

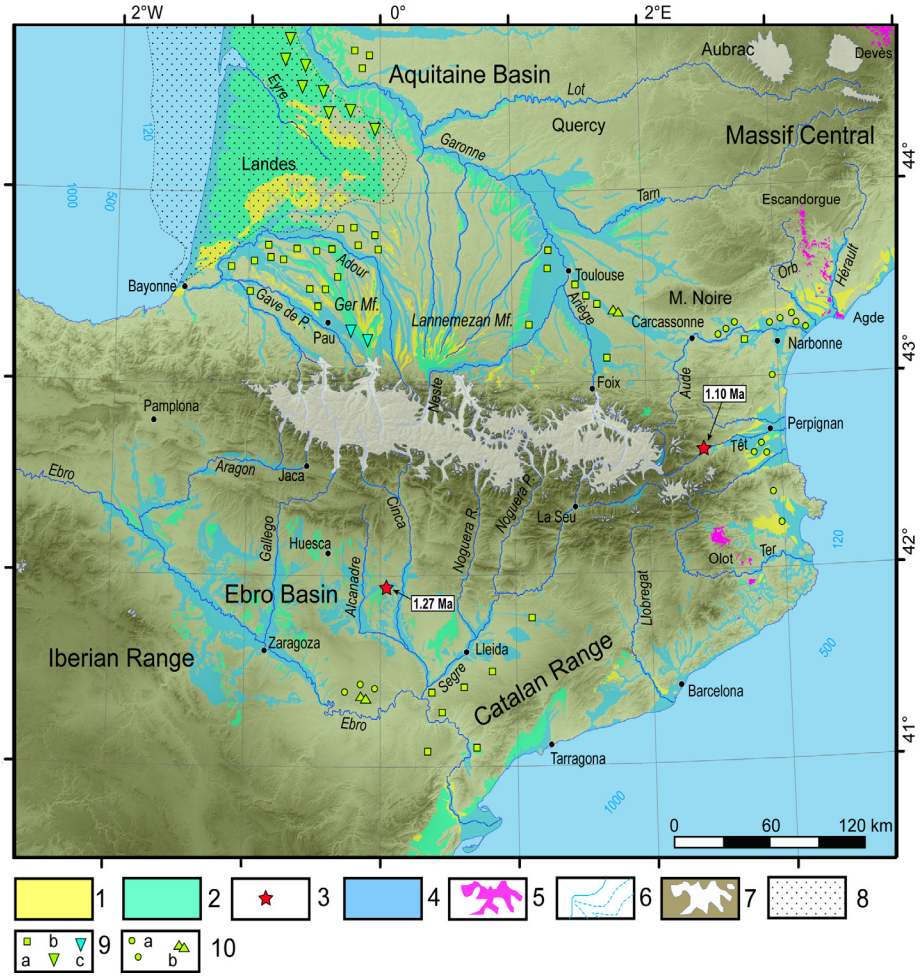

Figure 1. Quaternary geology of the Pyrenees and their piedmont zones: a simplified map. Key to symbols and ornaments – 1: Pliocene deposits (marine and continental); 2: early Pleistocene (upper alluvial and glacifluvial terraces); 3: dated alluvial deposits (ESR age); 4: middle and late Pleistocene alluvial deposits, Holocene alluvium; 5: Quaternary volcanism (late Pliocene to early Pleistocene); 6: offshore isobaths, including LGM isobath (–120 m); 7: outline of most Late Pleistocene extensive glaciation (differences with most extensive Quaternary glaciation are small); 8: middle and late Pleistocene coversands (erg of the Landes); 9: other periglacial features – 9a: loess, 9b: sand wedges, 9c: cryoturbation features; 10: aeolian landforms – 10a: deflation hollows, 10b: yardangs. Alluvial deposits after 1:1,000,000 geological map of France, Barrère et al. (2009), and 1:50,000 scale IGME sheets, with additional information from Mensua et al. (1977).

The spatial distribution of Quaternary glaciers was dictated by dual E–W and N–S asymmetries in the climatic and topographic configuration of the orogen (Fig. 2). The N–S asymmetry is the sharpest, with the northern mountain front open to Atlantic influence and concentrating 75% of the glaciated surface area.

The mean Equilibrium Line Altitude (ELA) for the Quaternary, when reconstructed from isolated cirque-floor altitudes, lay between 1200 and 1600 m among the massifs of the North-Pyrenean Zone, rising a little into the core of the Axial Zone. The largest outlet glaciers reached lowland altitudes of 350 m (Ariège) and 450 m (Garonne), with glacier lengths attaining 37 km along the Gave d'Ossau, 50 km along the Gave de Pau, 70 km for the Garonne, 65 km for the Ariège, with ice thicknesses in each case 0.8–1 km. Limiting factors of ice extent have been the narrowness of the Pyrenees (and therefore of the accumulation zone), the predominance of transverse drainage, and the limited opportunities for valley confluence that such a parallel drainage network imposes on ice flow patterns. The most elevated ridges of the mountain range always stood above the top of the icefield, and transfluence cols between parallel valleys are uncommon (Col de Lhers, Col du Portillon). Despite some fairly thin, localised plateau icefield occurrences on summit surfaces such as at the Arres d'Anie and in the Aston and Carlit massifs, the Pleistocene icefield was thus by no means an icecap. The larger ice accumulation on the north side of the range nonetheless contributed to spill over to the southern side via a number of transfluence cols across the main divide, each situated at increasingly lower elevations from east to west (Col de Puymorens: 1917 m; Port de Bonaigua: 2072 m; Pla de Beret: 1870 m; Col du Pourtalet: 1795 m; Col du Somport: 1631 m), with an additional number of more minor divide breaches at higher altitudes.

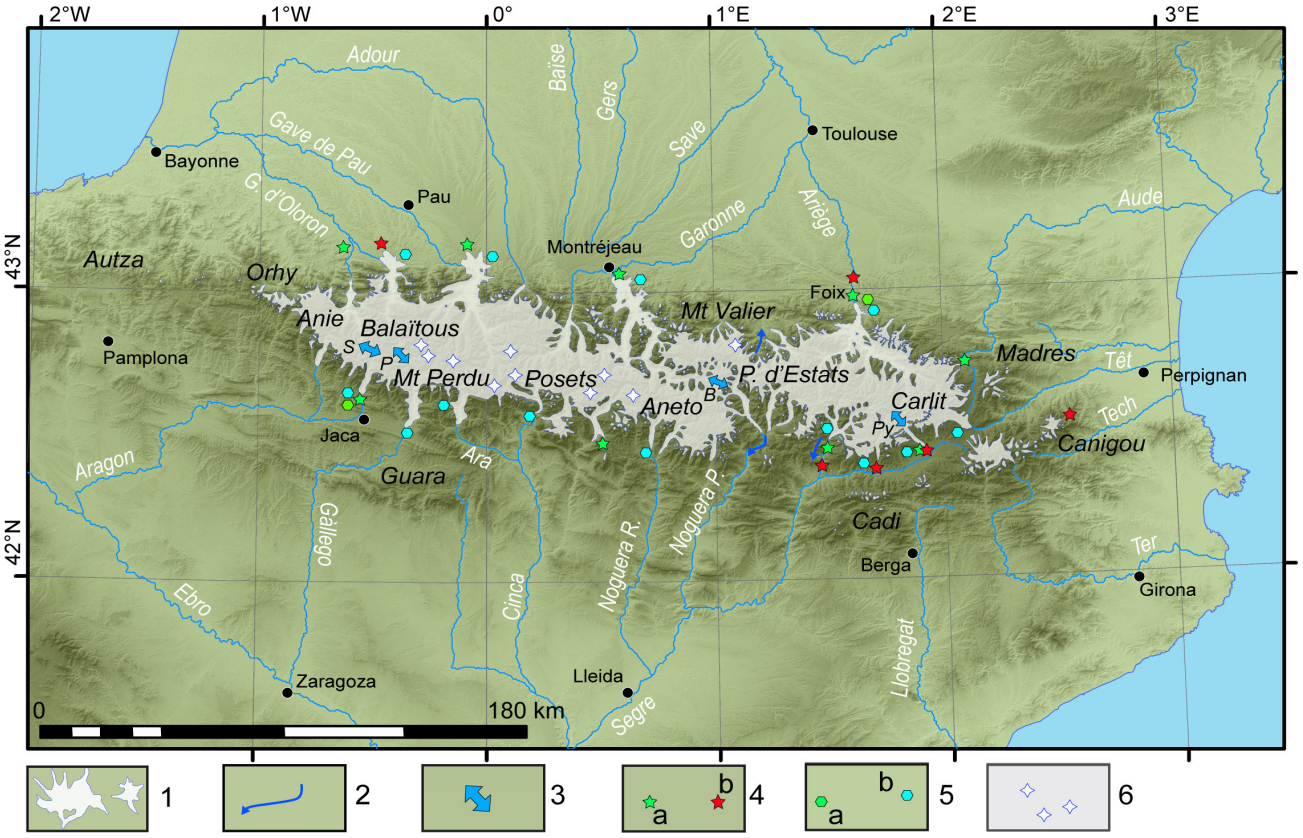

Figure 2. Glaciation and glacial deposits of the Pyrenees. Key to symbols and ornaments – 1: most extensive glaciation during the Late Pleistocene (numerous nunataks not shown); 2: possible Late Pleistocene maximum advance of some valley glaciers; 3: main transfluence cols between the north and south sides of the icefield divide; 4: pre-Late Pleistocene moraines and till occurrences – 4a: MIS 6 moraines (locally based on exposure ages); 4b: middle to early Pleistocene glacial till; 5: exposure-dated frontal moraines and ice-marginal deposits – 5a: MIS 6 frontal moraines (OSL- or 10Be-dated); 5b: MIS 4 to LGM frontal moraines (14C-, OSL-, or 10Be-dated); 6: massifs currently hosting residual glaciers (the population of massifs with a record of Little Ice Age glaciers is larger). After Calvet (2004), Calvet et al. (2011), and Delmas et al. (2022a, b, c).

The Iberian domain contained comparatively shorter and thinner (400–600 m) valley glaciers, with outlet glaciers terminating at elevations between 750 m and 940 m. Glacier lengths rarely exceeded 30 km. The Pallaresa and Valira trunk glaciers may have attained maximum lengths of 60 and 42 km, respectively, but mainly by virtue of the inputs from tributary valley glaciers that could feed into the main stem at points quite far down the trunk valley (Serrat et al., 1994; Turu et al., 2007; Turu et al., 2011; Turu, 2011).

The Late Pleistocene ELA rose rapidly southward to elevations above 2100–2200 m in the outermost massifs of the Axial Zone and Sierras Interiores, and to even higher altitudes in the case of south-facing slopes.

The glaciation gradient along the strike of the range was more gradual than across it. The icefield thinned eastward as a combined result of diminishing Atlantic moisture advection from the west and of the increase in aggregate sunshine hours under Mediterranean influence. Among the outlet glaciers along the northern mountain front, only the Gave de Pau at Lourdes and Gave d'Ossau at Arudy formed piedmont glacier lobes. The ELA was particularly low in the Basque Country (1100–1200 m; Viers, 1960). From there, it rose progressively along strike, reaching 1300–1400 m among the outermost massifs in the Ariège. The ELA attained 1600 m in the upper catchments of the Hers, Aude and Boulzane (Dourmidou massif), i.e., ~60 km from the Mediterranean coast. In the eastern Pyrenees, the greater fragmentation of relief resulting from Neogene extensional tectonics and relative aridity of the sheltered intermontane basins conspired to a confinement of glaciation to the most elevated massifs of the Axial Zone. Here, the ELA extended between 2000 and 2300 m, the valley glaciers were short (Têt: 18 km, Querol: 25 km) and never extended below the 1000–1500 m contour band. At these easterly longitudes, the icefield was often little more than a population of cirque glaciers (Fig. 3).

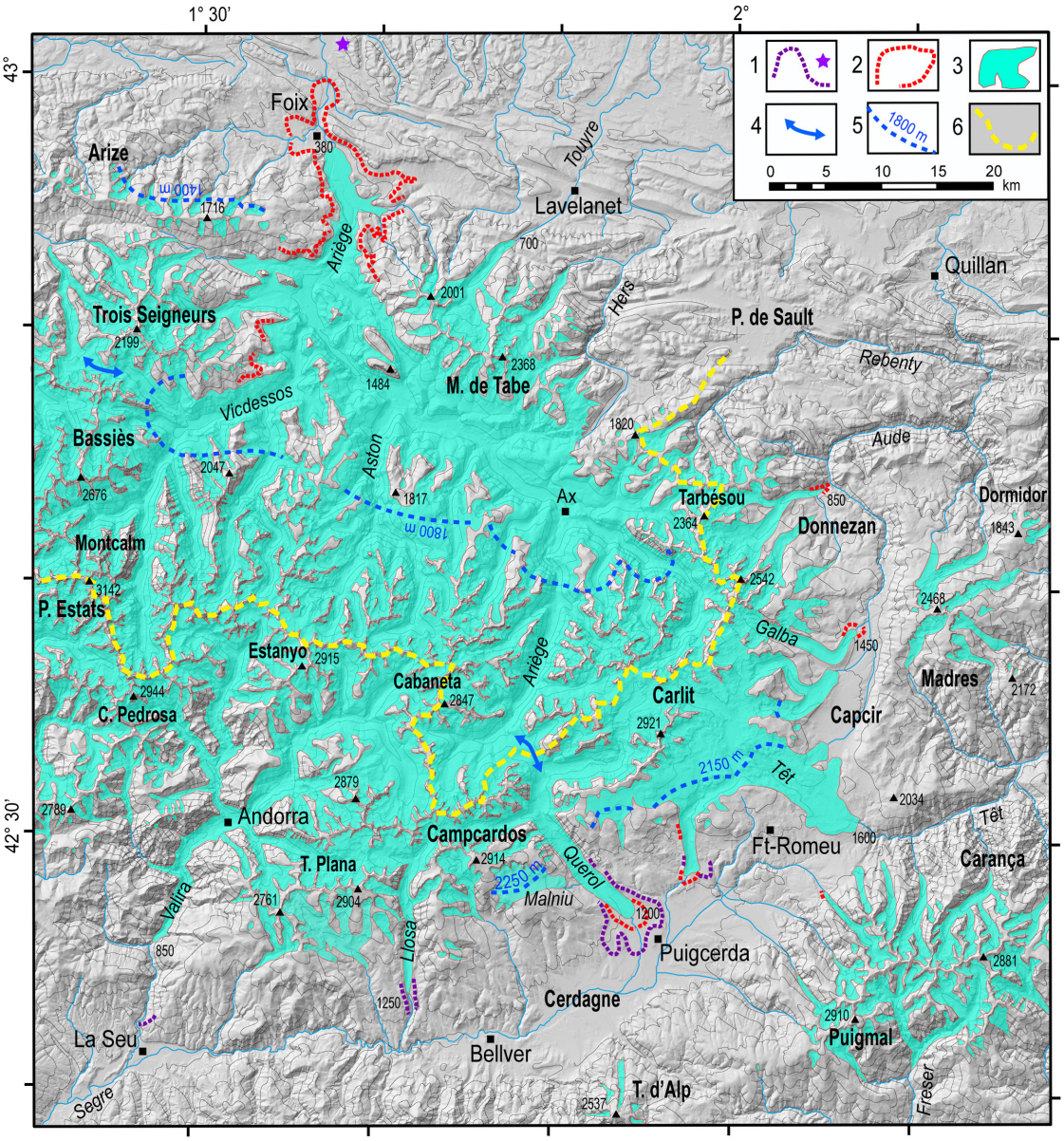

Figure 3. Extent of glaciation in the eastern Pyrenees (after Calvet et al, 2011; Delmas et al., 2011; Reixach et al., 2021). Key to symbols and ornaments – 1: early Middle Pleistocene deposits; star indicates isolated erratic boulders in lower Ariège valley. 2: mid to late Middle Pleistocene deposits (probably MIS 6). 3: Late Pleistocene deposits, here shown during the most extensive glaciation of that period. 4: Main transfluence cols. 5: Local LGM Equilibrium line altitude. 6: Drainage divide between Atlantic and Mediterranean catchments. 10Be-dated); 5b: MIS 4 to LGM frontal moraines (14C-, OSL-, or 10Be-dated); 6: massifs currently hosting residual glaciers (the population of massifs with a record of Little Ice Age glaciers is larger). After Calvet (2004), Calvet et al. (2011), and Delmas et al. (2022a, b, c).

These Quaternary glacial gradients were essentially an exaggerated version of present-day climatic contrasts, also reflected in the pattern of the modern winter snowline. It can thus be reasonably inferred that average climatic conditions and average atmospheric circulation patterns in the region remained similar throughout the Quaternary (Barrère, 1954; Taillefer, 1982; Calvet, 1996). These conditions include: (i) permanent air flow from the W to NW, bringing snow but also favouring its local redistribution over ridgetops, thereby supplying east- and southeast-facing cirques; (ii) the interference of Mediterranean air flow from the southeast, which is also a source of abundant snowfall in present-day conditions in the eastern part of the range; and (iii) the considerably greater dryness and warmth of the southern and eastern Pyrenees compared to anywhere else – with negative consequences on the thermal budget of glaciers in those areas.

The geomorphological legacy of Quaternary glaciation on Pyrenean landscapes and slope systems is widespread but not often intense. The glacial imprint is strongest in the cirque belt (Crest et al., 2017), which in some massifs displays characteristic arêtes and a few pyramidal peaks. In the eastern Pyrenees, however, the limited erosive power of the Pleistocene glaciers has, for example, failed to eradicate the erosion surfaces. Very deep mantles of saprolite, which at many places cover these elevated residuals of Neogene topography, have been preserved (Delmas et al., 2009). Most of the larger valleys nonetheless exhibit large bedrock steps, e.g., along the Ariège at Tarascon or at Les Cabannes. None of the wider glacial troughs are calibrated to a characteristic U shape; V-shaped gorge sections are frequent and even include entrenched fluvial meanders (such as between Ax-les-Thermes and Mérens in the Ariège). This relatively light erosional imprint of warm-based glaciers also explains the indecision among scholars as to the true terminal positions of valley glaciers in some V-shaped valleys such as the Noguera Pallaresa, Cinca, Valira, and Salat.

Chronology of glacial fluctuations in the Pyrenees

Pre-LGM chronology

Middle Pleistocene till exists in most outlet valleys of the Aquitaine foreland, whether stratigraphically beneath the Late Pleistocene till or slightly forward of Late Pleistocene terminal moraines (Synthesis in Delmas et al., 2022a). The earliest evidence of this was provided by the mapping and analysis of alluvial fill in limestone caves adjacent to ice-filled valleys. Depending on the ice thickness at each successive glaciation, certain cave levels would be supplied by glacifluvial deposits. When sandwiched between different generations of speleothems, the age of the gravel or varved silt units in the caves could be determined by U–Th dating the encasing calcite concretions. The Niaux–Lombrives cave system, which is situated at the junction between the Vicdessos and Ariège valleys, has in this way produced evidence of 4 glacial periods in the last 400 ka (Sorriaux, 1981, 1982; Bakalowicz et al., 1984; Sorriaux et al., 2016).

Producing a more detailed chronology of the last glacial cycle is still work in progress. The first evidence was obtained by 14C dating of ice-marginal lake sediments for the Late Pleistocene (Würmian Stage; Andrieu et al., 1988); and from caves, where U–Th dating of speleothems has placed the last glaciation between 90 and 20 ka (Bakalowicz et al., 1984). The most extensive glaciation was inferred from this evidence to have occurred during the first half of the Late Pleistocene, with deglaciation beginning at some time during MIS 3 (57–29 ka). Systematic OSL dating of deposits in the pro-wedge valleys (e.g., Lewis et al., 2009; Garcia Ruiz et al., 2013; Guerrero et al., 2018; Sancho et al., 2018); 10Be, 36Cl or 21Ne exposure dating at many sites across the range (Pallàs et al., 2006, 2010; Delmas et al., 2008, 2011, 2012; Turu et al., 2011, 2017; Palacios et al., 2015a, 2015b, 2017; Crest et al., 2017); systematic 14C dating (Turu et al., 2017); and Schmidt hammer proxy dating based on 10Be calibrations (Tomkins et al., 2018) have refined the chronology substantially and bring out some important components of regional variation. Note that, in the case of cosmogenic exposure ages, some allowance concerning apparent age discrepancies must be made for uncertainties relating to rock shielding by snow cover, and also for the older ages published before 2015 because the physical calibration of nuclide production rates has since been officially revised to lower values.

LGM and Post-LGM deglacial chronology

At the time of the LGM, a paradoxically reverse climatic contrast between the eastern and western Pyrenees appears to have prevailed: in the eastern Pyrenees, glaciers advanced at some places as far as their earlier (MIS 4) maximum positions, with the two moraine generations often bunching into a tight single mass in the case of the Têt, Querol, Malniu, Duran, Llosa, Aranser, and Noguera Ribagorçana glaciers. The LGM ice front stood 7 km upstream of the Local LLGM position in the Ariège valley, and at most 9 km in the Valira. In the west (Gàllego, Aragon, Ossau), the positions of LGM frontal moraines are unknown but LGM glaciers were probably also several kilometres shorter than their most extensive MIS 3/4 predecessors because of colder and drier conditions in the nearby Bay of Biscay than in the western Mediterranean (Delmas et al., 2011, 2022a, b, c).

New data have also provided constraints on the positions of LGM glacier fronts in the Esera and Ossau valleys (Reixach, 2022). Exposure ages obtained from the LLGM moraine at Chía (n = 18) and from the Cerler tributary glacier (n = 3) show that the LLGM position was attained several times during the Late Pleistocene by the fluctuating Esera glacier (Castejón de Sos and Benasque catchments), particularly during the LGM (19.0 ± 1.1 ka), during MIS 3 (35.2 ± 3.3 ka) and perhaps also MIS 5a-d (96.4 ± 10.3 ka; Reixach, 2022). The LLGM in the Ossau valley is defined by about ten sharply delineated frontal moraines around Buzy. These tend to bunch up and blur into a smaller population of moraines on the edges of the Arudy basin and upstream of the successive water gaps in the valley (where the Bilhères and Castet kame terraces are also positioned). These stadial moraines have benefited from exposure-age constraints provided by 22 10Be and 36Cl samples. Results show quite a large scatter of age values, but the oldest ages obtained, which are arguably the most relevant given the criteria and principles of exposure dating, suggest that this stadial position is compatible with the LGM and the end of MIS 3 (Reixach, 2022).

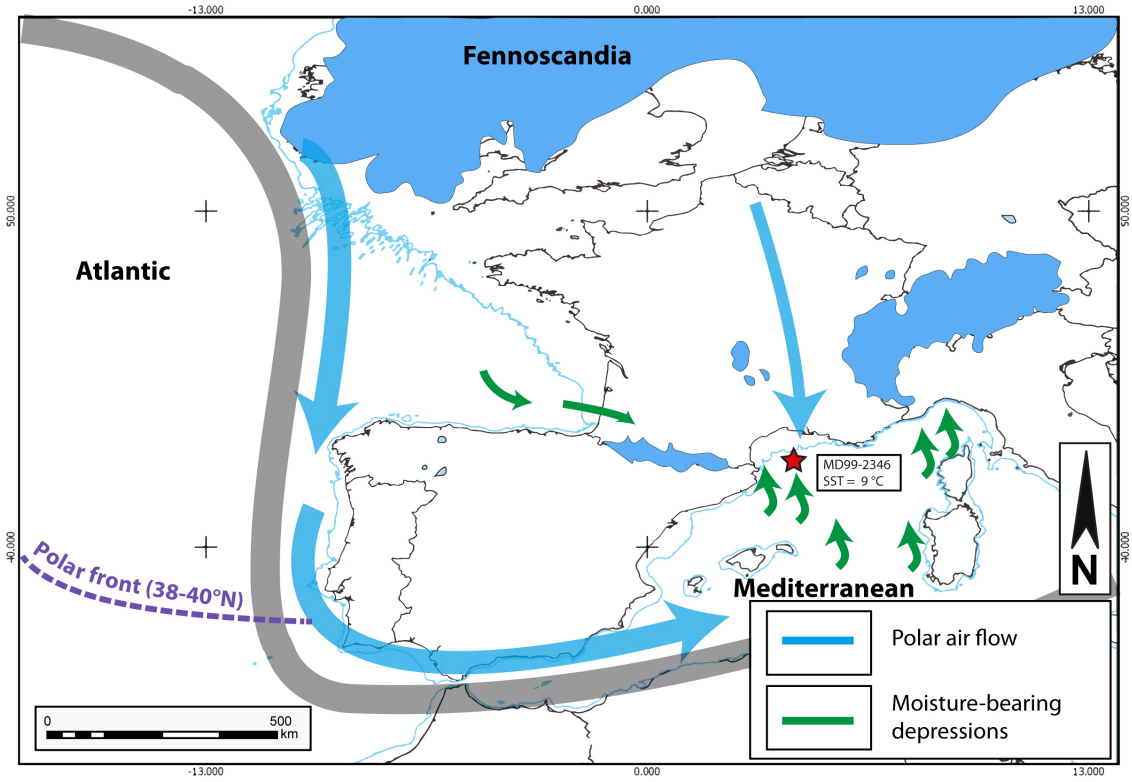

Figure 4. Prevailing air streams during the LGM over western Europe. Position of the Polar Front calibrated on the extent of sea ice in the Barents Sea (Mörner et al., 2020). Position of the Polar Jet in winter (Dec.-Jan.-Feb.) based on the CCSM4 climate model (Merz et al., 2015). Outline of LGM coastline (light blue) after GIS data from the Collaborative Research Centre (CRC) 806 (Zickel et al., 2016). LGM sea-surface water temperatures in the Mediterranean established from planktonic foramnifera assemblages (core MD99-2346, Melki et al., 2009). Extent of Fennoscandian ice sheet after Hughes et al. (2016).

These new results from Ossau and Esera entail a reconsideration of LGM atmospheric circulation patterns previously inferred from another population of valleys (Delmas et al., 2011, 2022a, b, c), as they appear to validate the existence of Atlantic weather systems sweeping along the northern mountain front, nonetheless weakening and generating less precipitation as they travelled eastward. In a LGM context where the Polar Front was positioned ca. 38°N, cold air masses would also detach from the Arctic air masses and travel from north to south, thereby promoting opportunities for convective instabilities over the Mediterranean and deflecting weather fronts to the southern mountain front of the Pyrenees, with precipitation reaching into Iberia at least as far as the Maladeta massif and its Esera valley (Fig. 4).
Finally, deglaciation appears to have been almost universally rapid at the end of the LGM, particularly in the eastern Axial Zone where the valley glaciers had receded all the way to the cirques by 20 ka (Delmas, 2005; Delmas et al., 2008, Delmas, 2015). A major glacial readvance during the Oldest Dryas, ca. 18 ka and persisting until 16–15 ka, has been documented. It produced glaciers ~20 km long in the upper Ariège, 7 km long in the Bassiès valley, 5 km in the Têt, 6 km in the Noguera Ribagorçana, 4 km in the Ésera, and 9 and 15 km, respectively, in two tributary valleys of the upper Gàllego catchment. By the end of the Allerød Interstadial (~13 ka), ice had disappeared even from the highest ranges of the eastern Pyrenees, with evidence of the tree line having risen to above 1800 m in the NE ranges of the orogen by that time (Reille and Andrieu, 1993). The last documented readvance during the Younger Dryas did not descend below the 2000 m contour in the eastern Pyrenees, remaining confined to the cirques and uppermost valley areas. Even at that time, the tree line stood around 1300 m. Many cirques of the eastern ranges became populated at this time with rock glaciers.

THE ROUTE

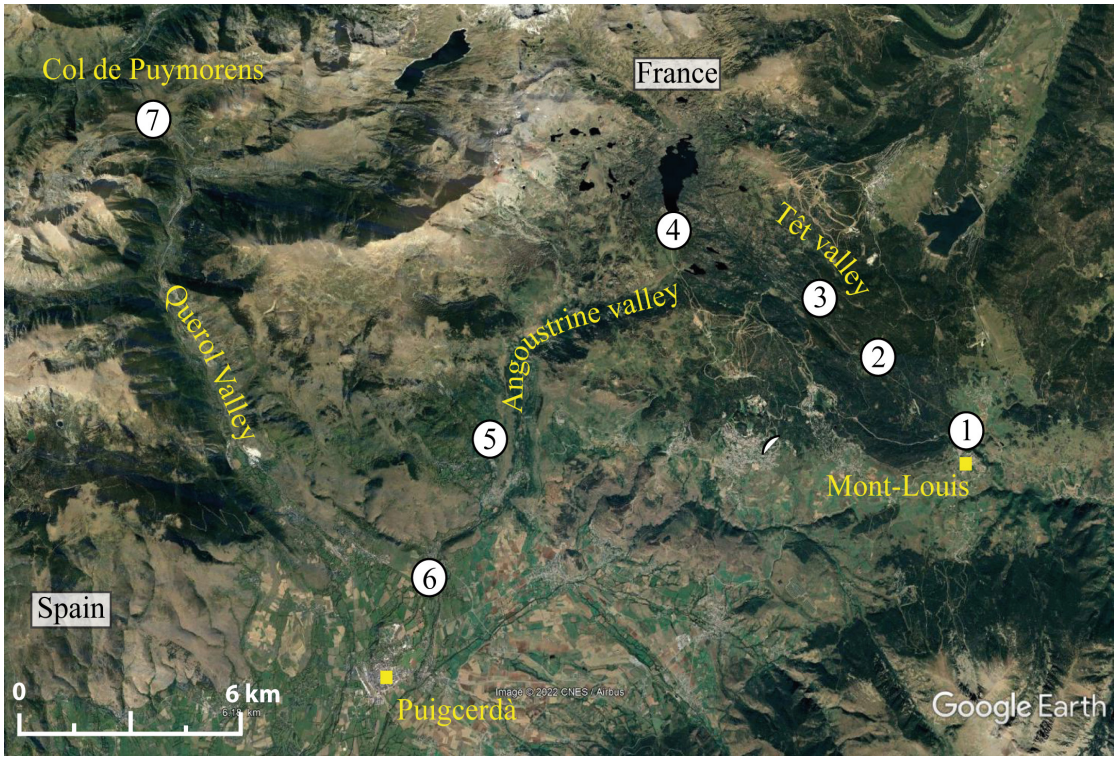

Figure 5. Itinerary of the field trip Têt - Angoustrine – Querol - Col de Puymorens.

1 Mont-Louis and the Late Pleistocene terminal moraines of the Têt valley.

Chronology of the local Last Glacial Maximum in the Eastern Pyrenees. Relative stratigraphy and surface exposure ages on the glacial sequence of deposits.

During the Late Pleistocene glaciation, the Local LGM (LLGM) Têt glacier was only 18 km long. As such, it was nonetheless the largest among the valley glaciers supplied by the Carlit icefield, which covered the massif between elevations of 2200 and 2400 m (Fig. 6) while leaving a few conspicuous nunataks rising above it (Viers, 1961, 1968; Delmas, 2005, 2009; Delmas et al., 2008). No record of Middle Pleistocene glaciations have been identified in the vicinity of the Mont-Louis terminal moraine system, either because their vestiges are buried beneath the mass of more recent debris, or because their (speculative) position farther out near the Têt knickzone has made them vulnerable to stripping and destruction. The chronology of the Late Pleistocene glacial cycle in the Têt valley has benefited from a large number of 10Be exposure ages from moraine boulders and glacially-polished bedrock steps (Delmas et al., 2008; Delmas, 2009). In this fieldguide, previously published exposure ages are updated on the basis of a uniform protocol incorporating revised decay constants, nuclide production rates, and corrections for snow cover (Reixach et al., 2021, Reixach, 2022). The LLGM frontal moraine at Mont-Louis (Fig. 7) is perfectly preserved, 60 to 90 m high. Its ridgetop actually consists of two to three elementary but closely bunched arcs. A 10Be exposure age of 24.3 ± 3.8 ka on a boulder embedded in this frontal moraine indicates that the LLGM Têt glacier was synchronous with the global LGM. Another sub-population of less imposing, but equally fresh, moraine occurs ~900 m further down valley below a scatter of detached houses west of Mont-Louis (Les Artigues), as well as on the plateau to the east of the D618 opposite the parking area (spot elevation: 1633 m). These less conspicuous frontal ribbons could be vestiges from the earlier part of the Late Pleistocene glacial cycle, as suggested by a calibrated Schmidt hammer proxy age of 40.9 ± 1.1 ka from Les Artigues (Tomkins et al., 2018).

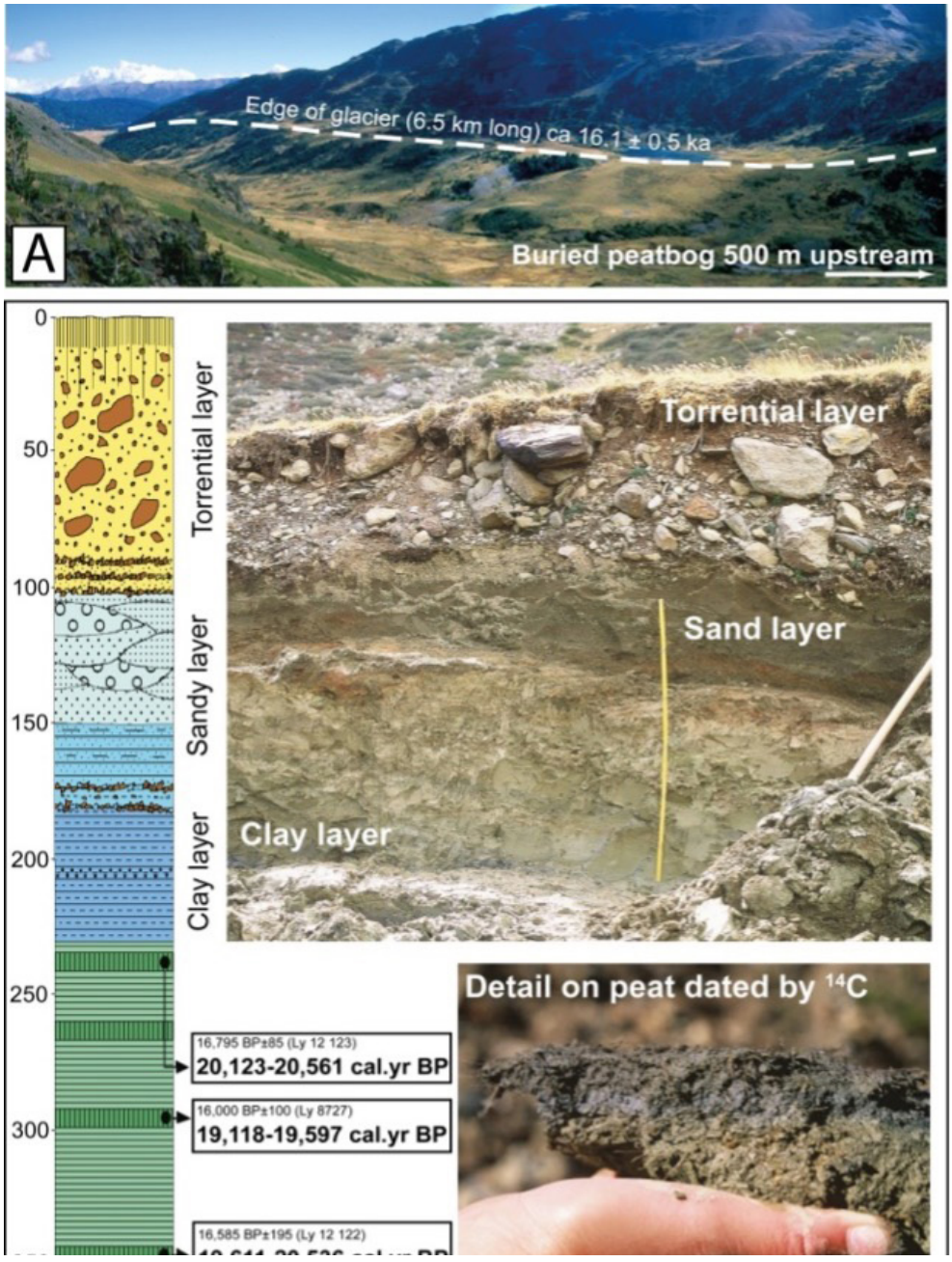

Figure 6. Glacial and glaciofluvial outwash deposits, with associated ages in the Têt and neighbouring catchments. 14C ages after Delmas (2005). 10Be exposure ages for sites I/CAL and P/CAC after Crest et al. (2017); all others after Delmas et al. (2008). Schmidt-hammer exposure dating (SHED) results after Tomkins et al. (2018). Geomorphological map (landforms and deposits) after Delmas (2005). Digital elevation data source: Institut Géographique National, ground resolution: 20 m.

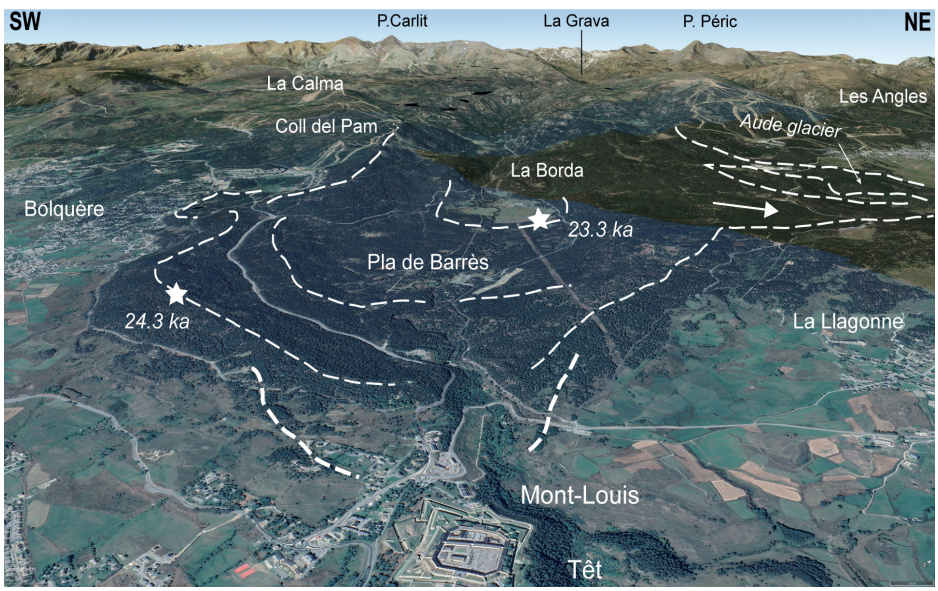

Figure 7. Late Pleistocene frontal moraines of the Têt glacier at Mont-Louis. Oblique aerial view of the Têt frontal moraine sequence, denoting the outlines of a piedmont lobe (CNES/Airbus imagery, here provided by Google Earth); note glacier diffluence towards the Capcir Basin.

A cut in the deposits along the D60, ca. 600 m to the west of the parking area (42°30'55.1"N, 02°06'24"E), reveals the internal facies of this mostly unweathered Late Pleistocene till (Fig. 8): ranker-type soil; grey to light beige silt- and sand-rich matrix containing less than 2% clay-sized particles; 50% of entirely fresh granite pebbles, with another 40% displaying oxidation features and vulnerable to hammering, and the remaining 10% characteristically friable – the latter exclusively consisting of granodiorite and biotite-rich monzogranite.

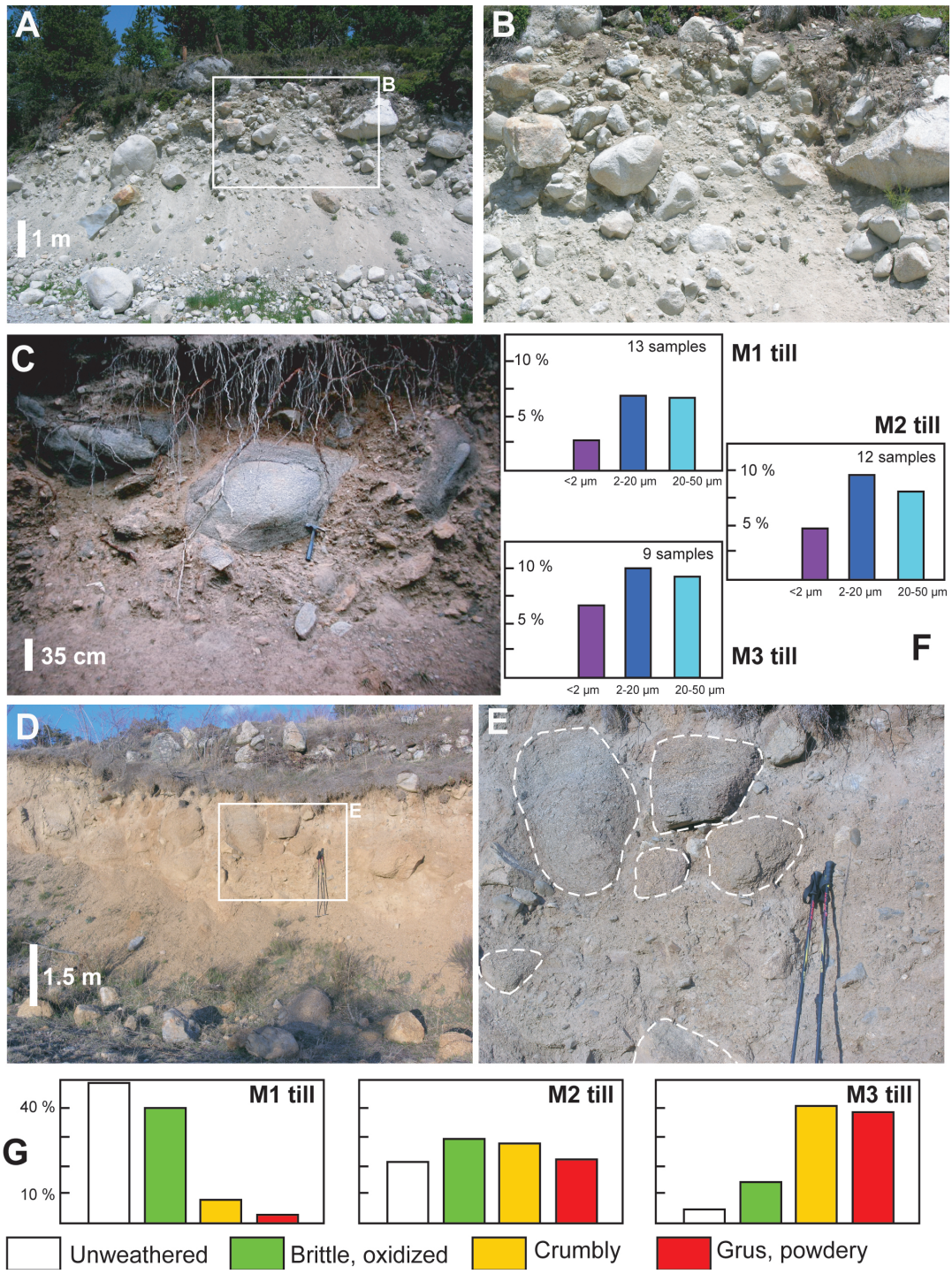

Figure 8. Itinerary of the field trip Têt - Aspects of the three generations of glacial depositional material in the eastern Pyrenees. A, B. Younger generation, M1 (Late Pleistocene); section through frontal moraine near Mont-Louis, D60 roadside. C. Intermediate generation, M2 (mid to late Middle Pleistocene); boulders are spheroidally weathered on the outside, but with a fresh core; Esposolla section. D, E. Older generation, M3 (early to mid-Middle Pleistocene); boulders are weathered to the core; Escaldes reservoir section. F. Proportion of matrix fines among the three till generations. G. Proportion of weathered clasts, and weathering intensity among granite pebbles 5–20 cm in length. The data are valid for till deposits from the Cerdagne and Capcir basins.

Driving up the Têt glacial stairway offers a chance to observe successive frontal moraines representing post-LLGM recessional standstills. These have been chronologically named Barrès (near the campsite), and La Borda (1 km upsteam). The Barrès stadial deposits have not yielded a robust age record, but the Borda moraine has provided three 10Be exposure ages of 20.4 ± 0.4, 21.6 ± 2.7 and 23.3 ± 3.3 ka. Stop at La Borda parking area and climb to the top of the rock bar (1690 m) situated just above the farm buildings.

2 Panoramic view of La Borda moraine and the Têt glacier terminal complex. Extent and chronology of the first stages of the post-LGM deglaciation in the Têt valley. Data on ELA fluctuations during the Late Pleistocene glaciation and the Last Glacial to Interglacial Termination in the Têt valley

The top of this granitic bedrock step provides a good vantage point from which to view the sequence of moraines, starting from the much taller LLGM terminal moraine at the far end of the valley to the smaller recessional occurrences in the middle ground (Fig. 9). The Borda moraine is covered by forest and closes off the large expanse of meadows and peatbog that currently fills the glacial rock basin. A 4.3 m sediment core from the peatbog has also sampled underlying lacustrine sediments. These have been chronologically tied to the LGIT on the basis of their pollen assemblages, and the '15,000 event' (Reille and Lowe, 1993), now calibrated to ~18 ka, ties in with the transition between GS2-1b and GS2-1a in the reference Greenland stratigraphy (Rasmussen et al., 2014).

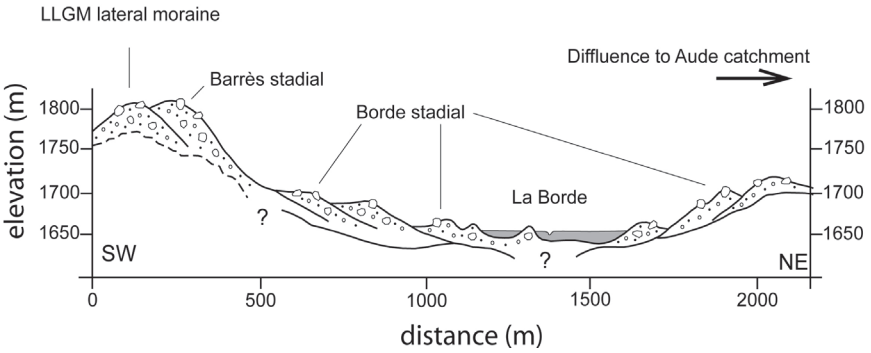

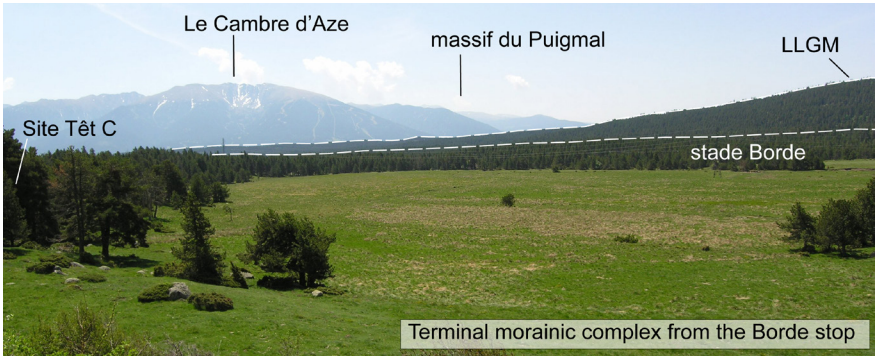

Figure 9. Têt terminal moraine complex around la Borde. A – La Borde glacial rock basin, looking south. B – Cross-section through the Têt terminal moraine complex (section strikes across the glacial trough axis).

The road next rises up a long break in slope where the glacial valley constricts into a gorge less than 300 m wide. Note the dominant NW–SE fracture pattern (Bollosa Fault) across this glacially-polished and plucked bedrock step. Stop as you enter the Avellans rock basin (spot elevation: 1706 m; avellan: 'hazel' in Catalan). Here you can ascend the 'Rocher des Bouillouses' (summit: 1755 m), also a rock-climbing spot, by skirting round to its more gently inclined north-end rock face through the woods. Once at the top, aim for the south end (42°32'25.4"N, 02°03'25"E).

3 Summit of Avellans bedrock step. Inherited exposure ages on bedrock steps and implications for Late Pleistocene glacial erosion rate.

The imprint of glaciation on the pre-Quaternary valley morphology appears modest compared to the impact of the tectonics-driven fluvial knickzone below Mont-Louis. The light touch of glacial denudation in this catchment (see Box 1) is confirmed by 10Be exposure ages on several bedrock steps that are much older than the LLGM.

Estimates of Late Pleistocene glacial erosion rates in the Carlit massif:

The SE-facing flank of the Carlit massif has provided constraints on spatial and chronological variation in depths of glacial erosion during the Late Pleistocene (Delmas et al., 2009). The unique advantage of this catchment is that the frontal and lateral moraines are remarkably well preserved in the landscape because the glaciers were contained within low-energy environments such as the Carlit plateau, the Cerdagne Basin, and the Capcir Basin. These elevated intermontane base levels, all situated above the major fluvial knickzones of the area such as the Têt gorge below Mont-Louis, the Segre canyon and the Aude gorges, have accordingly undergone comparatively limited postglacial denudation. The detailed chronology of glaciation in this area has been obtained from 10Be exposure dating, locally aided by 14C dating of peat deposits adjacent to glacial landforms. Three chronostratigraphic units have been reconstructed on that basis: (i) the Terminal Unit, which corresponds to moraines produced during the last most extensive glaciation, or local last glacial maximum (LLGM); the (ii) Recessional Unit, which collectively refers to the succession of moraines generated by receding glaciers between the LLGM and ~20 ka cal BP; the (iii) Cirques Unit, which represents the final glacial standstill (or local stade), by the end of which (i.e., by the end of the LGIT) the icefield had shrunk to a collection of cirque glaciers situated above 2400 m.

By dividing the total volume of moraine preserved in the Terminal and Recessional units by the surface area of the glaciated catchment at each standstill (supraglacial nunatak areas included), it was possible to estimate mean Late Pleistocene landscape denudation during each of these intervals. Given its coarse-grained texture (boulders, cobbles), debris angularity, and openwork fabric, the Cirques Unit was mainly supplied by cirque-wall rather than cirque-floor material. This youngest unit consequently provides a quantitative estimate of headwall recession rather than of basal erosion. Results (Delmas et al., 2009) show that denudation was ~10 times greater during the shorter Recessional period (0.6 mm/yr) than during the protracted glacial advance and LLGM (0.05 mm/yr). This is ascribable to contributions from paraglacial processes, which in the Carlit massif were quite active during the post-LLGM deglaciation. The glaciers at the time were mostly evacuating debris produced in the thinning accumulation zone as the ELA gradually rose to elevations in excess of 2200 m (this contour coincides with the low-gradient floor of pediment P1). Denudation rates remained high during the LGIT given that the Cirques Unit has yielded headwall recession rates of 0.1–0.3 mm/yr in granite and 0.6–1.2 mm/yr in schist (Fig. 10). These figures confirm the theory according to which cirques grow faster during deglacial and interglacial periods rather than during glacial maxima (Cook and Swift, 2012; Crest et al., 2017).

In summary, Late Pleistocene denudation achieved a catchment-averaged minimum denudation depth of 4 m (basic calculation using the total volume of moraine currently preserved in the SE Carlit landscape); this value should be doubled in order to allow for the evacuation of suspended load in streams. Despite the inevitable uncertainty around such estimates, cold-climate denudation calculated on the basis of these benchmark values and cumulated over the last ten or so 100,000-year Milankovitch cycles has been modest, and mainly exerted on cirque and glacial-trough walls. The impact of Quaternary glaciation on the landscape, at least compared to wetter areas of the central Pyrenees more directly exposed to Atlantic weather systems, has thus remained limited. Accordingly, this explains why deep weathering profiles have been widely preserved even under till at elevations impacted by Pyrenean glaciation (Fig. 10), and partly also why relict Neogene landforms such as high-elevation erosion surfaces are still so prominent in the landscape.

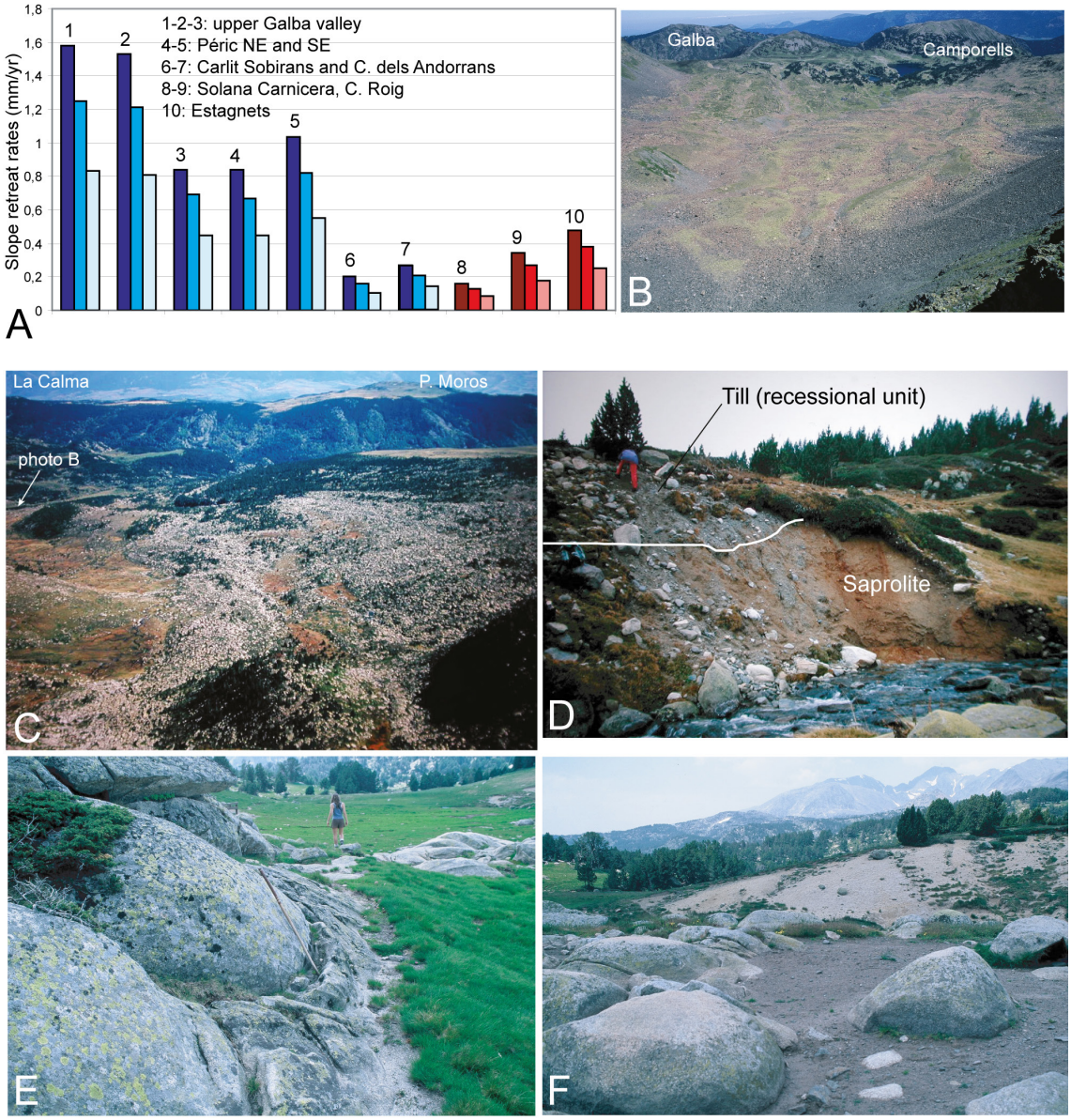

Figure 10. Aspects of the glaciated landscape in the Carlit massif. A. Post-LGM cirque headwall recession rates. Blue bars: cirques in schist; red bars: cirques in granite. The colour gradient represents headwall recession rates calculated for each cirque on the basis of three different density ratios between the debris and the bedrock (V63, V50 and V33, respectively). Cirques are numbered from NE to SW; units 6 and 8 coincide with a mixed lithology. B, C. Cirque moraines (bouldery facies: ablation till). B. La Coquilla cirque, in schist, NE of Pic Péric. C. Soccarade moraines (granite boulders), at the base of Pic de Col Rouge. D, E, F. In-situ saprolite and weathering front on pediment P1, covered by subglacial till, evidencing the weakness of Quaternary glacial erosion. D. Section through rubified saprolite at Els Forats. E. La Balmette bedrock step, barely stripped of its spheroidally weathered granite envelope. F. La Balmette weathering front with corestones, covered by recent till further in the background (after Delmas, 2009 and Delmas et al., 2009, merged and modified).

An example is the summit of the Avellans rock mass (Fig. 11A, B), which has yielded an exposure age of 21.3 ± 3.6 ka, consistent with the deglaciation chronology, whereas perfectly preserved glacial polish on the flank of the rockface documents an exposure age of 74.0 ± 7.2 ka. This implies extremely limited bedrock erosion at this location during most of the Late Pleistocene glacial cycle (the anomalously old age is a composite of 10Be atoms acquired since the last deglaciation of the glacially-polished bedrock step, i.e., after the LGM, but also of a preserved contingent of atoms produced prior to the Late Pleistocene, i.e., during MIS 5e). Other sites also record varying levels of nuclide inheritance, with anomalously old ages likewise indicating only partial resetting of the radiometric clock. They also, therefore, testify to shallow bedrock denudation depths during the Late Pleistocene – too shallow to attain depths of bedrock where the 10Be radiometric clock would be entirely reset (i.e., much less than 3 m).

Similar age dispersal has been observed at other bedrock steps, where a sensitivity test was applied by sampling various points at the top and on the front or sloping lateral face of the glacially-polished bedrock steps (Fig. 11C,D). The bedrock step at Les Bouillouses (1995 m), for example, yielded an age of 40.5 ± 4.6 ka, clearly suggesting nuclide inheritance at that location. Higher up in the catchment, the Sobirans step (2270 m) on the Carlit plateau likewise provided three ages of 22.3 ± 3.0 ka, 27.2 ± 4.0, and 27.3 ± 4.5; and the uppermost step of the glacial stairway, in the Grave cirque (2380 m), records one age at 27.7 ± 1.4 ka among other much younger results (Fig. 11D), suggesting a strong component of short-range spatial heterogeneity in subglacial erosion.

The road continues across the sediment-filled Avellans glacial rock basin. At Avellans, the glacial trough is deeper (300 m) than further down the valley. The frontal lobe of the corresponding recessional moraine is positioned at the top end of the Avellans basin floor. The road next winds along the edge of the lateral moraine and finally rises up the large bedrock step at les Bouillouses. The latter is probably a glacially-retouched fluvial knickzone, similar to (but smaller than) the one previously encountered below Mont-Louis. The dead-end road terminates at Bouillouses dam.

Figure 11. Nuclide inheritance on ice-polished rock-bar surfaces in the Têt glacial trough. A. Avellans bedrock step, also a rock-climbing spot. B. Detail of ice-polished rock exposure sampled for 10Be dating, Avellans rock outcrop. C. La Grava bedrock step (upper site: 2350 m). D. Detail of exposure-dating sample locations, La Grava (upper site).

4 Panoramic view from Lac des Bouillouses (La Bollosa). Very early post-LGM deglaciation of the upper Têt valley (Grave catchment).

On the west side of the valley, the dam rests against the lateral branch of a recessional moraine; it joins its frontal lobe ~500 m further down the valley. The impounded reservoir fills a glacial rock basin mostly containing postglacial alluvium, and it was still blanketed by peat at the time of dam construction. To the west, the extensive Carlit plateau is a knock-and-lochan landscape, i.e., it was partly covered by Pleistocene plateau ice, unevenly scoured, and is dotted with variously sized lakes. To the north, the Camporells plateau is also a vestige of middle Miocene pediment (Fig. 12).

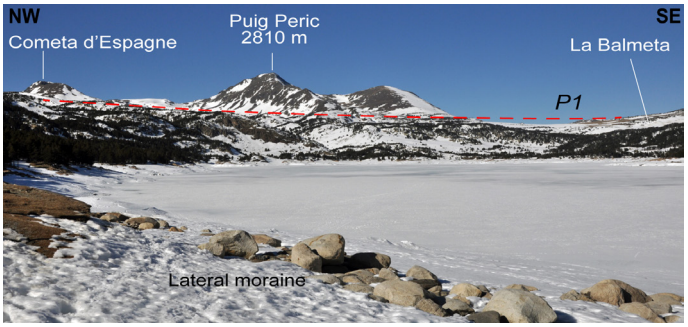

Figure 12. Bouillouses Reservoir (La Bollosa) in winter (frozen lake), looking north.

Rising above it, the Puig Carlit and Puig Peric rock masses are Cenozoic inselbergs or monadnocks, lightly retouched by cirque glaciation during the Pleistocene. Off to the south, the Angoustrine glacial trough previously encountered is a dry valley, its drainage having been beheaded by the Têt River in the vicinity of Avellans knickpoint – perhaps as recently as the LGIT and in relation to the massive recessional moraine accumulation situated just below Bouillouses dam.

Upper Têt (Grava) glacial valley (5 hours walk return)

This catchment-head valley provides good opportunities for observing a closely-spaced succession of lateral and frontal moraines generated by fluctuating glaciers. At the bottom end of the Grava valley, a double ribbon of left-margin lateral moraines located between 2200 and 2100 m marks out the past existence of a 6.5-km-long glacier, its tip located around 2020 m. After walking another 1 km up the valley, you will encounter a frontal moraine ca. 2050 m produced by a shorter glacier. Still further by another 2 km, you will pass three other frontal and lateral moraines, in this case all generated at a time when glaciation was confined to the cirques, with successive glacier fronts at 2150 and 2160 m. 10Be and Schmidt-hammer exposure ages on boulders embedded in these frontal and lateral moraines indicate 16.1 ± 0.5 ka for the 6.5-km-long trunk glacier, and 14.5 ± 1.9 ka and 12.4 ± 1.9 ka for the two cirque glaciers terminating respectively at 2150 and 2160 m. On that basis, the older stadial position correlates with the Oldest Dryas, and the younger positions with the Younger Dryas or earliest Holocene (9.4 ± 0.6 ka Schmidt-hammer age for the upper ridge ~2200 m, Fig. 13; Tomkins et al., 2018; Reixach et al., 2021). A radiocarbon-dated fossil peatbog (~20 ka cal BP) situated ca. 2150 m a.s.l. on the upper Grava valley floor suggests that the three LGIT stadial deposits listed above were generated after an interval of pronounced deglaciation in this valley segment, thus allowing the peat to develop in a proglacial position before subsequent glacier readvance (Fig. 13). This peat-forming event highlights how fast post-LGM deglaciation of the SE Carlit massif occurred. This situation is at least partly ascribable to the hypsometry of the glaciated catchment, which contained extensive plateau surfaces. When contained within the accumulation zone, such as during the LGM, these plateau surfaces could host volumes of ice large enough to feed several valley glaciers 15 to 20 km long, such as the Angoustrine, Têt, and Vallsera. Any small upturn in palaeotemperatures, such as occurred after the LGM, would raise the ELA, and even a small increment would drastically reduce the size of the accumulation zone and hasten the retreat of those valley glaciers far back into the cirque zone.

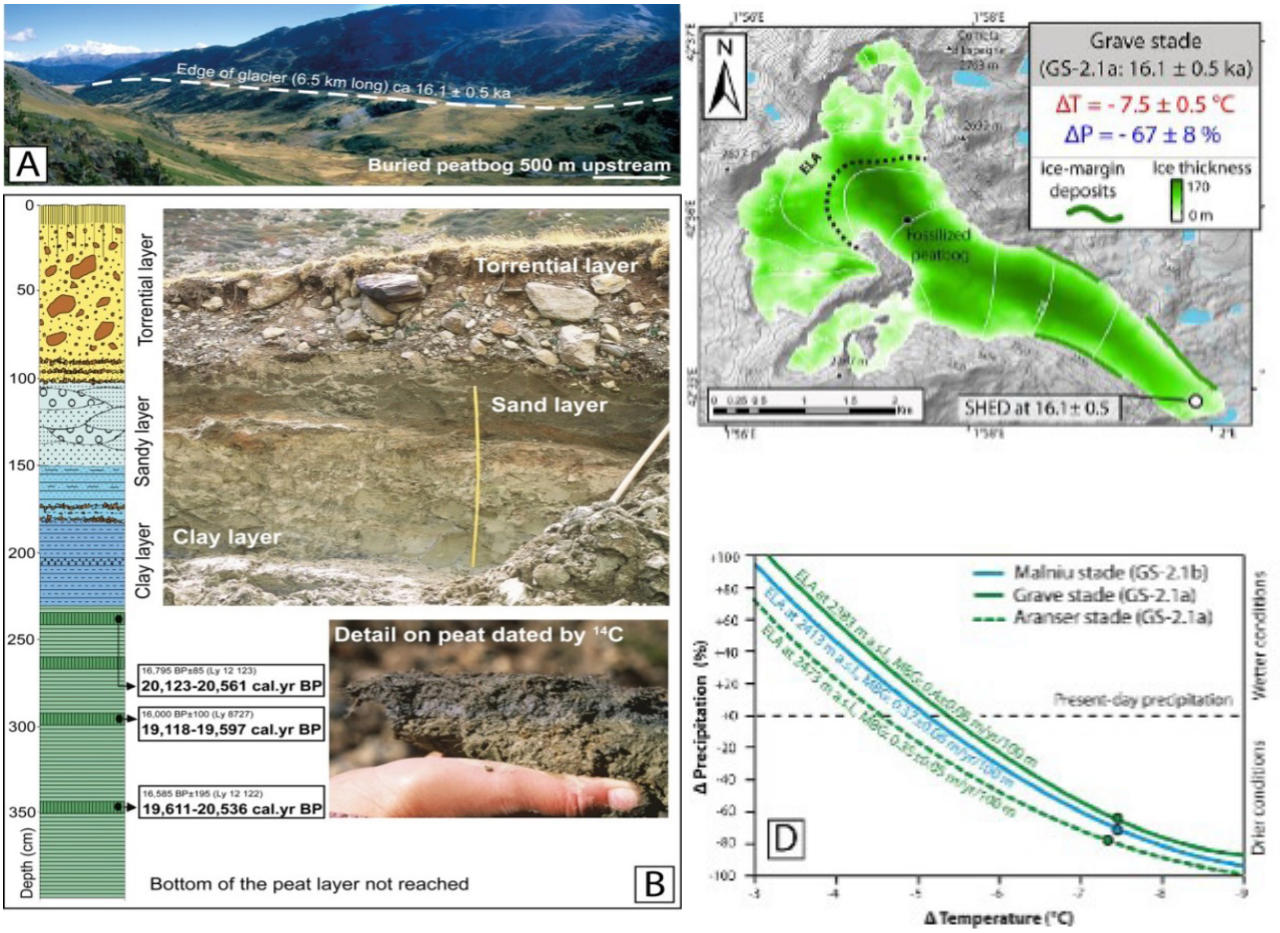

Figure 13. Post-GLGM deglaciation and early LGIT glacier re-advance in the Grave valley. A- Lateral moraine, legacy of the GS-2.1a glacial readvance in the Grave/upper Têt valley. B- Radiocarbon ages and stratigraphy of the buried peat bog and lacustrine, deltaic, and high-energy, poorly sorted fluvial deposits. After Delmas (2019) and Reixach et al. (2021).

5 Les Escaldes: stratigraphy of ancient saprolite and moraines. Angoustrine and the Middle to Late Pleistocene glacial deposits in the Cerdagne Basin. Section on a weathered lateral moraine ascribed to a Middle Pleistocene glaciation. Picnic with a panoramic view on the Cerdagne Basin. (40 min walk return)

A good section through thick saprolite containing corestones appears at the foot of the slope (Fig. 14). The tor and boulder field on the catchment slopes of the Coma Ermada where exposed after stripping of this regolith mantle. This site became the focus of intense stone quarrying from the late 19th century to the 1950s, and its products contributed to many buildings, walls, bridges and railway viaducts throughout this region. A few tors emerge here and there, but the saprolite overall drapes the entire hillslope as far as a track leading to a water reservoir. At this point (42°29'34.4"N, 01°57'18.2"E) you will encounter the first occurrence of ancient till capping the saprolite (Fig. 14). The till contains granite boulders often 1 m in diameter, characteristically rotten to the core, in association with pebbles of dark schist and hornfels often displaying striation marks. This patch is the oldest among three local generations of glacial deposit which were inventoried (Fig. 14), classified, and regionally correlated on the basis of their weathering attributes (Calvet, 1996). Based on systematic counts of granitoid clasts and a number of laboratory analyses, the attributes of this older generation of deposits are as follows: 7% of clay-sized fraction in the matrix, 80% of granite pebbles intensely weathered, 5% still unweathered.

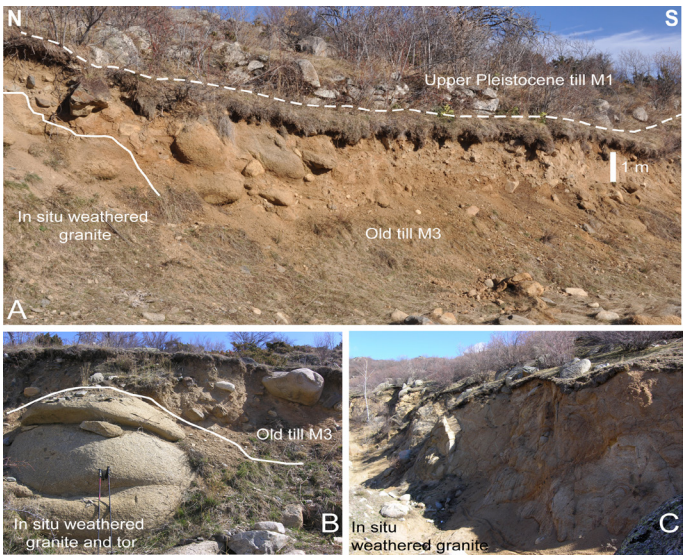

Figure 14. Exposures at Les Escaldes hospital. A Deeply weathered ancient till. Exposure near the water tank. B Granite tor, initially partly exhumed and subsequently buried by the till. C Deep grus at slope base; section ~ 10 m high

The till deposit is itself overridden by the right-margin moraine of the Late Pleistocene Angoustrine glacier, from which you can gain a more commanding view of the area. The stratigraphy overall clearly indicates that (i) the saprolite is pre-Middle Pleistocene, and probably mostly pre-Quaternary; (ii) the successive glaciers merely covered the saprolite without energetically ploughing into it or stripping it. This evidence corroborates conclusions previously drawn at Stop 3 (Aveillans) concerning the relative infirmity of glacial erosion in these transitional Mediterranean mountain environments where, additionally, the mountain hypsometry is attenuated by the elevated base levels of Cerdagne and Capcir and by the extensive occurrence of low-gradient topography in the glaciated catchments.

6 Ur–Llaurà, a deep section into the elevated alluvial deposits of Puigcerdà.

Middle and Late Pleistocene glacial and glaciofluvial outwash system of the Querol valley. Extent and chronology of three generations of ice-margin deposits based on surface exposure ages, vertical 10Be profiles and burial dating.

This abandoned gravel quarry face, now converted to a roadside rest area, has deteriorated substantially over the years (for comparison, Fig. 15C, D shows the state of the quarry face in 1984) but still displays some of its key features (Fig. 15A, B). The 30 m vertical exposure consists of two types of deposit resting unconformably on the tilted Vallesian beds (Unit 1, southerly dip, i.e., towards the Cerdagne Basin depocentre), which are faintly distinguishable in the north corner of the section. The base of the overlying sequence (Unit 2) is a high-energy deposit (rolled cobbles, imbricate structures, ochre sandy matrix). The upper part (Unit 3) is glacial till (abundant clasts of fine-grained, glacially striated grey schist, beige to grey silty sand matrix). These are the remains of a frontal or left-margin lateral moraine of the Querol glacier. The entire sequence is deeply weathered, with many granite boulders rotten to the core. The shallowest levels are enriched in quartz, quartzite, and quartz phyllite debris displaying thick weathering rinds. The colloidal fraction (fines) in these levels represents, on average, 7 to 8% (compared to 2% in the most recent generation of moraines), and 4% among specimens of the intermediate generation.

The Ur–Llaurà section was initially interpreted as a single outwash deposit (Unit 2) grading vertically and laterally to a coeval till deposit (Unit 3) (Calvet, 1996, 2004; Calvet et al., 2011), and the Puigcerdà terrace (here part of the Segre catchment) was correlated with alluvial generation T4 in the Roussillon catchments. That interpretation has now been revised. What appeared to be a simple paraconformity between Units 2 and 3 is actually a sharp unconformity, with a wide time gap between the two formations documented by electron spin resonance and cosmogenic burial age data (work in progress). A fresh examination of the section and borehole logs from the 'Banque du sous-sol' archive (Bureau de Recherches Géologiques et Minières) have likewise revealed that the glacial till fills two washout channels cut in the underlying glacifluvial debris (Fig. 15A, B, G). Similar gully fills have been observed further up-valley in a section exposed by the Riu de Brangoli channel (42°27'42"N, 01°56'02.8"E) and in freshly cut exposures below the new hospital building at Puigcerdà, at the base of the terrace riser (Fig. 16C, 42°26'37.2"N, 01°55'28.5"E). At this site, the base of the deeply weathered till crosscuts both the outwash formation and the Vallesian mudstone.

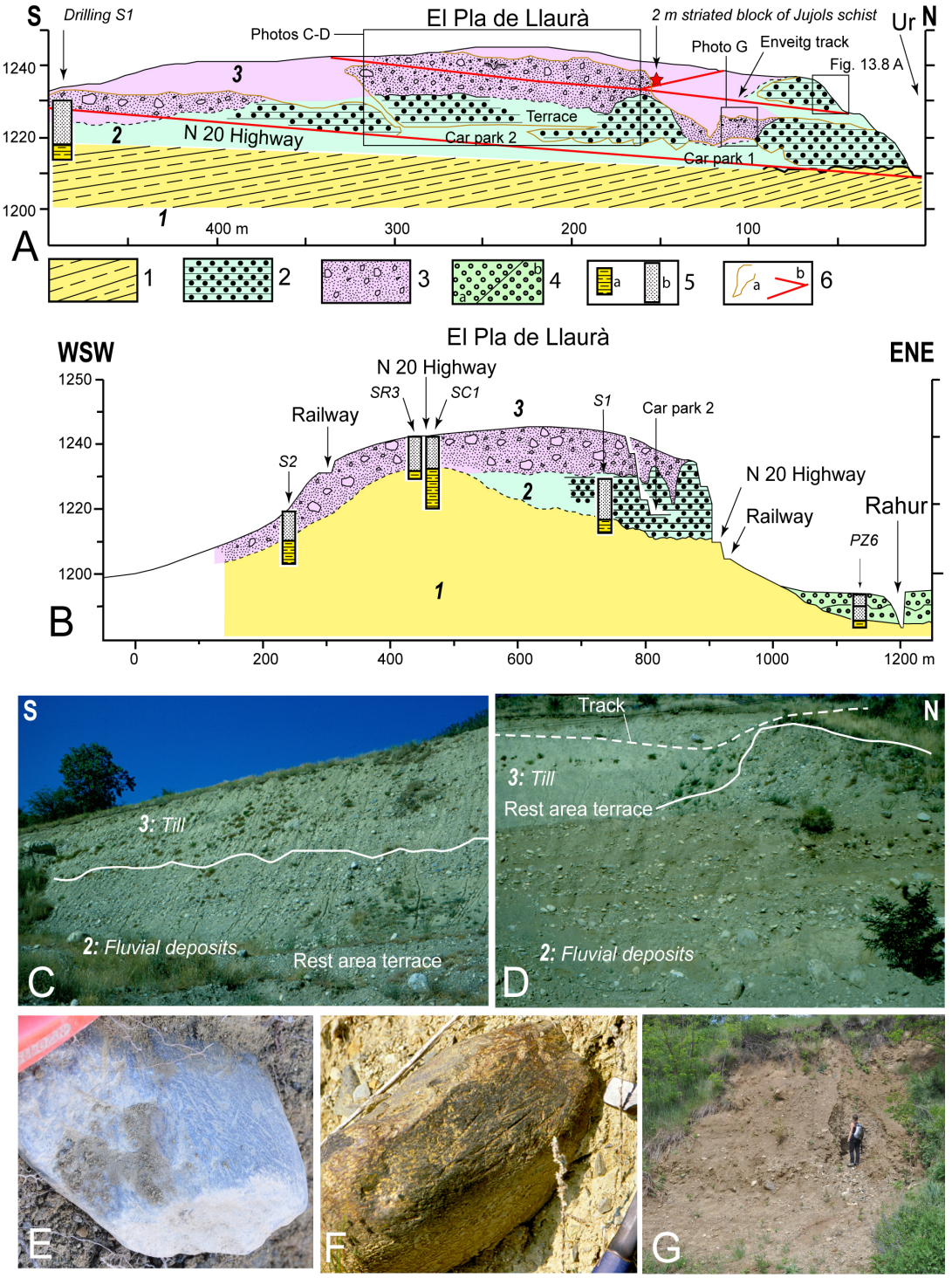

Figure 15. Sections through Early Pleistocene deposits near Ur (highway N20). A. Road-parallel view of the section; positions of the footpath ('Enveitg track') and engineered terrace in the quarry face (a tourist rest area) are indicated. B. Road perpendicular section. Key to ornaments – 1: Vallesian sandy clay; 2: High-energy fluvial deposit (lower unit); 3: Deeply weathered ancient till; 4: Low alluvial level, Rahur stream (4a: alluvium T1; 4b: weathered older alluvium or Vallesian sand); 5: Borehole data (5a: Vallesian clays; 5b: alluvium or till); 6: Other features (6a: outcrops; 6b: roads and tracks). C, D. View of the vertical section at Car park 2 in 1984. Note clear stratigraphy, with the unsorted till facies over the bedded fluvial deposits. 'Rest area terrace' indicates position of the engineered platform area recently cut into the quarry-face stratigraphy. E, F. Glacially-striated schist pebbles observed in situ withing the fine-textured till matrix. G. Recent section at car park 1 (in 2020) revealing the disconformity between the till and the underlying alluvium (figure, for scale, is standing on the alluvium). Positions of photographs (ph.) C, D, and G are indicated on cross-section A.

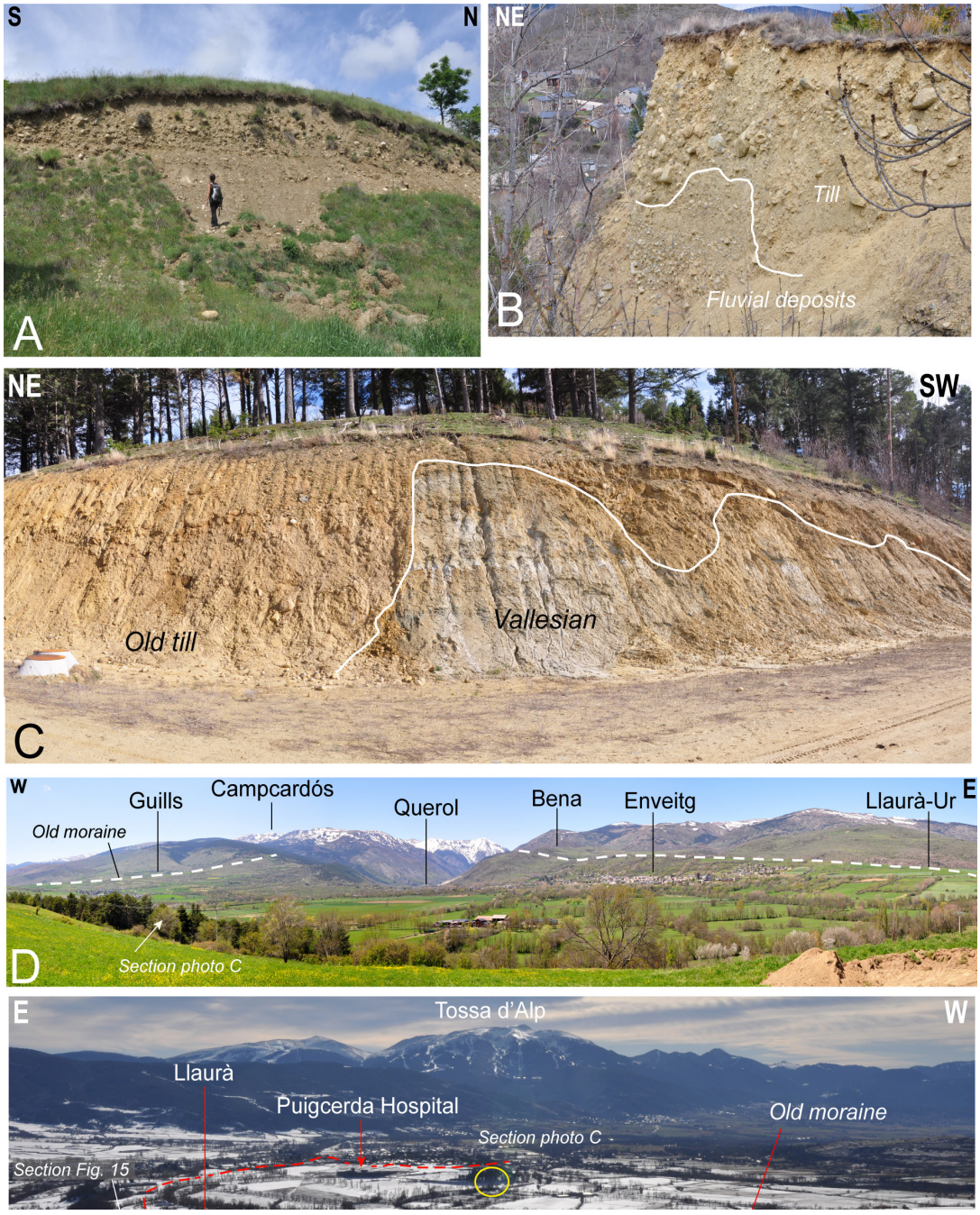

Figure 16. Ancient moraines of the Querol (landscape views and deposit exposures). A. Enveitg section (located in panel E and Figure 15), showing high-energy fluvial deposits. B. Brangoly stream, above Ur, showing disconformity between the till and the underlying alluvium (location in panel E). C. Puigcerdà hospital terrace section, with a ravinement surface between the ancient till and Vallesian clays exposed in a cutting through a steep slope corresponding to the edge of the uppermost outwash terrace (here seen in 2013; see panel E for location). D. Piedmont lobe at the mouth of the Querol valley, here seen from the terminal moraine at Puigcerdà hospital. E. Outline of Querol piedmont lobe viewed from Belloc.

Dating of the stratigraphy at Ur has so far revealed that the alluvium (Unit 2) is ancient (1–2 Ma; electron spin resonance and cosmogenic nuclide burial dating, work in progress): given that the alluvial deposit is vertically inset by 25 m here at Llaurà and by 35 m at Puigcerdà hospital, the till is likely Middle Pleistocene, probably coeval with outwash deposits labelled elsewhere as generation T3. When standing in the meadow at the top of the Ur–Laurà section, the convex shape of the ancient lateral moraine is distinguishable; the corresponding ribbon of glacial till rises gently to the NW, curving round to the WNW from Pla de Llaurà (SE of Enveitg) all the way to the hamlet of Bena, a further 5 km to the NW (Fig. 17).

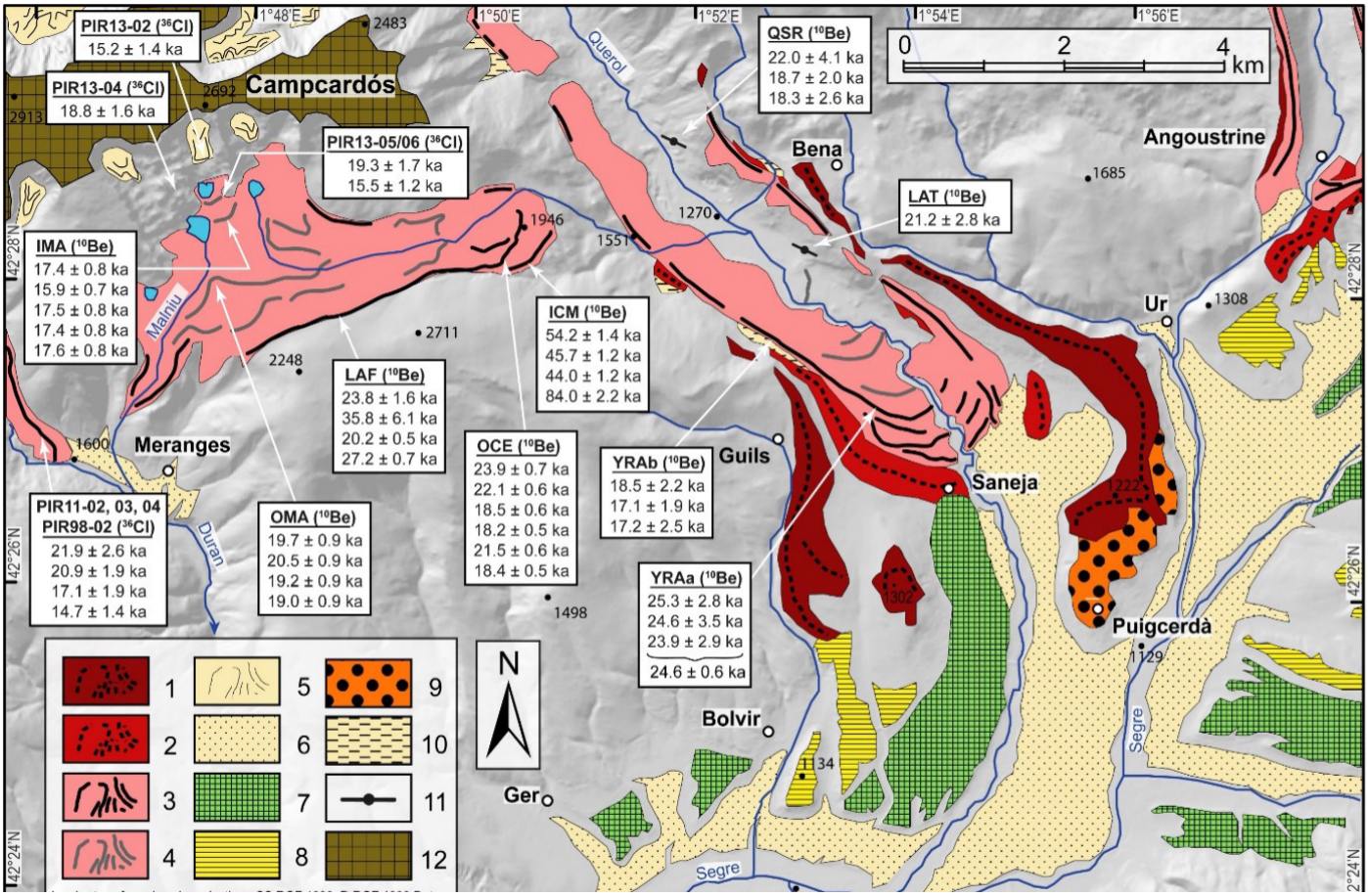

Figure 17. Glacial and glaciofluvial outwash deposits, with associated ages in the Querol and neighbouring catchments. After Delmas et al. (2022c), see figure 6 for keys.

Along the Querol glacial trough to Col du Puymorens

At Latour-de-Carol, take the N20 northbound. Note the landslide scar in the hornfels outcrop above the village, most likely produced in paraglacial conditions soon after Late Pleistocene glacier recession. The cross-section of the Querol (Carol) valley is reasonably U-shaped, but its floor was not substantially overdeepened and is thus populated by a large number of bedrock 'whalebacks', mostly in granite, rather than by large and sediment-filled rock basins. Three 10Be exposure-dating results obtained from ice-polished exposures along the valley have yielded a succession of ages (21. 2 ± 2.8 at Latour, 22 ± 4.1 at Quers, and 21.7 ± 3.4 at la Fullatera bridge, just downstream of Porta rock basin), all indicating rapid deglaciation towards the end of the LGM (Pallàs et al., 2010). This chronology conforms exactly to the scenario documented along the Têt glacial stairway. The road eventually reaches Porta rock basin, located at the junction with the Campcardós tributary valley. The treads of LGM ice-marginal kame terraces (elevation: 1950 m) suggest a glacier ~450 m thick at the time. A large number of avalanche corridors occur on the valley sides. Those at Montfilla (carriages of a passing train overturned by a powder-snow avalanche in 1935) and Serradal (road and railway line cut off in 1972) are particularly threatening. The corridor at Coma Cervera used to be a threat to the village of Porta (one death in 1826), but forest regrowth indicates a decline in avalanche frequency at this location. By continuing towards Porté, you can reach the upper Querol valley and join up with Lake Lanoux (Lanòs). This was the largest glacial lake of the Pyrenees even before it was further enlarged after being closed off by a dam (3 hr walk, round trip). Another option is to drive up to Col du Puymorens (1917 m) to reach Stop 7.

7

Col du Puymorens (Coll Pimorent).

Chronology of the post-LGM deglaciation in the upper valleys of the Querol and Ariège rivers. Paleoclimatic reconstruction based on paleoglaciologic modelling and implication for atmospheric circulation pattern at large scale.

This mountain pass is in fact a very broad palaeovalley which suffered drainage beheading from an agressor stream in the north and now feeds to the Ariège catchment. This drainage capture is explained by the greater steepness of the Ariège stream channel compared to the Segre, which in this area lies comparatively much further from its marine base level and initially flows through the elevated Cerdagne Basin instead of dropping off rapidly to its nearest piedmont. During the Late Pleistocene, the Puymorens operated as a transfluence col through which the Ariège glacier, which was more abundantly supplied by precipitation from the Atlantic and accordingly endowed with a much lower equilibrium line altitude (1800 m vs. 2200 m), spilled southward into the Querol valley. This lasted until the end of the LGM, extending to 18–17 ka as shown by numerous 10Be exposure ages obtained from lateral moraines in the Ariège and Orri glacial troughs (Fig. 18).

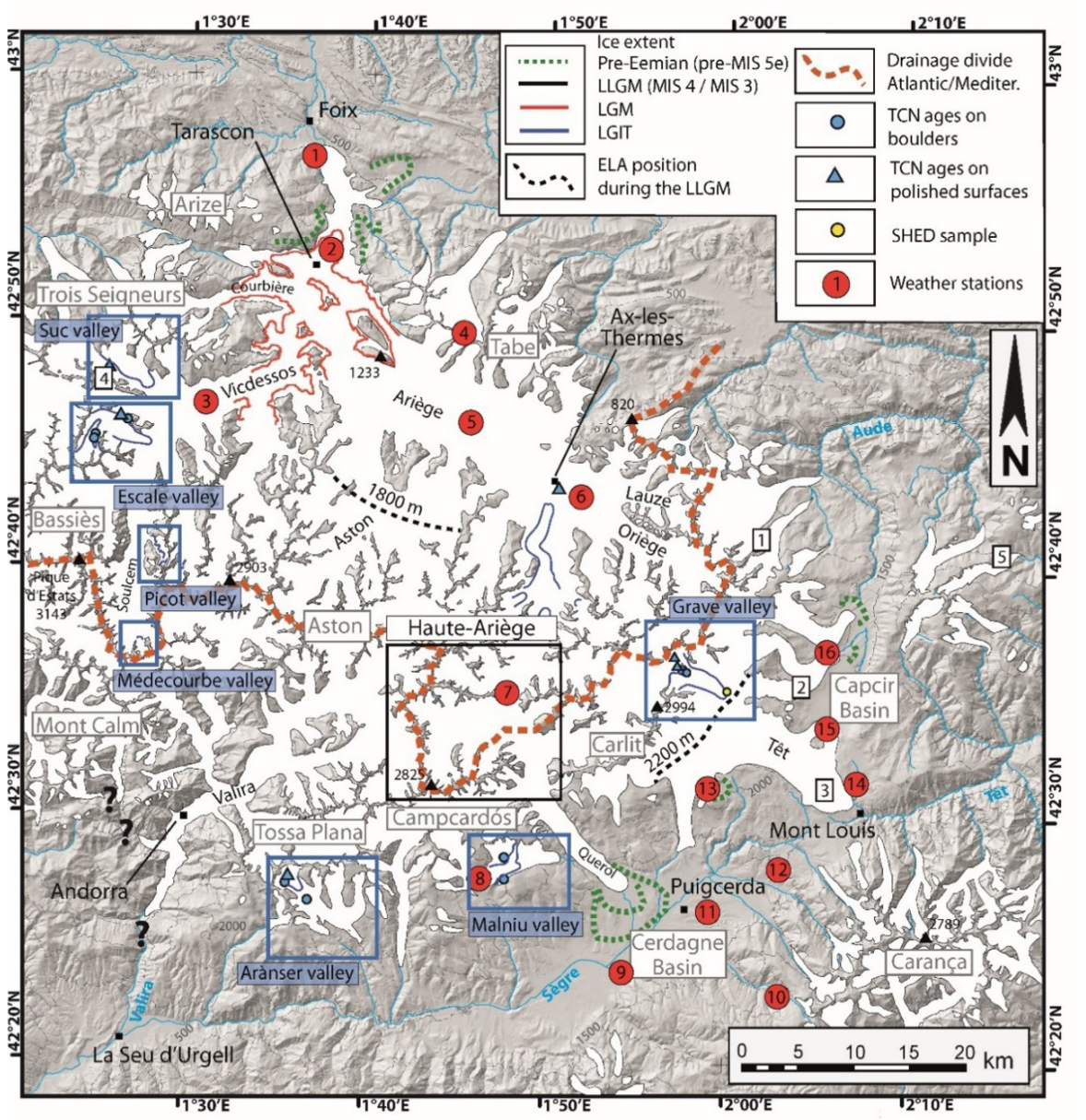

Figure 18. Pleistocene glacial extent in the eastern Pyrenees. Dashed red line: modern drainage divide between Atlantic and Mediterranean streams. Black and blue boxes define study areas. Numbered red circles: weather stations providing data used in the climate modelling. Numbered white squares: peatbogs. After Reixach et al. (2021), modified.

A total of 22 10Be exposure ages were obtained from a population of moraines in the upper Ariège valley and around Col du Puymorens (Fig. 19, Reixach et al., 2021). Puymorens straddles the drainage divide between the north-flowing Ariège and south-flowing Querol rivers, each tributaries of the Garonne (under Atlantic influence) and the Ebro (under more Mediterranean influence), respectively.

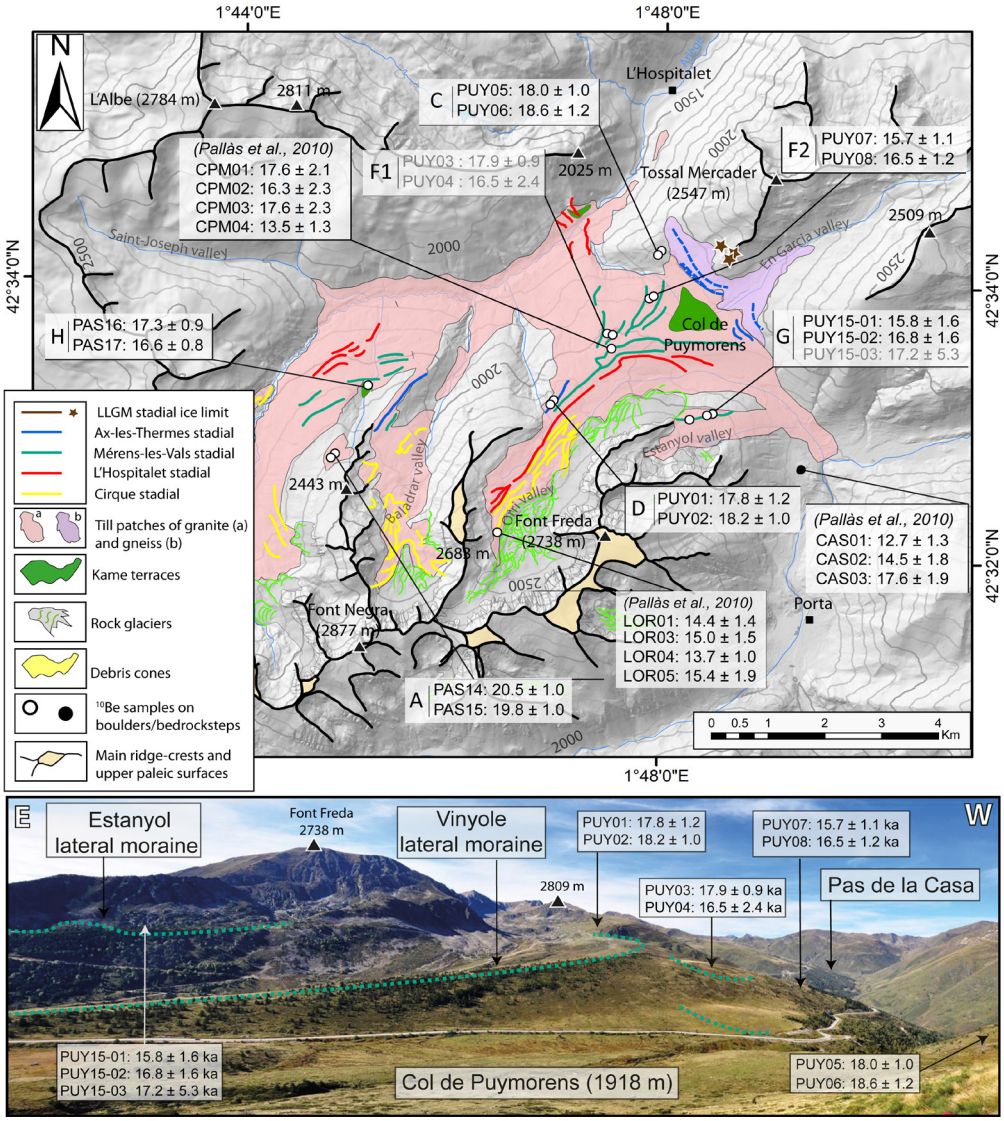

Figure 19. Geomorphological map and 10Be exposure ages at and around Col de Puymorens. After Reixach et al. (2021), modified.

A detailed analysis of chronological and palaeogeographical evidence from this valley segment has documented the extent of the Ariège glacier at four successive stades during the last glacial to interglacial transition (Fig. 20):

(1) At the time of the Ax-les-Thermes stadial (Fig. 20A), the valley hosted a composite glacier ca. 20 km long, its presence outlined today by vestiges of the lateral moraines at Petches (upstream from Ax-les-Thermes) and by the outermost band of lateral moraines further up the valley. At the time, the glacier was connected to the south-facing Querol valley glacier by transfluent ice at Puymorens. Exposure ages on the lateral moraine at Petches and from a ribbon of glacier-margin boulders in the upper valley (Fig. 20A) position the Ax stadial during the Oldest Dryas (GS-2.1b: 18.0 ± 0.5 ka).

(2) At the time of the Mérens stadial (Fig. 20B), the glacier was ~15 km long, had lost several tributaries, and the Ariège icefield was now cut off from the Querol at Puymorens. Frontal moraines at Mérens-les-Vals and in disconnected tributary valleys in the catchment indicate that the Mérens stadial coincided with the Oldest Dryas (GS-2.1a: 16.5 ± 0.5 ka).

(3) At the time of the Hospitalet stadial (Fig. 20C), the glacier was ~10 km long and produced several, closely-spaces frontal moraines upstream

of the village of l'Hospitalet. The precise age of this stadial position currently remains unknown because of unsuitable dating material. Given the ages of local stades 2 (see above) and 4 (see below), it nonetheless appears that glacier recession was occurring fast at the time. .

(4) The cirques stade is the last episode of the deglacial history, a time when the landscape was hosting a population of small cirque and short valley glaciers such as Orri and Baladrar (Fig. 20D). Updated age models of exposure data previously obtained by Pallàs et al. (2010) from lateral moraines above Puymorens (Orri valley) indicate that Figure 20D illustrates the landscape during the Bølling–Allerød (GI-1: 14.5 ± 0.6 ka).

Amplitudes of palaeotemperatures and palaeoprecipitation have been retrieved from glaciological and palaeoclimatic models calibrated on the positions of each successive generation of glacial landforms (Fig. 21). Results indicate that climate in the upper Ariège valley was overall colder and drier than today, with an acceleration towards milder conditions between GS-2.1b and GI-1. The ELA rose by 410 m over than period, and the increase in mass-balance gradient (MBG) by 0.04 m/yr/100 m testifies to an increase in temperature and precipitation of 4.2 °C and 38 %, respectively.

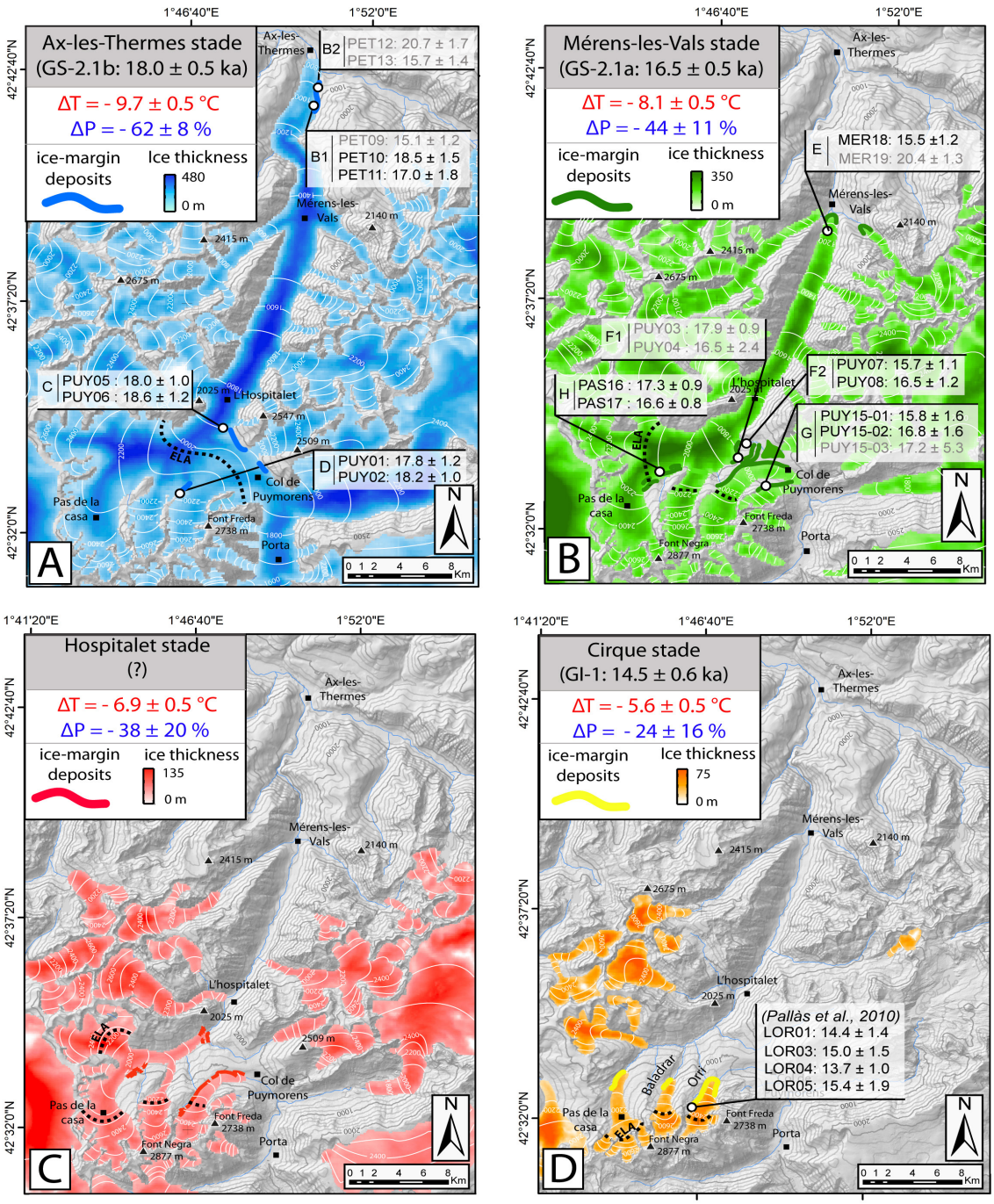

Figure 20. Extent of successive glacial stages in the upper Ariège valley. After de Reixach et al. (2021).

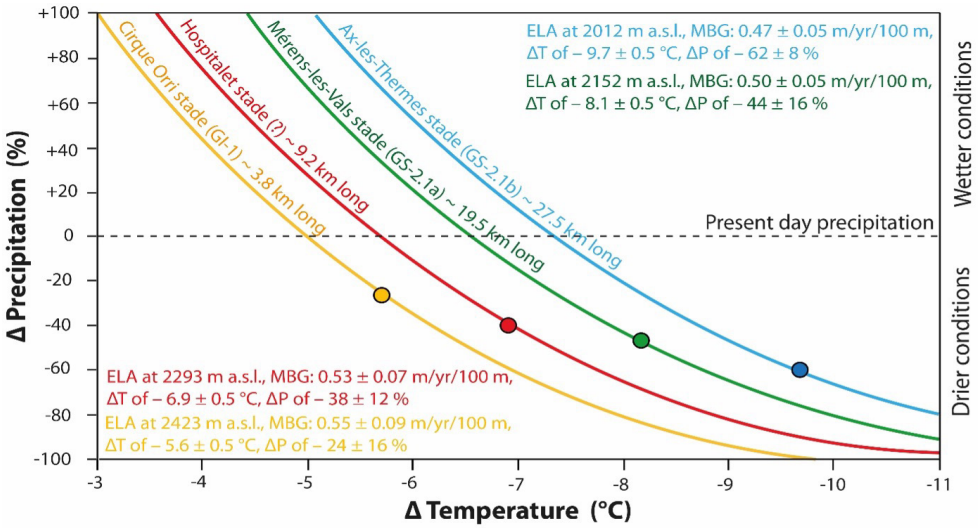

Figure 21. Reconstructed P and T pairs relative to present conditions, here applied to the four glacial stillstands (local stades) identified in the upper Ariège catchment. Extrait de Reixach et al. (2021).

CONCLUSIONS

The Ariège results have been integrated into a wider database of palaeoenvironmental proxy evidence and age results (n = 64) from seven other valleys distributed across the eastern Pyrenees (Suc, Escale, Picot, Médecourbe, Aránser, Malniu and Grave) (Fig. 18 and Table 1). Collectively, these data provide a basis for inferring patterns of climatic conditions during the LGIT, and for linking these with evolving climate dynamics over western continental Europe and the western Mediterranean at the time. The data suggest that deglaciation in the eastern Pyrenees occurred fast, with only small cirque glaciers remaining ca. 12.3 ka (GS-1) wherever local climatic conditions (typically controlled by slope aspect) allowed it (e.g. Grave valley, Médecourbe). Glaciological modelling highlights a contrast between the colder and wetter north-facing mountain front and massifs, and the milder south-facing mountain front under Mediterranean influence. In the north, ELAs were thus systematically lower and MBGs systematically steeper that in the south (2012 m and 0.47 ± 0.05 m/yr/100 m at Ax, and 2413 m and 0.37 ± 0.06 m/yr/100 m at Malniu during GS-2.1b; 2152 m and 0.50 ± 0.05 m/yr/100 m at Mérens, and 2473 m and 0.35 ± 0.05 m/yr/100 m at Aranser during GS-2.1a). Such a north–south contrast is still observed today but is much less pronounced. It appears to have prevailed as such since at least the LGM (~19 ka).

Location	Chronological data			Glaciological reconstructions				Climatic reconstructions	
Relative position within mountain range	INTIMATE stratigraphy	Local glacial stade	Age (ka ± 1 sigma)	Glacier length (km)	Area above ELA (km^2)	ELA (m a.s.l.)	Mass-balance gradient ($m.yr^{-1}.100\ m^{-1}$)	ΔT (°C)	ΔP (%)
North	GS-2.1 b	Ax-les-Thermes	18.0 ± 0.5	27.5	90.7	2012	0.47 ± 0.05	−9.7 ± 0.5	−62 ± 8
North		Outer Picot	17.8 ± 0.3	2.6	No data	2425[a]	No data	No data	No data
South		Malniu	19.2 ± 0.7	3.1	2.1	2413	0.37 ± 0.06	−7.5 ± 0.5	−70 ± 9
North	GS-2.1a	Mérens-les-Vals	16.5 ± 0.5	19.5	25.3	2152	0.50 ± 0.05	−8.1 ± 0.5	−44 ± 11
North		Freychinède	16.7 ± 1.0	4.9	3.6	1700[a]	0.65 ± 0.09	−9.1 ± 0.5 [b]	+45 ± 25 [d]
North		Légunabens	16.1 ± 0.2	6.6	4.4	2012	0.44 ± 0.05	−9.1 ± 0.5	−45 ± 11
North		Inner Picot	16.7 ± 0.1	1.9	0.4	2449[a]	0.23 ± 0.04	−9.1 ± 0.5 [b]	−80 ± 5 [d]
South		Aránser	Indirectly dated	2.4	0.5	2473	0.35 ± 0.05	−7.4 ± 0.5	−77 ± 7
South		Grave	16.1 ± 0.5	6.5	3.8	2383	0.40 ± 0.06	−7.5 ± 0.5	−67 ± 8
North	No data	Hospitalet	No data	9.2	16	2293	0.53 ± 0.07	−6.9 ± 0.5	−38 ± 12
North	GI-1	Cirque Orri	14.5 ± 0.6	3.8	2.8	2423	0.55 ± 0.09	−5.6 ± 0.5	−24 ± 16
North	GS-1	Mouscadous	12.3 ± 0.2	3.4	2.1	2203	0.52 ± 0.09	− 7.0 ± 0.5	−21 ± 16
North		Médecourbe	13.2 ± 0.9	1.6	0.4	2525[a]	0.41 ± 0.03	− 7.0 ± 0.5[c]	−60 ± 7[d]

Table I. Synthesis of glaciologic and climatic reconstructions of east-Pyrenean LGIT glacial stades.
Notes. [1] ELA calculated using the AABR method (Balance ratio of 1.59; Rea, 2009). [2] ΔT value obtained for Légunabens glacial stade. [3] ΔT value obtained for Medecourbe glacial stade. [4] ΔP value modeled on the basis of a ΔT value obtained from an adjacent catchment during the same glacial stade.

REFERENCES

- Andrieu, V., Hubschman, J., Jalut, G., Hérail, G., 1988. Chronologie de la déglaciation des Pyrénées françaises. Dynamique de sédimentation et contenu pollinique des paléolacs : application à l'interprétation du retrait glaciaire. Bulletin de l'Association Française pour l'Étude du Quaternaire 34/35, 55–67.
- Bakalowicz, M., Sorriaux, P., Ford, D.C., 1984. Quaternary glacial events in the Pyrenees from U-series dating of speleothems in the Niaux–Lombrives–Sabart caves, Ariège, France. Norsk Geografisk Tidsskrift 38, 193–197.
- Barrère, P., 1954. Equilibre glaciaire actuel et quaternaire dans l'Ouest des Pyrénées centrales. Revue Géographique des Pyrénées et du Sud-Ouest, XXIV, 2, 116–134.
- Barrère, P., Calvet, M., Courbouleix S., Gil Peña I., Martin Alfageme S., 2009. In: Courbouleix, S., Barnolas, A. (eds), Carte géologique du Quaternaire des Pyrénées, 1:400,000 scale. BRGM and ITGM.
- Calvet, M., 1996. Morphogenèse d'une montagne méditerranéenne : Les Pyrénées Orientales. Thèse de Doctorat d'Etat, Document du BRGM n° 255, BRGM ed., Orléans, 1177 p.
- Calvet, M., 2004. The Quaternary glaciation of the Pyrenees. In: Ehlers, J., Gibbard, P. (eds), Quaternary Glaciations – Extent and Chronology, part I: Europe. Elsevier, Amsterdam, 119–128.
- Calvet, M., Delmas, M., Gunnell, Y., Braucher, R., Bourlès, D., 2011. Recent advances in research on Quaternary glaciations in the Pyrenees. In: Ehlers, J., Gibbard, P.L., Hughes, P., Eds. Quaternary Glaciations. Extent and Chronology, a closer look Part IV. Developments in Quaternary Science 15, Elsevier, 127–139.
- Cook, S.J., Swift, D.A., 2012. Subglacial basins: their origin and importance in glacial systems and landscapes. Earth Sci. Rev. 115, 332–372.
- Crest, Y., Delmas, M., Braucher, R., Gunnell, Y., Calvet, M., ASTER Team, 2017. Cirques have growth spurts during deglacial and interglacial periods: evidence from 10Be and 26Al nuclide inventories in the central-eastern Pyrenees (France, Spain). Geomorphology 278, 60–77.
- Delmas, M., 2005. La déglaciation dans le massif du Carlit (Pyrénées orientales) : approches géomorphologique et géochronologique nouvelles. Quaternaire 16, 45–55.
- Delmas, M., 2009. Chronologie et impact géomorphologique des glaciations quaternaires dans l'est des Pyrénées. Thèse de doctorat, université Paris 1 Panthéon-Sorbonne, 529 pp.
- Delmas, M., 2015. The last maximum ice extent and subsequent deglaciation of the Pyrenees: an overview of recent research. Cuadernos de Investigación Geográfica 41, 109–137.
- Delmas, M., Gunnell, Y., Braucher, R., Calvet, M., Bourlès, D., 2008. Exposure age chronology of the last glacial cycle in the eastern Pyrenees. Quaternary Research 69, 231–241.
- Delmas, M., Calvet, M., Gunnell, Y., 2009. Variability of erosion rates in the Eastern Pyrenees during the last glacial cycle–a global perspective with special reference to the Eastern Pyrenees. Quaternary Science Reviews 28, 484–498.
- Delmas, M., Calvet, M., Gunnell, Y., Braucher, R., Bourlès, D., 2011. Palaeogeography and 10Be exposure-age chronology of Middle and Late Pleistocene glacier systems in the northern Pyrenees: implications for reconstructing regional palaeoclimates. Palaeogeography, Palaeoclimatology, Palaeoecology 305, 109–122.
- Delmas, M., Calvet, M., Gunnell, Y., Braucher, R., Bourlès, D., 2012. Les glaciations quaternaires dans les Pyrénées ariégeoises : approche historiographique, données paléogéographiques et chronologiques nouvelles. Quaternaire 23, 61–85.
- Delmas, M., Gunnell, Y., Calvet, M., Reixach, T., Oliva, M., 2022a. Glacial landscape of the Pyrenees (chapter 16). In: Palacios, D., Hughes, P., García-Ruiz, J.M., Andrés, A. (Eds.), European Glacial Landscapes (volume 1): Maximum Extent of Glaciations. Elsevier, 123–128.

- Delmas, M., Gunnell, Y., Calvet, M., Reixach, T., Oliva, M., 2022b. The Pyrenees: glacial landforms prior to the Last Glacial Maximum (chapter 40). In: Palacios, D., Hughes, P., García-Ruiz, J.M., Andrés, A. (Eds.), European Glacial Landscapes (volume 1): Maximum Extent of Glaciations. Elsevier, 295–307.
- Delmas, M., Gunnell, Y., Calvet, M., Reixach, T., Oliva, M., 2022c. The Pyrenees: glacial landforms from the Last Glacial Maximum (chapter 59). In: Palacios, D., Hughes, P., García-Ruiz, J.M., Andrés, A. (Eds.), European Glacial Landscapes (volume 1): Maximum Extent of Glaciations. Elsevier, 461–472.
- Delmas, M., Gunnell, Y., Calvet, M., Reixach, T., Oliva, M., 2023a. The Pyrenees: environments and landforms in the aftermath of the LGM (chapter 21). In: Palacios, D., Hughes, P., García-Ruiz, J.M., Andrés, A. (Eds.), European Glacial Landscapes (volume 2): Last Deglaciation. Elsevier, 185–200.
- Delmas, M., Oliva, M., Gunnell, Y., Fernandes, M., Reixach, T., Fernández-Fernández, J.M., Calvet, M., 2023b. The Pyrenees: glacial landforms from the Bølling–Allerød Interstadial (chapter 38). In: Palacios, D., Hughes, P., García-Ruiz, J.M., Andrés, A. (Eds.), European Glacial Landscapes (volume 2): Last Deglaciation. Elsevier, 361–368.
- Delmas, M., Oliva, M., Gunnell, Y., Reixach, T., Fernandes, M., Fernández-Fernández, J.M., Calvet, M., 2023c. The Pyrenees: glacial landforms from the Younger Dryas (chapter 56). In: Palacios, D., Hughes, P., García-Ruiz, J.M., Andrés, A. (Eds.), European Glacial Landscapes (volume 2): Last Deglaciation. Elsevier 441–452.
- García-Ruiz, J.M., Martí-Bono, C., Peña-Monné, J.L., Sancho, C., Rhodes, E.J., Valero-Garcés, B., González-Sampériz, P., Moreno, A., 2013. Glacial and fluvial deposits in the Aragón Valley, central-western Pyrenees: Chronology of the Pyrenean Late Pleistocene glaciers. Geografiska Annaler Series A Physical Geography 95, 15–32.
- Guerrero, J., Gutiérrez, F., García-Ruiz, J.M., Carbonel, D., Lucha, P., Arnold, L.J., 2018. Landslide-dam paleolakes in the Central Pyrenees, Upper Gállego River Valley, NE Spain: timing and relationship with deglaciation. Landslides 15, 1975–1989.
- Hérail, G., Hubschman, J., Jalut, G., 1987. Quaternary glaciation in the French Pyrenees. Quaternary Science Review 5, 397-402.
- Hughes, A.L.C., Gyllencreutz, R., Lohne, Ø.S., Mangerud, J., Svendsen, J.I., 2016. The last Eurasian ice sheets - a chronological database and time-slice reconstruction, DATED-1. Boreas 45, 1–45.
- Lewis, C.J., Mc Donald, E.V., Sancho, C., Peña, J.L., Rhodes, E.J., 2009. Climatic implications of correlated Upper Pleistocene and fluvial deposits on the Cinca and Gállego Rivers (NE Spain) based on OSL dating and soil stratigraphy. Global and Planetary Change 67, 141–152.
- Martí Bono, C.E., García Ruiz, J.M. Eds., 1994. El glaciarismo surpirenaico: nuevas aportaciones, Logroño, Geoforma édit., 142 p.
- Melki, T., Kallel, N., Jorissen, F.J., Guichard, F., Dennielou, B., Berné, S., Labeyrie, L., Fontugne, M., 2009. Abrupt climate change, sea surface salinity and paleoproductivity in the western Mediterranean Sea (Gulf of Lion) during the last 28 kyr. Palaeogeography, Palaeoclimatology, Palaeoecology 279 (1–2), 96–113.
- Mensua S., Ibañez J., Yetano M. (1977) □ Sector central de la depresion del Ebro, mapa de terrazas fluviales y glacis. Departamento de Geografia, Universidad de Zaragoza, 5 hojas al 1:100 000, Comentario a los mapas, 18 p.
- Merz, N., Raible, C.C., Woollings, T., 2015. North Atlantic eddy-driven jet in interglacial and glacial winter climates. Journal of Climate 28, 3977–3997.
- Mörner, N., Solheim, J., Humlum, O., Falk-Petersen, S., 2020. Changes in Barents Sea ice Edge Positions in the Last 440 years: A Review of Possible Driving Forces. International Journal of Astronomy and Astrophysics, 10, 97-164.
- Palacios, D., Gómez-Ortiz, A., de Andrés, N., Vázquez-Selem, L., Salvador-Franch, F., Oliva, M. 2015a. Maximum Extent of Late Pleistocene Glaciers and Last Deglaciation of La Cerdanya Mountains, Southeastern Pyrenees. Geomorphology 231, 116–129.
- Palacios, D., de Andrés, N., López-Moreno, J.I., García-Ruiz, J.M. 2015b. Late Pleistocene deglaciation in the central Pyrenees: the upper Gállego valley. Quaternary Research 83, 397–414.

- Palacios, D., García-Ruiz, J.M., Andrés, N., Schimmelpfennig, I., Campos, N., Léanni, L., ASTER Team, 2017. Deglaciation in the central Pyrenees during the Pleistocene-Holocene transition: timing and geomorphological significance. Quaternary Science Reviews 162, 111–127.
- Pallàs, R., Rodés, A., Braucher, R., Carcaillet, J., Ortuño, M., Bordonau, J., Bourlès, D., Vilaplana, J.M., Masana, E., Santanach, P., 2006. Late Pleistocene and Holocene glaciation in the Pyrenees: a critical review and new evidence from 10Be exposure ages, south-central Pyrenees. Quaternary Science Reviews 25, 2937–1963.
- Pallàs, R., Rodés, A., Braucher, R., Bourlès, D., Delmas, M., Calvet, M., Gunnell, Y., 2010. Small, isolated glacial catchments as priority targets for cosmogenic surface exposure dating of Pleistocene climate fluctuations, southeastern Pyrenees. Geology 38, 891–894.
- Penck, A., 1883. La période glaciaire dans les Pyrénées. Bulletin de la Société d'histoire naturelle de Toulouse 19, 105–200.
- Penck, A., 1894. Studien über das Klima Spaniens während der Jüngeren Tertiärperiode und der Diluvialperiode. Zeitschrift der Gesellschaft fur Erdkunde zu Berlin 29, 109–141.
- Rasmussen, S.O., Bigler, M., Blockley, S.P., Blunier, T., Buchardt, S.L., Clausen, H.B., Cvijanovic, I., Dahl-Jensen, D., Johnsen, S.J., Fischer, H., Gkinis, V., Guillevic, M., Hoek, W.Z., Lowe, J.J., Pedro, J.B., Popp, T., Seierstad, I.K., Steffensen, J.P., Svensson, A.M., Vallelonga, P., Vinther, B.M., Walker, M.J.C., Wheatley, J.J., Winstrup, M., 2014. A stratigraphic framework for abrupt climatic changes during the Last Glacial period based on three synchronized Greenland ice-core records: refining and extending the INTIMATE event stratigraphy. Quaternary Science Reviews 106, 14–28.
- Rea, B.R., 2009. Defining modern day area-altitude balance ratios (AABRs) and their use in glacier-climate reconstructions. Quaternary Science Reviews 28, 237–248.
- Reille, M., Andrieu, V., 1993. Variations de la limite supérieure des forêts dans les Pyrénées (France) pendant le Tardiglaciaire. Compte rendu de l'Académie des Sciences de Paris Série II 316, 547–551.
- Reille, M., Lowe, J.J., 1993. A re-evalutation of the vegetation history of the eastern Pyrenees (France) from the end of the last glacial to the present. Quaternary Science Reviews, 12, 47-77.
- Reixach, T., Delmas, M., Braucher, R., Gunnell, Y., Mahé, C., Calvet, M. 2021. Climatic conditions between 19 and 12 ka in the eastern Pyrenees, and wider implications for atmospheric circulation patterns in Europe. Quaternary Science Reviews 260, doi.org/10.1016/j.quascirev.2021.106923.
- Reixach, T. 2022. Chronologie des fluctuations glaciaires dans les Pyrénées au cours du Pléistocène supérieur - implications paléoclimatiques. Thèse de doctorat, Université de Perpignan Via Domitia, 382 p.
- Sancho, C., Arenas, C., Pardo, G., Peña-Monné, J.L., Rhodes, E.J., Bartolomé, M., García-Ruiz, J.M., Martí-Bono, C., 2018. Glaciolacustrine deposits formed in an ice-dammed tributary valley in the south-central Pyrenees: New evidence for late Pleistocene climate. Sedimentary Geology 366, 47–66.
- Serrat, D., Bordonau, J., Bru, J., Furdada, G., Gomez, A., Marti, J., Marti, M., Salvador, F., Ventura, J., Vilaplana, J.M., 1994. Síntesis cartográfica del glaciarismo surpirenaico oriental. In: Martí Bono, C.E. and García Ruiz, J.M. (eds), El glaciarismo surpirenaico: nuevas aportaciones, Logroño, Geoforma édit., 9-15.
- Sorriaux, P., 1981. Étude et datation de remplissages karstiques : nouvelles données sur la paléogéographie quaternaire de la région de Tarascon (Pyrénées ariégeoises). Comptes Rendus de l'Académie des Sciences série II 293, 703–706.
- Sorriaux, P., 1982. Contribution à l'étude de la sédimentation en milieu karstique. Le système de Niaux-Lombrives-Sabart (Pyrénées Ariégeoises). Thèse de 3° cycle, Université Toulouse Paul Sabatier, 255 p.
- Sorriaux, P., Delmas, M., Calvet, M., Gunnell, Y., Durand, N., Pons-Branchu, E., 2016. Relations entre karst et glaciers depuis 450 ka dans les grottes de Niaux-Lombrives-Sabart (Pyrénées ariégeoises). Nouvelles datations U/Th dans la grotte de Niaux. Volume spécial en Hommage à R. Maire, Karstologia 67, 3–16.
- Taillefer, F., 1957. Le glaciaire pyrénéen : versant nord et versant sud. Revue Géographique des Pyrénées et du Sud-Ouest, XXVIII, 3, 221-244.

- Taillefer, F., 1967. Le néoglaciaire pyrénéen. In : Mélange offerts à O. Tulippe, Deculot & Gembloux, 134–147.
- Taillefer, F., 1969. Les glaciations des Pyrénées. In Actes VIII° congrès international INQUA, Supplément au Bulletin de l'Association Française pour l'Etude du Quaternaire, Paris, 19–32.
- Taillefer, F., 1982. Les conditions locales de la glaciation pyrénéenne. Pirineos, 116, 5-12.
- Tomkins, M.D., Dortch, J.M., Hughes, P.D., Huck, J.J., Stimson, A., Delmas, M., Calvet, M., Pallas, R. 2018. Rapid age assessment of glacial landforms in the Pyrenees using Schmidt hammer exposure dating (SHED). Quaternary Research 90, 26–37.
- Turu, V., 2011. Los complejos morrenicos terminales del Valira (Andorra-Alt Urgell). Resúmenes XIII Reunion Nacional de Cuaternario, Andorra 2011, Simposio de glaciarismo, guía de campo, 1-8.
- Turu i Michels, V., Boulton, G.S., Ros i Visus,, X., Peña Monné J.L., Martí i Bono, C., Bordonau i Ibern, J., Serrano-Cañadas, E., Sancho-Marcén, C., Constante-Orrios, A., Pous i Fábregas, J., Gonzalez-Trueba, J.J., Palomar i Molins, J., Herrero i Simón, R., Garcia-Ruiz, J.M., 2007. Structure des grands bassins glaciaires dans le nord de la péninsule ibérique : comparaison entre les vallées d'Andorre (Pyrénées orientales), du Gallego (Pyrénées centrales) et du Trueba (Chaîne cantabrique). Quaternaire, 18, 309-325.
- Turu, V., Ventura, J., Ros, X., Pèlachs, A., Vizcaino, A., Soriano, J.M., 2011. Geomorfologia glacial del tram final de la Noguera Pallaresa i Riu Flamicell (Els Pallars). Resúmenes XIII Reunion Nacional de Cuaternario, Andorra 2011, Simposio de glaciarismo, 37-43.
- Turu, V., Vidal Romani, J.R., Fernández Mosquera, D., 2011. Dataciones con isótopos cosmogénicos (10Be): el "LGM" (Last Glacial Maximum) y the "Last Termination" en los valles del Gran Valira y la Valira del Nord (Principado de Andorra, Pirineos orientales). Resúmenes XIII Reunion Nacional de Cuaternario, Andorra 2011, Simposio de glaciarismo, 19-23.
- Turu, V., Calvet, M., Bordonau, J., Gunnell, Y., Delmas, M., Vilaplana, J., Jalut, G., 2017. Did Pyrenean glaciers dance to the beat of global climatic events? Evidence from the Würmian sequence stratigraphy of an ice-dammed palaeolake depocentre in Andorra. In: Hughes, P.D., Woodward, J.C., Eds. Quaternary Glaciation in the Mediterranean Mountains. Geological Society, London, Special Publications 433, 111–136.
- Viers, G., 1960. Le relief des Pyrénées occidentales et leur piémont. Pays Basque français et Barétons. Thèse de Doctorat d'Etat, Privat, Toulouse, 604 p.
- Viers, G., 1961. Le glaciaire du massif du Carlit (Pyrénées-Orientales) et ses enseignements. Revue Géographique des Pyrénées et du Sud-Ouest 32, 5–33.
- Viers, G., 1968. La carte du relief glaciaire des Pyrénées. Feuille Mont-Louis au 1/50 000°. Revue Géographique des Pyrénées et du Sud-Ouest 39, 429–434.
- Zickel, M., Becker, Daniel., Verheul, J., Yener, Y., Willmes, C., 2016. Paleocoastlines GIS dataset, computed land masks of past sea level models. CRC806-Database, 10.5880/SFB806.20.

3 Field trip to:

Clot de la Menera rock glaciers, Envalira mountains, Andorra

Turu, V. [1], Ros, X [1], Echeverria, A[2], Ventura, J. [1,3]

[1]Igeotest, Fundació Marcel Chevalier
2Andorra Recerca + Innovació
3Universitat de Barcelona

Clots de la Menera rock glaciers, Envalira mountains, Andorra

Turu, V. [1], Ros, X [1], Echeverria, A [2], Ventura, J. [1,3]
[1]Igeotest, Fundació Marcel Chevalier
2Andorra Recerca + Innovació
3Universitat de Barcelona

INTRODUCTION

The tour visits the Valira valley located in the small Pyrenean state of Andorra (Principat d'Andorra), a transition zone between the central and eastern Pyrenees.

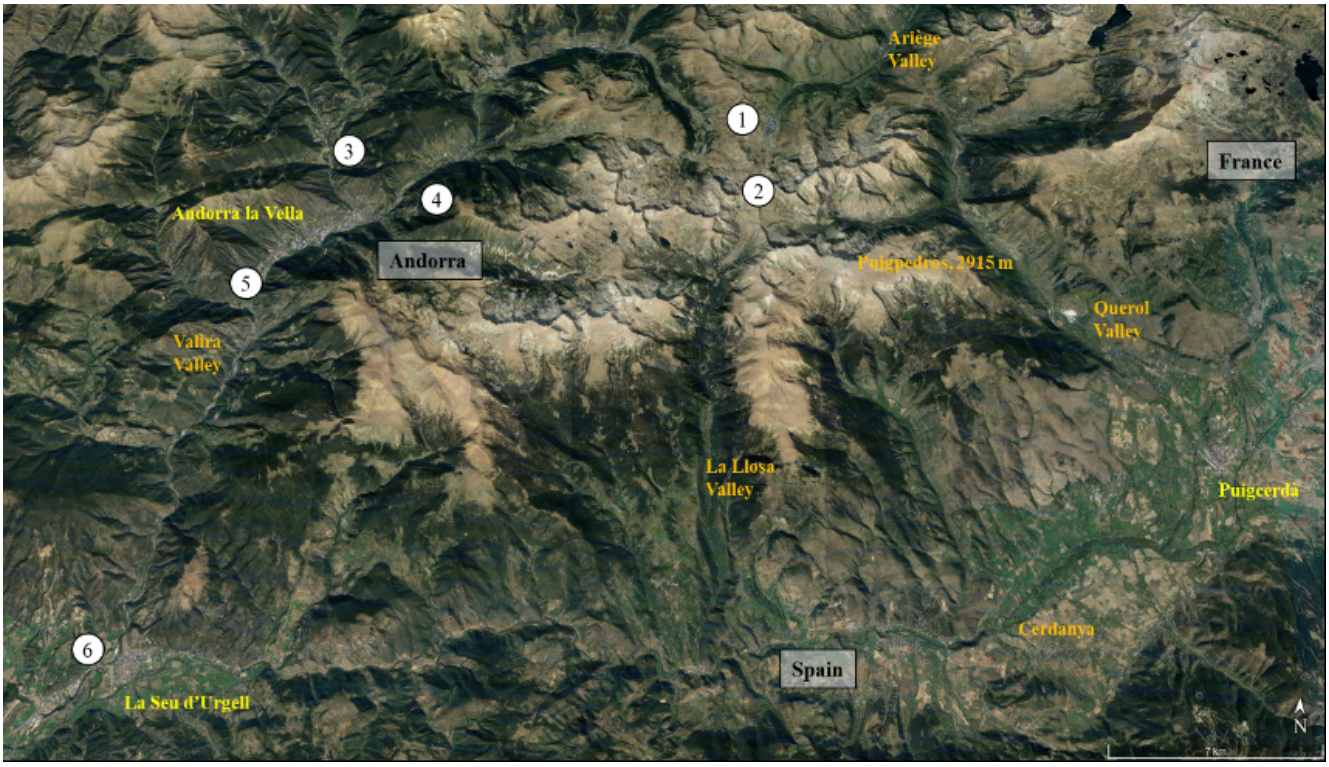

Figure 1. General view of the Andorra valley and the various stops

THE ROUTE

The first stop was made at Port d'Envalira to make the presentation of the geographical setting, glacial landscape and chronology of the Ariège and Valira valleys (North and South slope respectively). Here it will start hiking to Clots de la Menera (stop-2) rock glaciers and Grau Roig (4h). After lunch in Grau Roig you can make some of the following optional stops (their completion will be conditioned by the total time spent on the excursion to Clot de la Menera and the weather conditions):

- Stop-3 (Sant Cristòfol d'Anyòs), La Massana glacial complex. Formation of a paleolake by the obturation of the main glacier (Valira glacier) between 32 and 17 ka cal BP. Different levels of tills, glaciolacustrine rhythmites and deltaic sediments.
- Stop-4, Engolasters lake. Different moraines, deposits in the Andorra la Vella overdeepened basin, glacial phases detected and chronology of the LGC (Last glacial cycle) on the Valira glacier.
- Stop-5, La Margineda. Visit to the outcrops of the Aixovall frontal moraine (Valira Glacier).
- Stop-6, Torre Solsona-Castellciutat (La Seu d'Urgell), view of the Valira-Segre terrace system and the Tossal Bordar moraine (Valira Glacier).

The return to Puigcerdà will be made from La Seu d'Urgell following the N-260 road that crosses the N area of Alt Urgell and La Cerdanya.

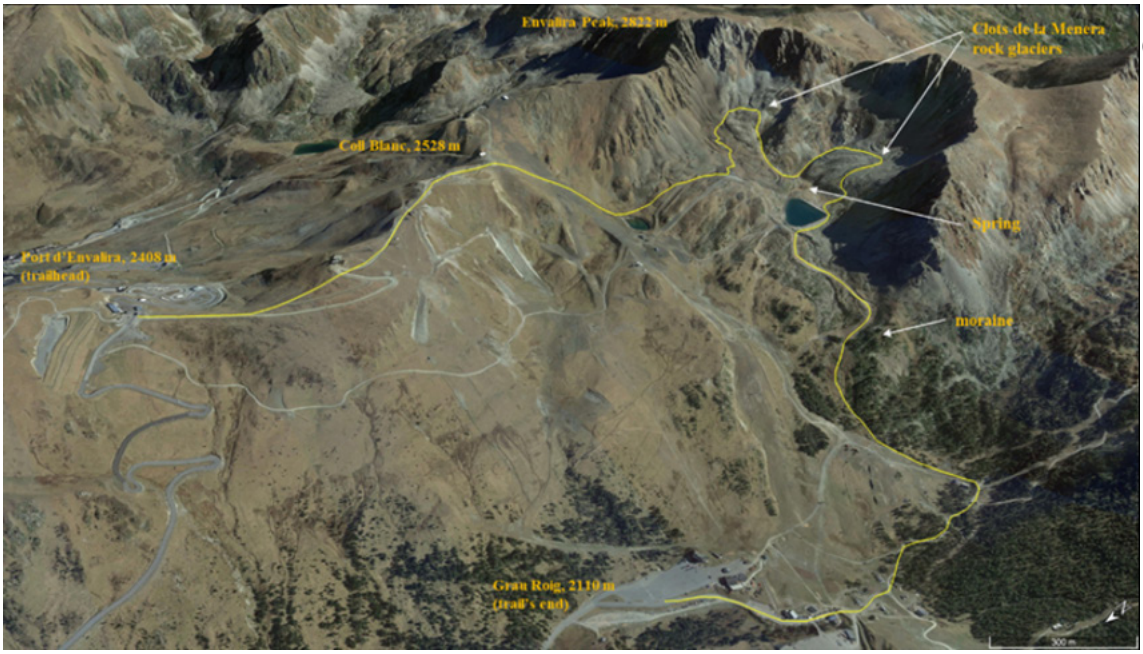

Figure 2. Tour itinerary (stop-2) from Port de Envalira, Clot de la Menera cirque and Grau Roig ski resort.

The geographic characteristics of Andorran mountains and their geomorphological evolution have been recently described in the book "Iberia, Land of Glaciers" (Oliva et al. (Eds.), 2021), specifically in the chapter dedicated to the Central-Eastern Pyrenees (Ventura & Turu, 2021).

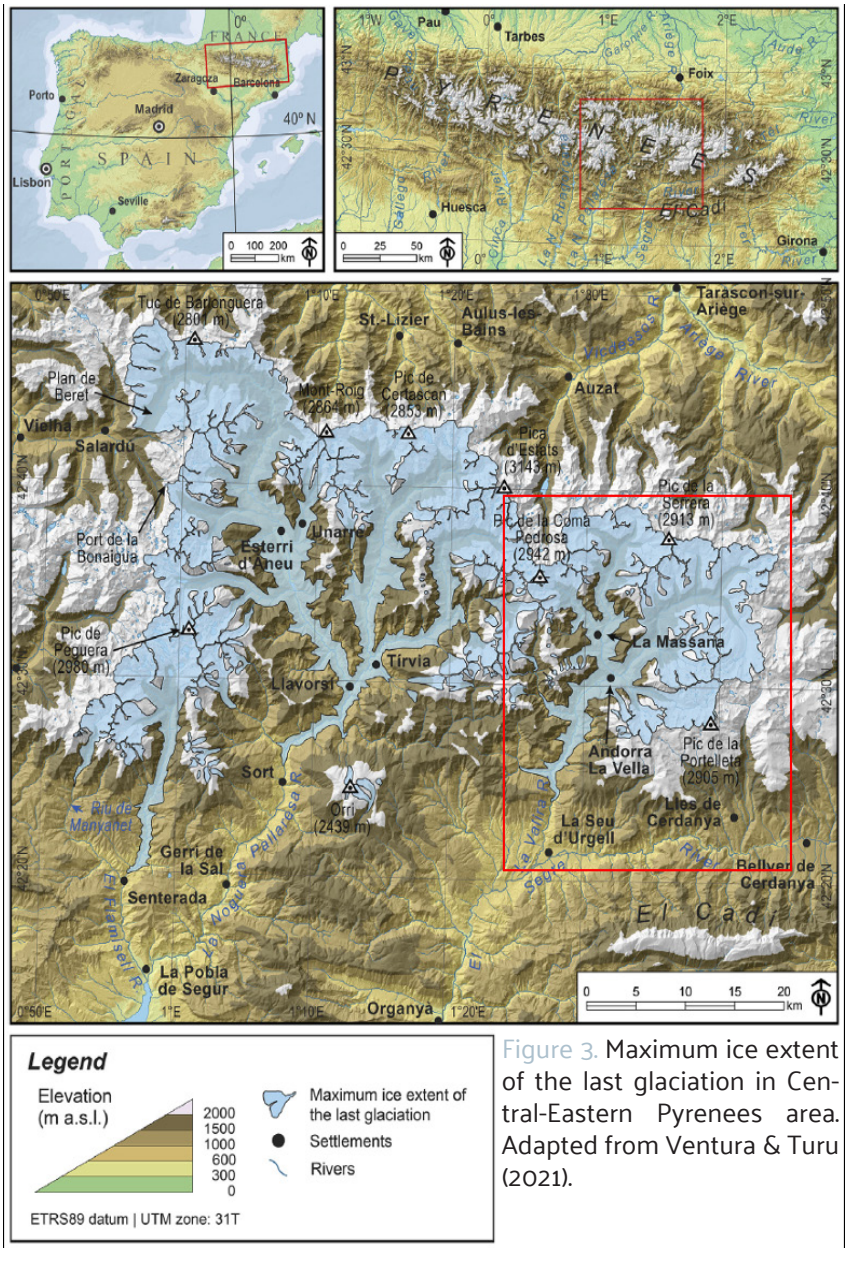

Figure 3. Maximum ice extent of the last glaciation in Central-Eastern Pyrenees area. Adapted from Ventura & Turu (2021).

1

Port d'Envalira

Presentation of the geographical setting, glacial landscape and chronology of the Ariège and Valira valleys (North and South slope respectively).

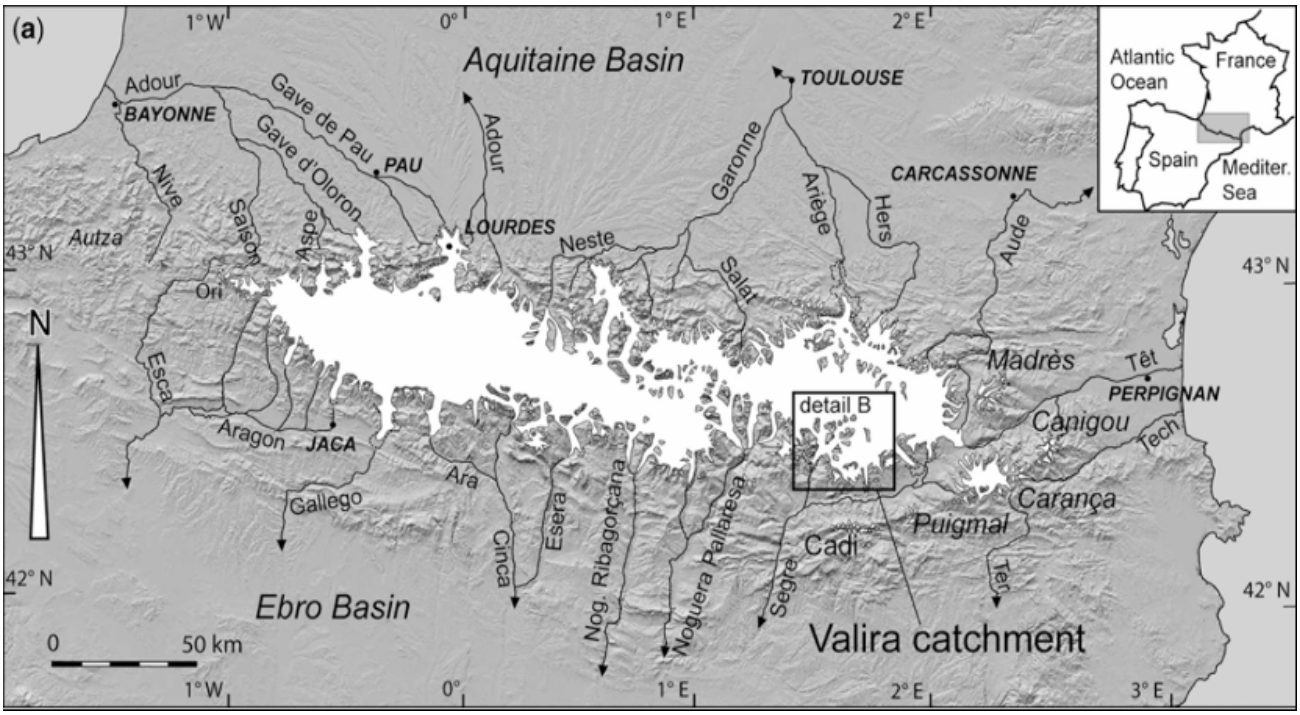

LGM and LLGM asynchrony

Ariège glacier (NE - Pyrénées)

T. Reixach, M. Delmas, R. Braucher et al. *Quaternary Science Reviews 260 (2021) 106923*

Delmas, M., Calvet, M., Gunnell, Y., Braucher, R., Bourlès, D., 2012. Les glaciations quaternaires dans les Pyrénées ariègeoises : approche historiographique, données paléogéographiques et chronologiques nouvelles. Quaternaire 23, 61–85.

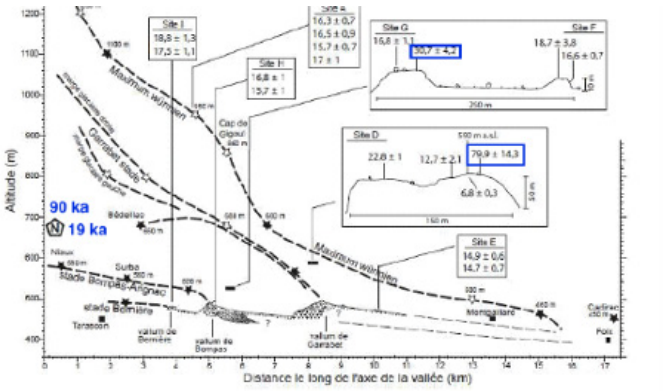

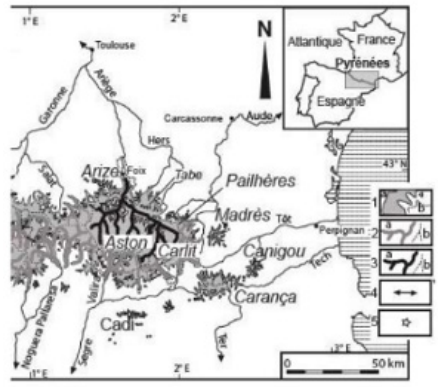

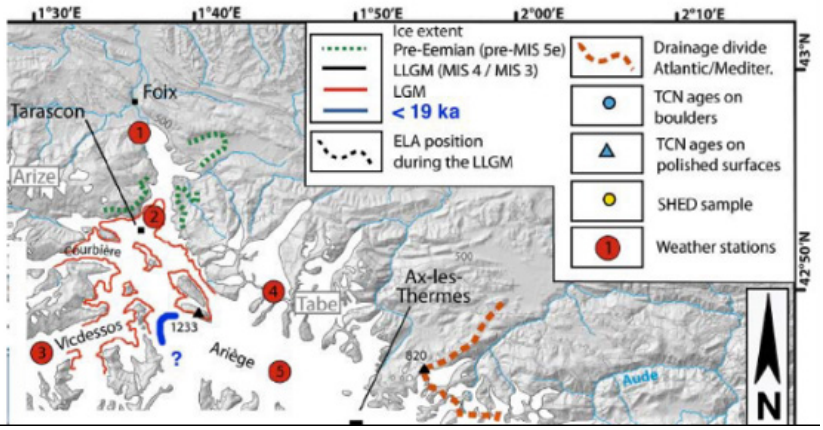

The Last Termination

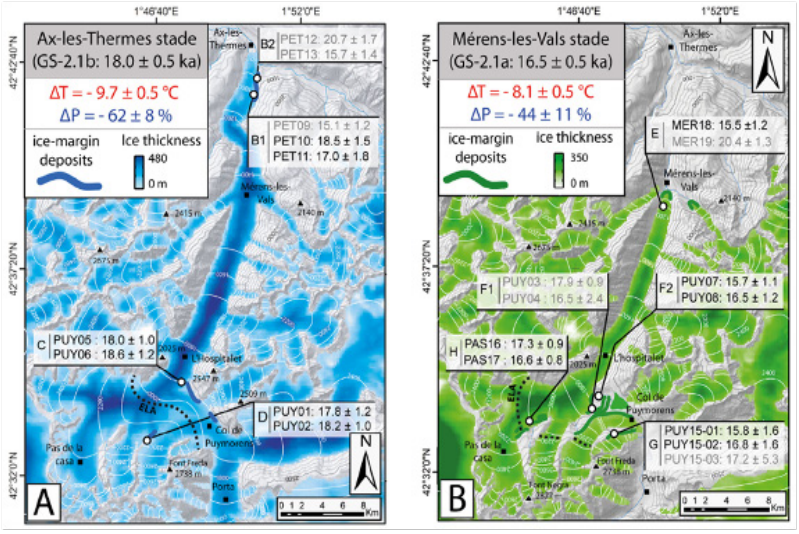

Reixach et al. (2021)

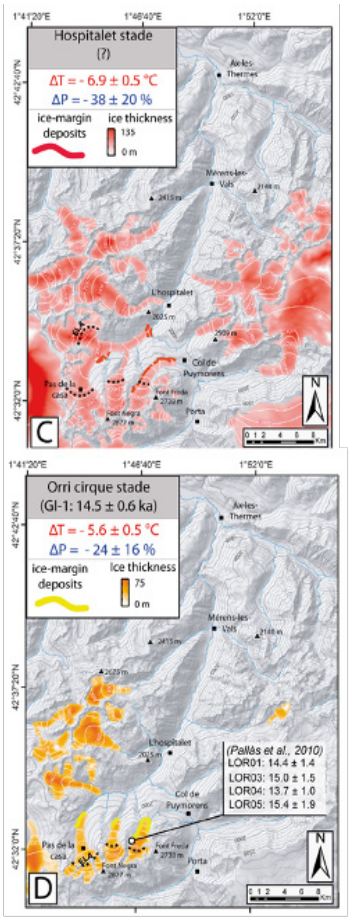

Glacial phases in the Pyrenees

LGM = Last Glacial Maximum (Global)

NLVGP = No Large Valley Glacier Period

GTP = Glacial Thinning Period

LIME = Last Ice Maximu Extent

EGR = Early Glacial Recession

EW = Early Würm

WMHP = Western Mediterranean Humid Periods

LGC = Last Glacial Cycle

PGC = Penultimate Glacial Cycle

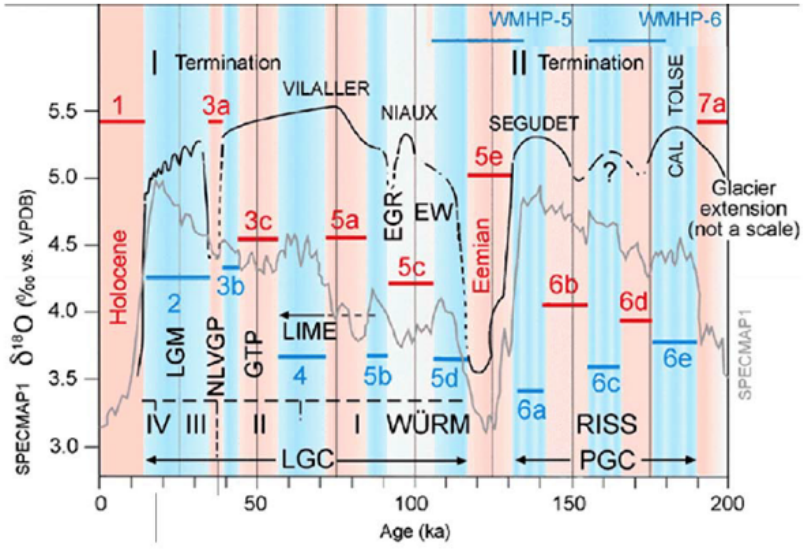

Turu et al. (2023)

The Valira d'Orient down valley - The Encampadana (15.3 ka) and El Forn landslide

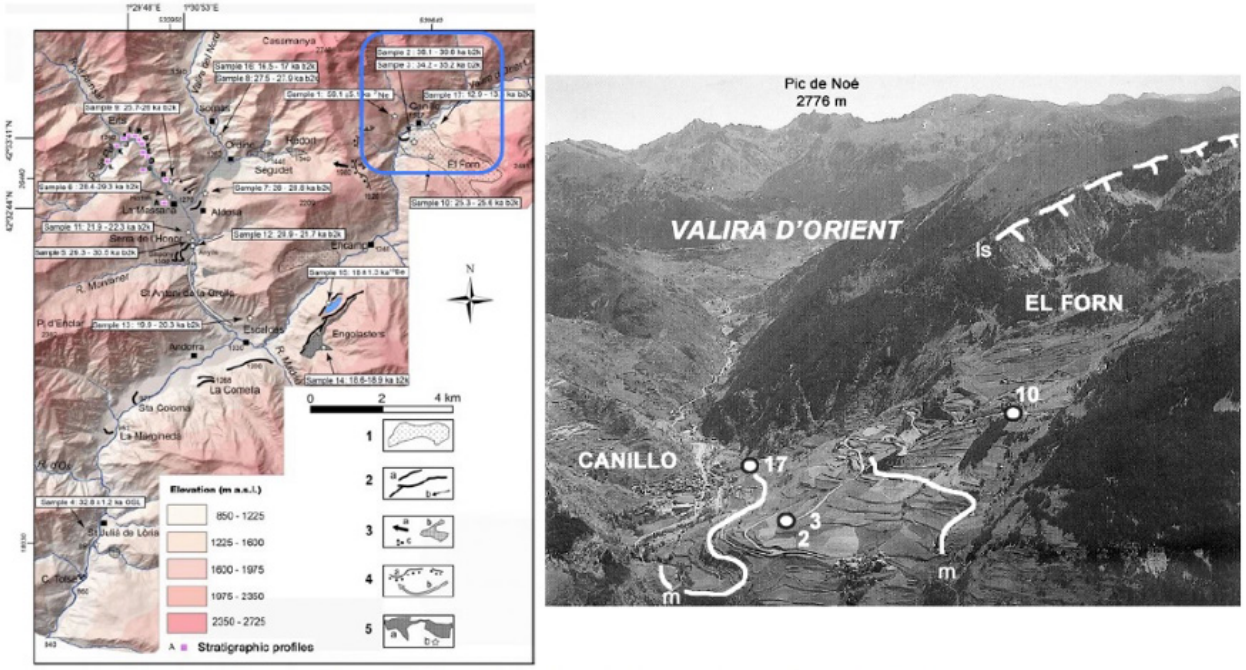

2, 3, 10 and 17 dating localities. Turu et al. (2016)
McCalping and Corominas, (2016)

2 Clot de la Menera cirque and rock glaciers

The Clot de la Menera cirque forms part, together with the great coalescing cirque of Pessons, of the head of the Valira paleoglacier (43 km long during the local LGM). Circular in shape (1.2 km2) and oriented to the N, it is mostly excavated in granodiorite rocks (Carboniferous-Permian), with schists, conglomerates and quartzites (Cambro-Ordovician and Ordovician) outcropping on its right side. The ridge line remains above 2650 m a.s.l. (Pic d'Envalira, 2823 m a.s.l.) and the rocky threshold that closes the cirque is located between 2370 and 2450 m a.s.l.

Figure 4. The rock glaciers of the Clot de la Menera cirque.

Inside (Figures 4 and 5) from E to W there are three rocky glaciers: a) GR-1, with lobed morphology, situates its front at 2420 m a.s.l). It is oriented to the NW and has an area of 4.8 ha (width: 370 m). It is the only rocky glacier in the cirque not excavated in a granite substratum; b) GR-2, tongue-shaped, is polymorphic (two units) with fronts at 2428 m and 2493 m a.s.l. respectively. It is 700 m long, has a surface area of 13.9 ha and an external front 20 m high. Orientation N-NW; c) GR-3, oriented to the N, tongue-shaped, presents a massive aspect in its front part. It has a maximum length of 445 m and an area of 11.5 ha. The front (25 m high) which is located at 2414 m a.s.l. It has a fountain at its base. At the bottom of the cirque there are also abundant morainic deposits with blocks on the surface (open-work structure).

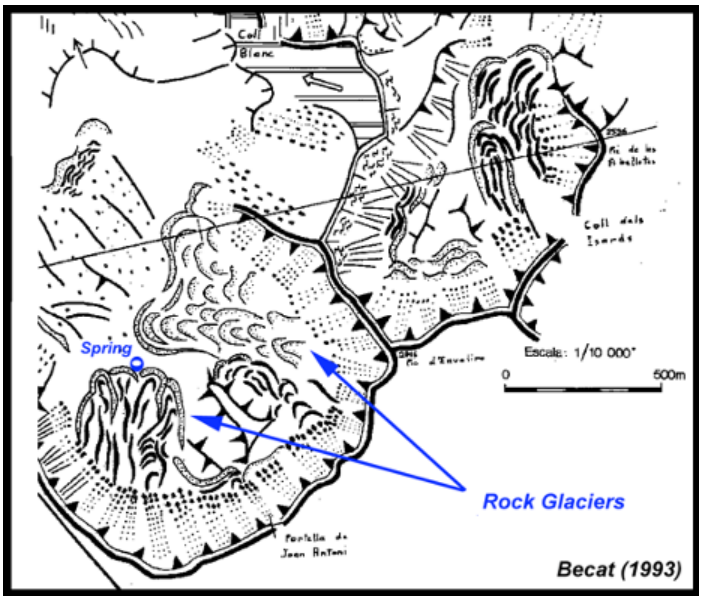

Figure 5. The upper Valira d'Orient basin at Grau Roig and the rock glaciers that had been estudied are indicated. Original from Bécat (1993).

Groundwater tracers / Isotope analysis

By doing a rutinary hydrogeological study on the upper Valira d'Orient bassin, and warned by the extremely low temperature of a particular spring, a specific study was conducted in order to identify fossil meltwater from a buried ice mass on a rock glacier core, northfaced located within a glacier cirque. The sampling took place on 26th September 2008 and the site is known as "Clot de la Menera" (Figure 6). The sampling was repeated a month later; however, budgetary difficulties no more samples were taken.

The sampling campaign was included in the technical report from Igeotest (2008), that look for the origin of groundwater supply for the Grandvalira ski resort (Figure 7), its catchment (N42°31'36.33"– E01°42'09.52"–2208 m a.s.l.) and related springs. The particular spring is located at the foothill of the Clot de la Menera rock glacier (N42°31'10.84"–E01°42'42.08"–2414 m a.s.l.).

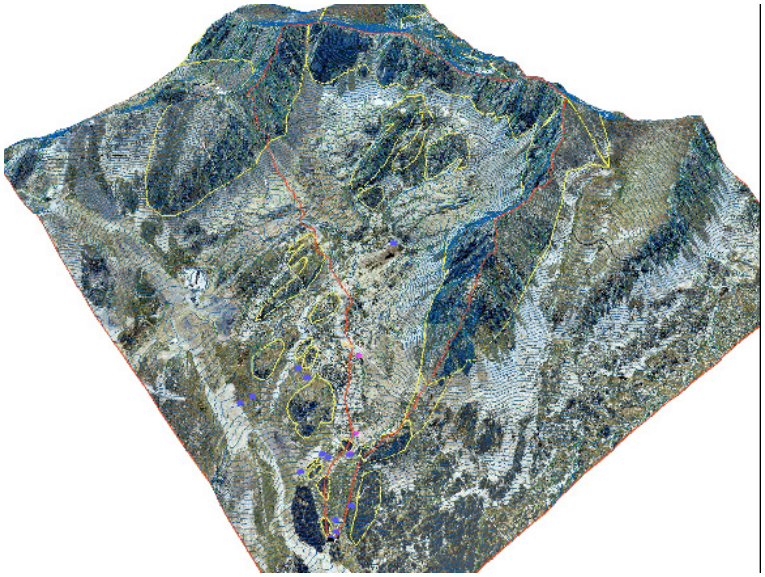

Figure 6. A 3D view of the studied area. Hydrographic basin (red line), water springs (blue points), the bedrock (yellow lines). Original from Igeotest, 2008.

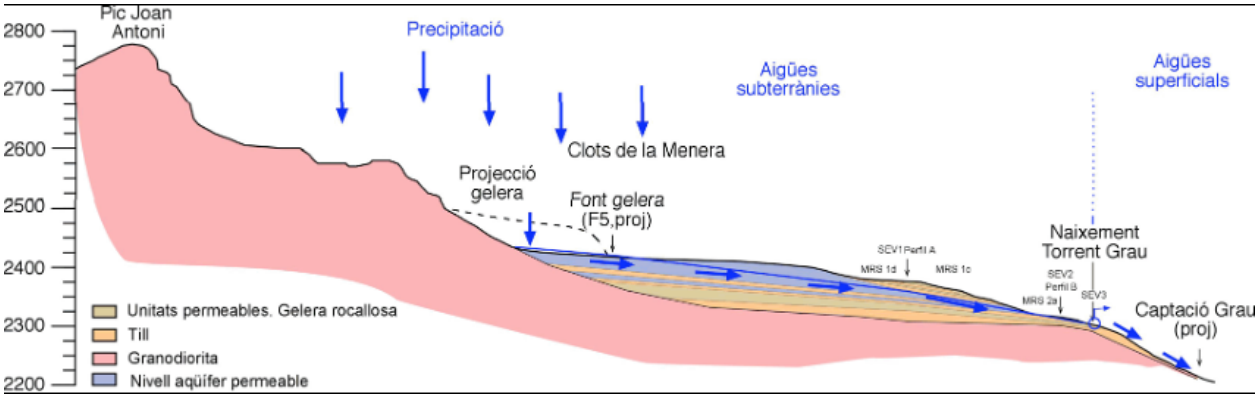

Figure 7. Original from the technical report from Igeotest (2008) showing the hydrogeological conceptual model. Meteoric water infiltrates through permeable layers beneath the rock glacier, until the catchment.

Routinary redox measurements were taken while sampling. The pH was 6.8 in the catchment and 6.8 – 7.2 in the spring, while the Eh was 29.8 mV in the catchment and 3.7 in the spring, advocating for a slighty low alkalinity relatively of pour oxigenated waters. Electrical conductivity indicates a very low mineralised water having 38.2 µS in the catchment and 37.0 – 38.5 µS in the spring. Finally, the temperature of the water was of 2.5 – 3.9°C in the catchment and 1.3 – 1.8 °C in the spring. A comparison between the spring water temperature and the average daily atmospheric temperature (Figure 8) of the public Grau-Roig station (elevation 2083 m) indicates an anomalous temperature behaviour of this particular spring.

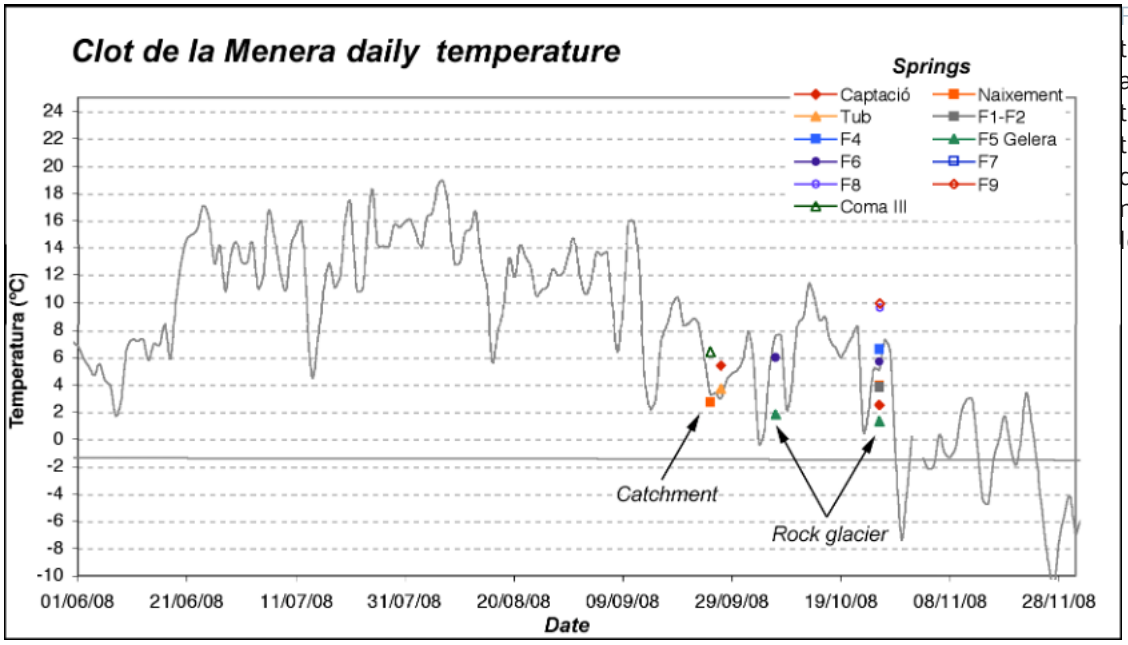

Figure 8. Daily temperature from summer 2008 at 2083 m a.s.l. and the temperature of the water springs from the Clot de la Menera over 2200 m a.s.l. Original from Igeotest (2008).

Deuterium and Oxygen-18

Analysing Tritium, Deuterium, Oxygen-18 and Carbon-13 and Carbon-14 content of two water samples collected at Clots de la Menera (Figure 9), allows determining the origin of the groundwaters (2H - 18O – 13C) and their age (3H and 14C).

A total of 2 samples were analysed and collected on the same day, the 25th October 2008. The results were analiticaly processed in the Jaume Almera Institute (CSIC). The ∂D was -65.3 ‰ in the catchment and -65.2 ‰ in the spring, while the ∂18O was -10.2 ‰ in the catchment and -10.26 ‰ in the spring, the excess of deuterium ΔD was 16.3 in the catchment and 16.88 in the spring, calculated according to the well known equation ΔD=∂D-8∂18O (Custodio and LLamas, 1996). The ∂D- ∂18O plot (Figure 10) show the relative isotopic fractionation of the two isotopes comparing to the global meteoric waters obeying to ∂D=8·∂18O+10 (Custodio and Llamas, 1996, and references therein).

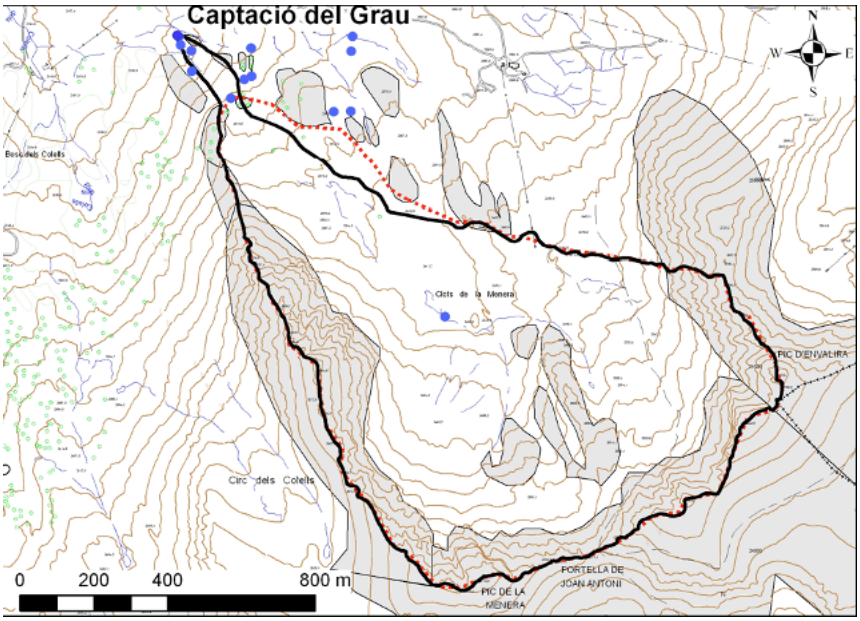

Figure 9. Localization of the Clot de la Menera and the isolated spring having an anomalous low temperature of the water (in the middle of the figure) and a spot of springs around the catchment for the ski resort on top of the figure. Original from the technical report of Igeotest (2008).

The samples fall into the left of the global meteoric water line (GMWL), indicating that these waters have not undergone any evaporation process. Usually, values ΔD > 10 ‰ may from areas having a high lack of moisture deficit (Custodio and LLamas, 1996) tipical from precipitation comming from the Mediterranean and not from the Atlantic (Igeotest, 2008). The Andorra local meteoric water line (LMWL) is ∂D=8·∂18O+13.3 (Figure 11) accordingly to a Mediterranean influence and relatively low moisture (Igeotest, 2008).

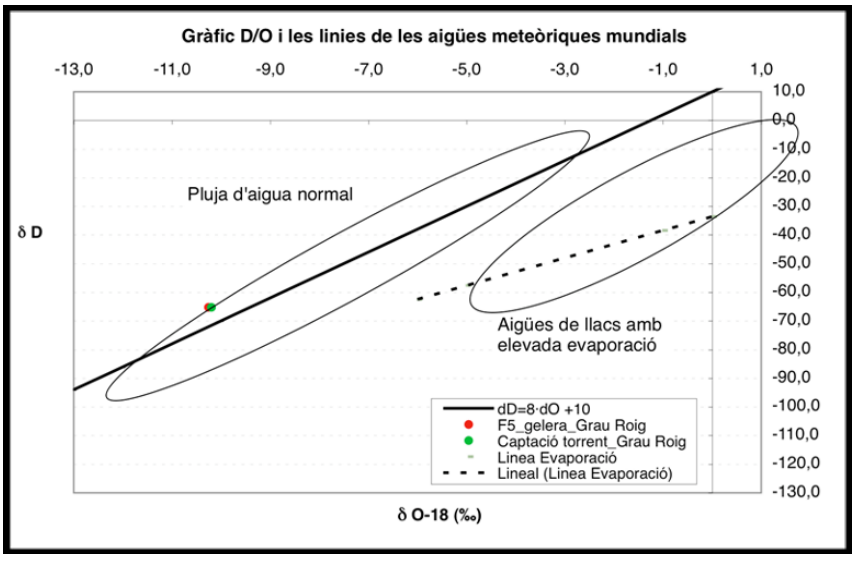

Figure 10. Solid line the Global Meteoric Water Line. Doted line the behaviour of meteoric waters that experienced evaporation. Original from the technical report of Igeotest (2008).

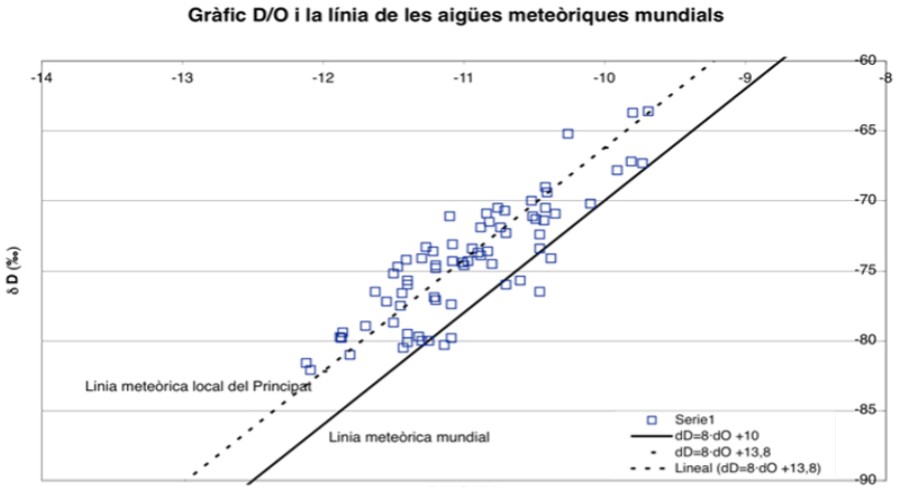

Figure 11. Local Meteoric Water Line (LMWL) of Andorra (dotted line) and the GMWL (solid line) conducted between 2000 and 2008. Original from the technical report from Igeotest (2018).

The ∂18O data allows to obtain the infiltration height of the samples. Because isotope values of the precipitation had some variability, a relationship between both parameters over a long period (5-10 years) may reduce biases. However, Andorra is exposed to some additional variability within the Pyrenees (Figure 12), also shown by palaeoclimate models (WRF model) from Ludwig et al. (2018), that should be aware because do not allow applying the same regression line throughout the Principality. Differences between the W-S and NE sector of Andorra and the NNE area exist (Igeotest, 2008). In the first case the gradient adjusts to 0.26‰ for every 100 meters and for the second area the gradient is close to 0.28‰ every 100 meters. So, for Grau-Roig the reference correspond to the W-S-NE sector must be applied (Figure 13). Doing the latter, a recharge altitude of 2580 ± 100 m is for the catchment located at 2208 m a.s.l. and 2602 ± 100 m is for the particular spring located at 2414 m a.s.l.

The results cannot be taken as absolute values because analytical errors accompaining the measurements are, in this case, of ± 0.2 ‰ for ∂18O and ± 2‰ for ∂D, conducting to calculation error of 40-50 meters for every 0.1 ‰ ∂18O of analytical error (Yehdegho & Reichl, 2002).

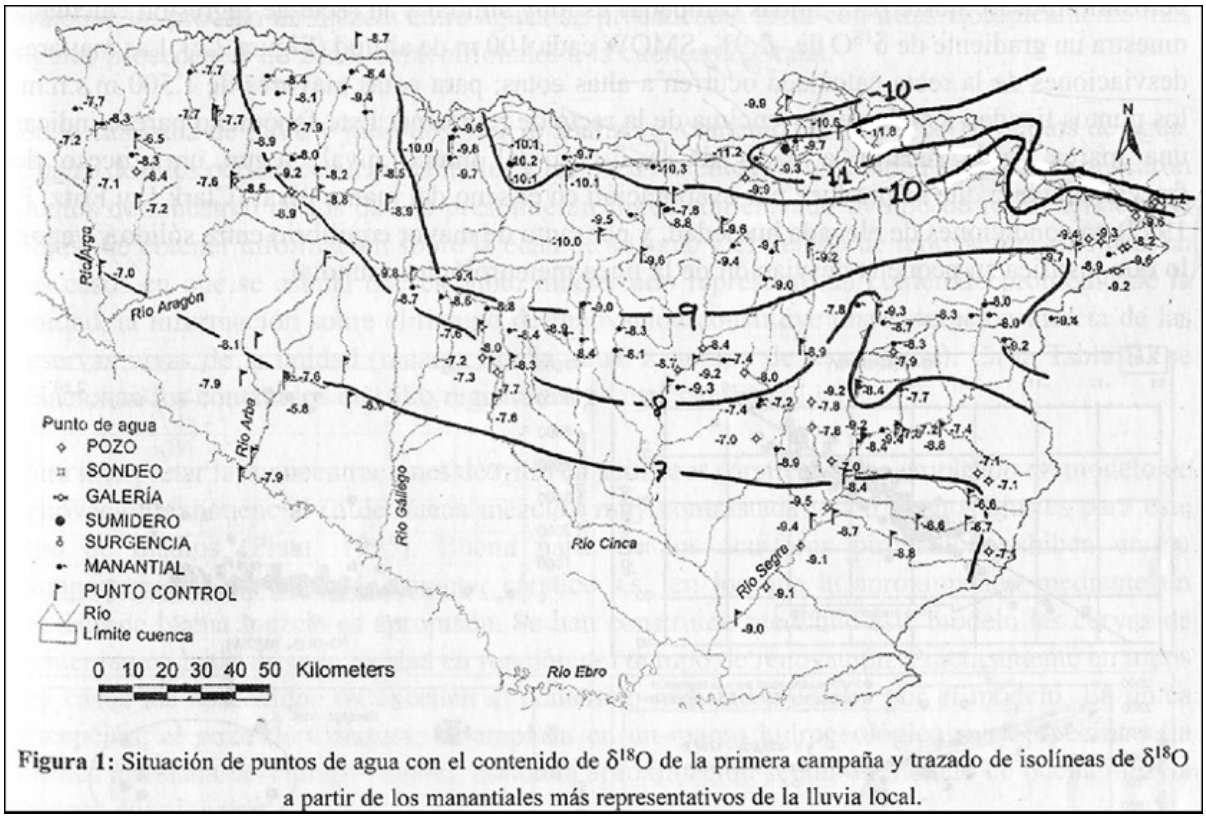

Figure 12. Modified from Arce et al. (2001) showing the anomalous isotope elbow folded isolines within the Principality (original from the technical report of Igeotest 2008).

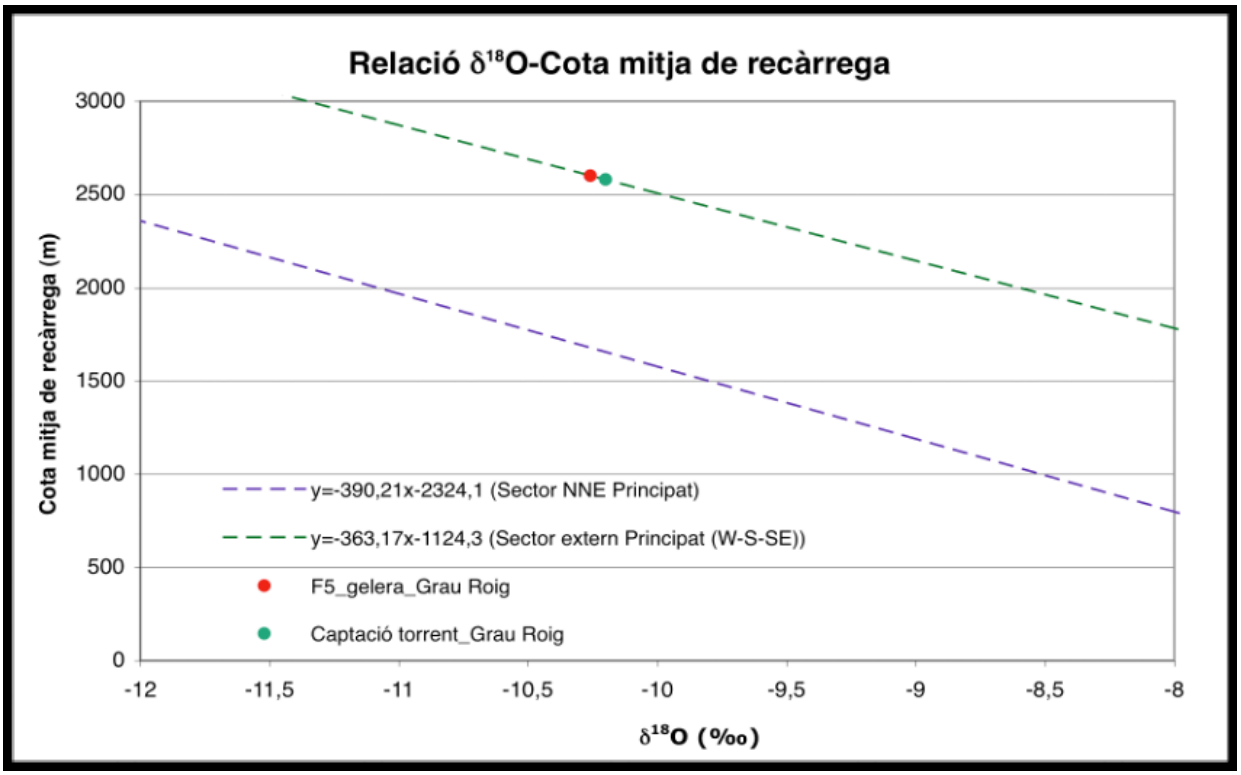

Figure 13. Infiltration altitude for the Clot de la Menera samples. Red point the particular spring, green dot at the catchment. Original from the technical report from Igeotest (2008).

Tritium

The samples were analysed at the "Centro de Estudios de Técnicas Aplicadas (CETA)" of CEDEX (Centro de Estudios y Experimentación de Obras Públicas) in Madrid, to determine the tritium content by using the electrolytic concentration method. The units of measurement of tritium content are in UT, which correspond to a ratio 3H/1H equal to 10-18 atoms. The result from the above mentioned samples were of 6.38 ± 0.43 sampled the 06th October 2008 in the spring and 6.64 ± 0.44 in the catchment, sampled the 25th.

DIC radiocarbon AMS results

The resulting ages refer to RCYBP (radiocarbon years past present, where "present" = AD 1950). By international convention, the modern reference standard is 95% of the 14C activity of the National Institute of Standards and Technology (NIST) Oxialic Acid (SRM 4990C) and calculated using Libby's half- life (5568 years). The 13C/12C ratio (∂13C) measurement has been calculated relative to the PDB-1 standard. The result from the above mentioned samples were of 450 ± 40 yrs. BP and ∂13C = -8.7 ‰ for the spring and 1,110 ± 40 yrs. BP and ∂13C = -10.7 ‰ for the catchment, both sampled the 25th October 2008.

The last glaciers in Andorra

The last glacial ice evidence is directly inferred from very cold springwater from the Clot de la Menera rock glacier, located at 2414 m a.s.l. at Grau-Roig (upper Valira d'Orient basin). Their tritium content and moderate 14C activity advocates for a mixing of young waters of meteorological origin and old waters of unknown age.

Both empirical methods converge at the end of the Younger Dryas and the beginning of the Holocene (10,900 – 11,820 yrs cal BP). At that time the Clot de la Menera rock glacier was active and an ice core may remained in beneath during the Holocene. The original position of the rock glacier boulders may change during the melting of the ice core, and such boulders are still moving.

Empirical approach

An empirical approach allows determining the factor better in directly defining the assumed age of disolved inorganic carbon (DIC) in groundwaters. The last was by Verhagen et al. (1991) applied in systems where the groundwater incorporated post-nuclear CO2, as evidenced by the occurrence of measured tritium activities more significant than the background, and involves the construction of a "3H/14C" diagram (Figure 14). The appropriate initial 14C activity is then assumed to occur where the curve intersects the tritium detection limit; however, the large analitical error determining tritium produces a large range of possible 14C activity (54 < Ao < 31.5 pMC). The basic reasoning here is that a groundwater sample not containing "bomb" tritium will also be free of anthropogenic 14C. Applying the correlation laws from Figure 14, the range is from 5045 – 9548 yrs. BP. The calibrate age may range 5,790 – 10,900 yrs. cal BP by using Reimer et al. (2020) calibration datasets.
Nevertheless, aquifer systems incorporating an increasing tritium content by the flow (open system), the mean residence time rather than the water age of groundwater may be estimated by applying the exponential model to the specific activity of tritium. The tritium exponential model is known for Andorra and was made by Plata-Araguas in 2008 (Figure 15) as an average of Madrid and Thonon-Les-Bains from the International Atomic Energy Agency database (IAEA/WMO, 2008).

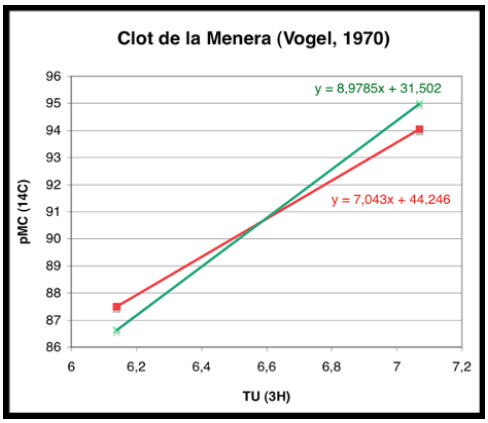

Figure 14. Pairs of values from the particular spring and the catchment at Clot de la Menera plotted twice depending on the analytical error of tritium.

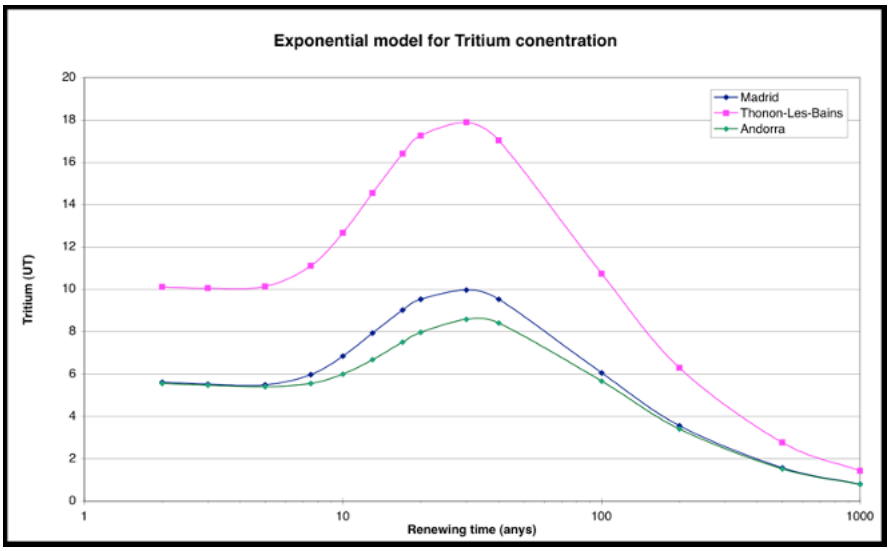

Figure 15. Exponential model of Tritium renewing time. To reduce the computing time consuming and potential errors, a full year has been divided by 10 portions. For a given value of 6 Ut a couple of ages are possible, 9 years and 90 years, because the exponential curve is intersected twice.

If the contribution of the old and modern water is known by modeling, the latter can be also applied to the 18O content obtaining the original recharging altitude solving the isotopic dilution (A x+ B [1-x] = C). Old water concentration (A) and recent water concentration (B) will show an apparent age (C) depending on their proportion (x). For the Clot de la Menera, proportions are known from the technical report of (Igeotest, 2008) being 4% of old water for the catchment and a higher portion of contribution (9%) for the spring, because the last is older. Thus, applicating the same proportion to the 18O concentration for the spring (-10,2 ‰) and the catchment (-10.26 ‰) regarding their apparent recharge altitude of the spring (2602 m a.s.l.) and the catchment (2580 m a.s.l.), the corresponding altitudes applying a 9% and 4% respectively the recharge height are practically the same, 2932 m a.s.l. for the spring and 2928 m for the catchment.

Since the exponential model of infiltration matches for the open framework of the rock glacier aquifer, by applying an exponential best fit between both apparent values and 14C activity (Figure 16), an original activity ranging 24.85 for the spring and 27.49 for the catchment is obtained. Their radiocarbon age range between 11,510 – 10,675 yrs. BP, and calibrating by using Calib 8.2 software allowed by Reimer et al. (2020) calibration datasets, the age of the meltwater is 13,050 ± 430 yrs. cal BP for one sigma and ranging

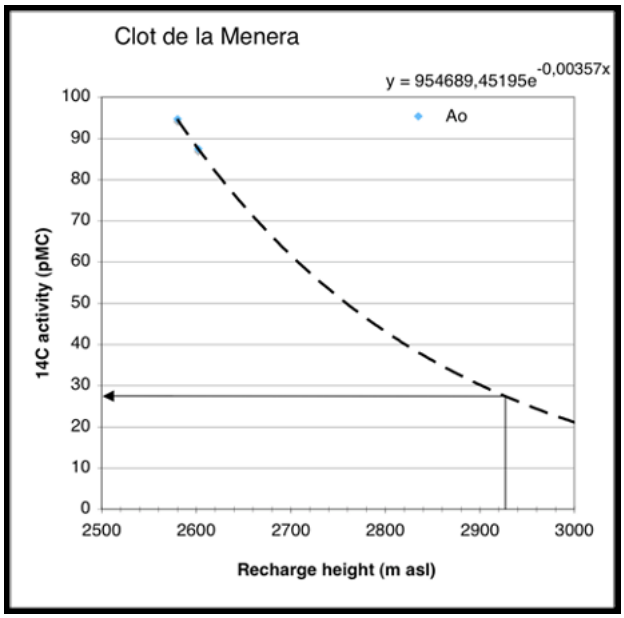

Figure 16. Exponential best fit for the original 14C activity of the melting waters from the Clot de la Menera rock glacier.

Latest activities in Clot de la Menera

During MOMPA project (Interreg V-A Spain-France-Andorra program POCTEFA 2014-2020) interferometric SAR technique has been used in the Pyrenees (Barra et al., 2017), including Clot de la Menera area. The medium-resolution satellite images (4 x 14 m2) were from Sentinel-1 satellite (descending geometry) for the 2015-2019 period. Figure 17 shows the map of the obtained deformation velocities in the line-of-sight, with an average sensitivity of 3.5 mm/yr. Measurements show movements of boulders from Clot de la Menera rock glacier, within the sensibility range of the method (Figure 17), interpreted in this work as a fingerprint of the ice melting (Figure 18).

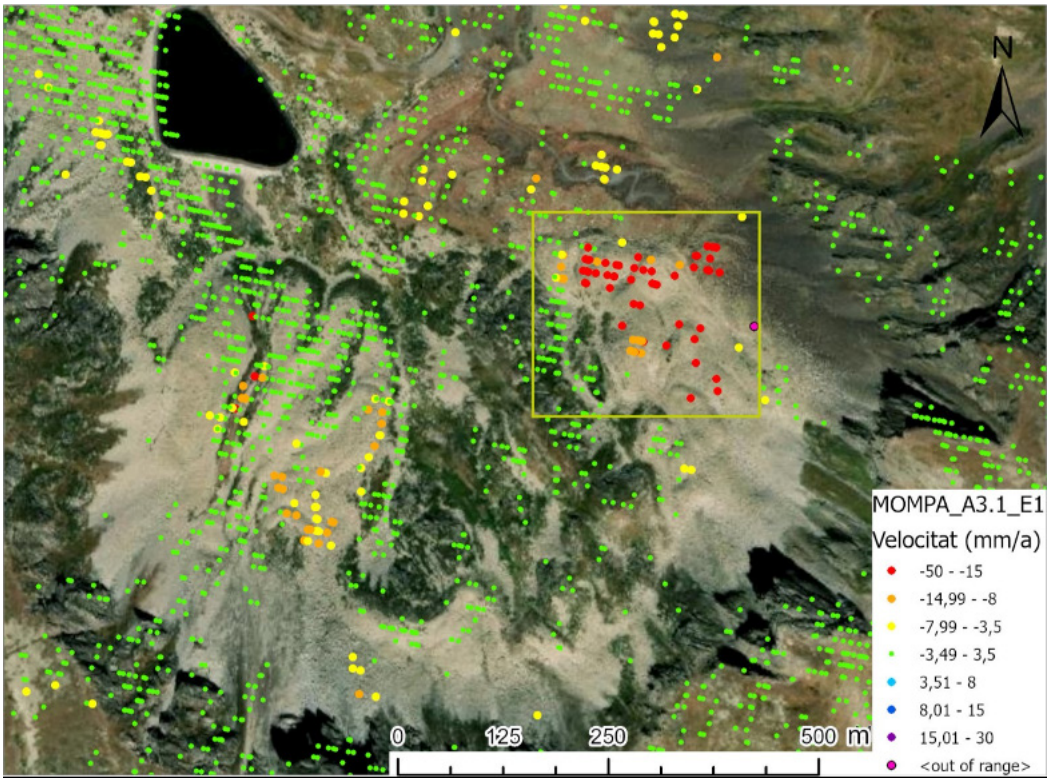

Figure 17. InSAR velocities of the Clot de la Menera rock glacier masses. Dots are mainly boulders that have moved, especially red dots (higher movements).

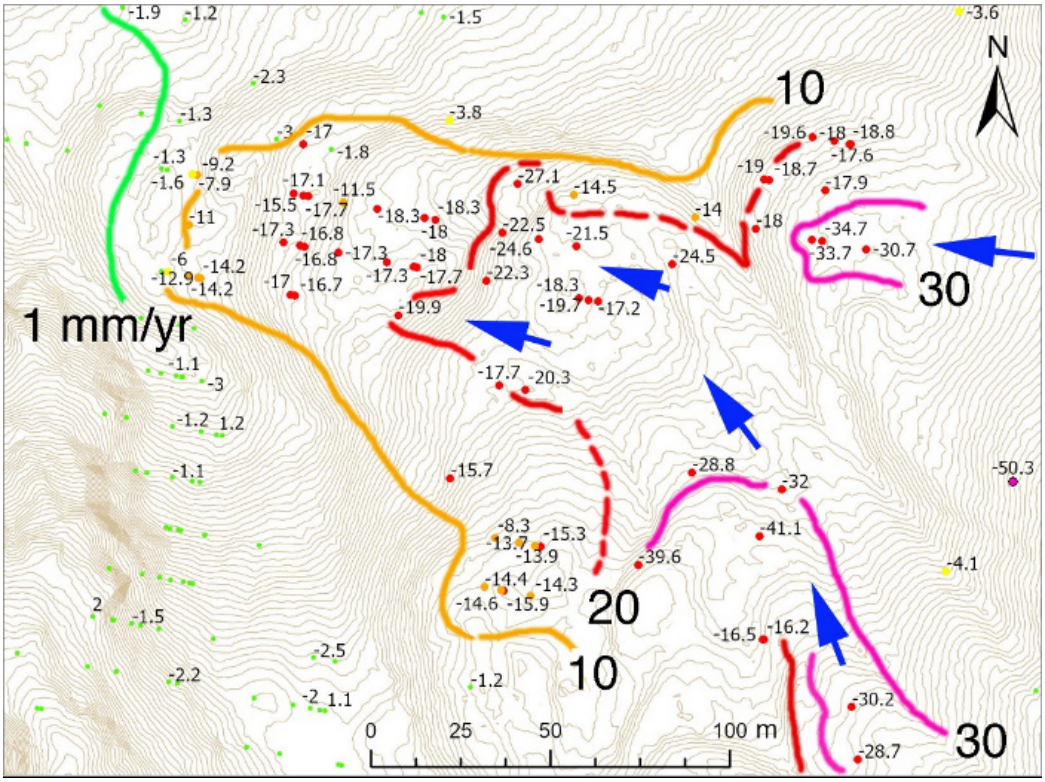

Figure 18. Movement interpretation (mm/yr) in the Clot de la Menera E rock glacier (yellow square in Fig. 17). Subsidence or flow.

With the intention of continuing the studies in the rock glaciers of the Clot de la Menera, in September 2022 a series of continuous temperature sensors (dataloggers) were installed at 90-50-20-10 and 5 cm (Figure 19) in the upper area of the frontolateral lobe (right) at 2533 m a.s.l. (GR-2). In future campaigns, electrical surveys and drilling (15 m) are planned to install temperature sensors to map and monitor the existing permafrost.

Figure 19. .Installation of dataloggers in the Menera rock glacier.

3 Sant Cristòfol d'Anyòs

Presentation of La Massana glacial complex. Formation of a paleolake by the obturation of the main glacier (Valira glacier).

The the ice-dammed palaeolake area - Valira del Nord basin

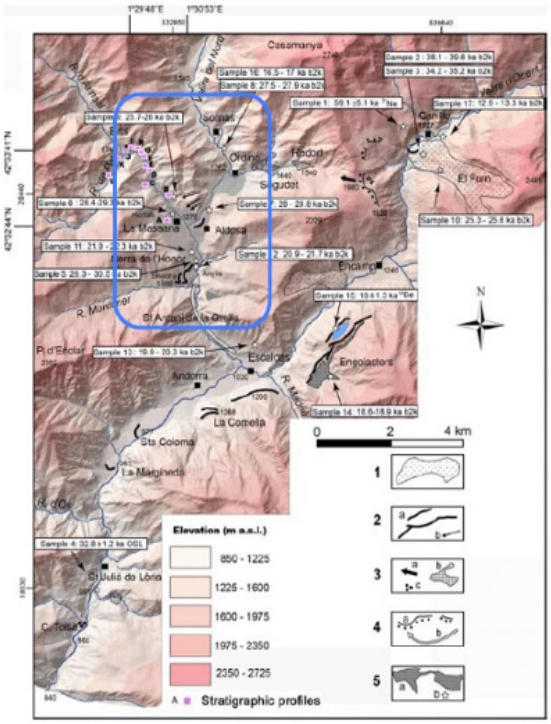

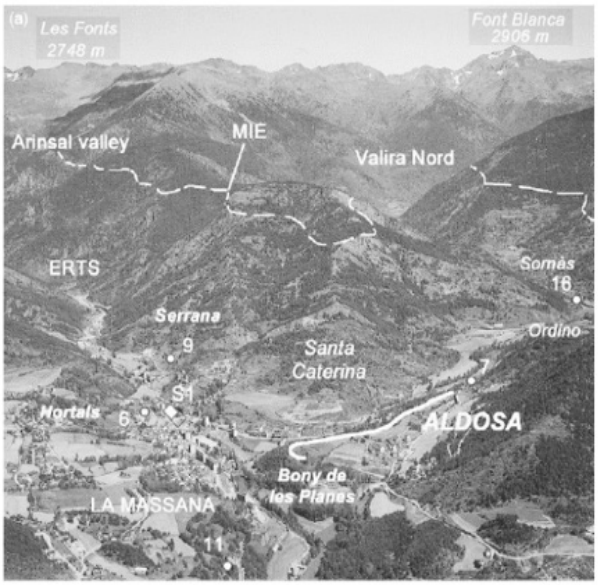

Turu et al. (2016)

The La Massana palaeolake

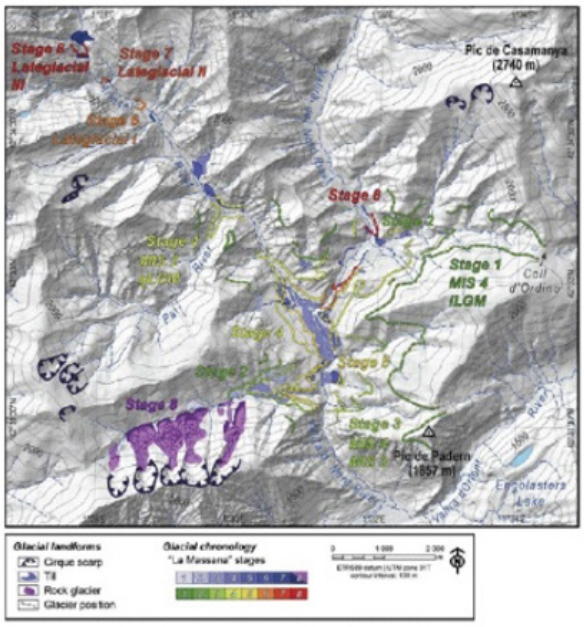

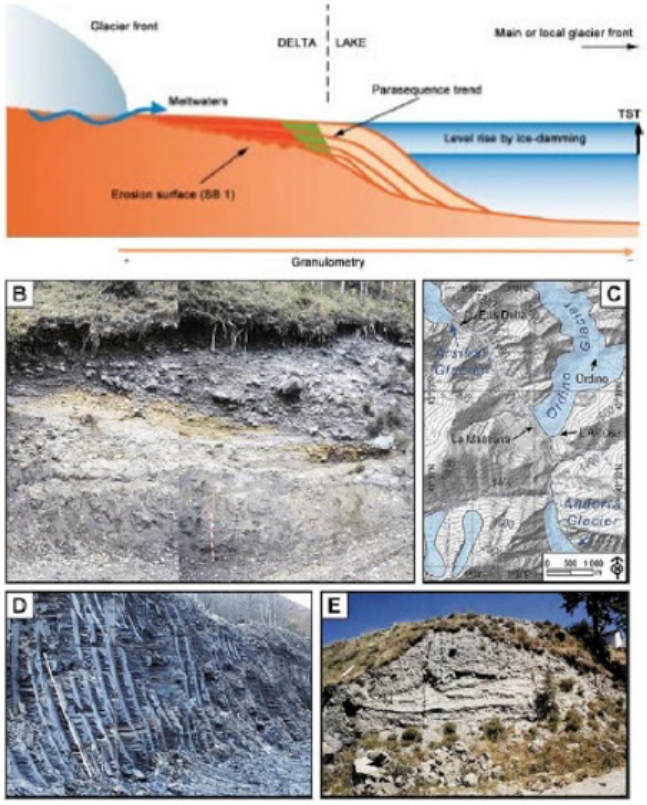

Ventura & Turu (2022)

The base level signification within the palaeolake

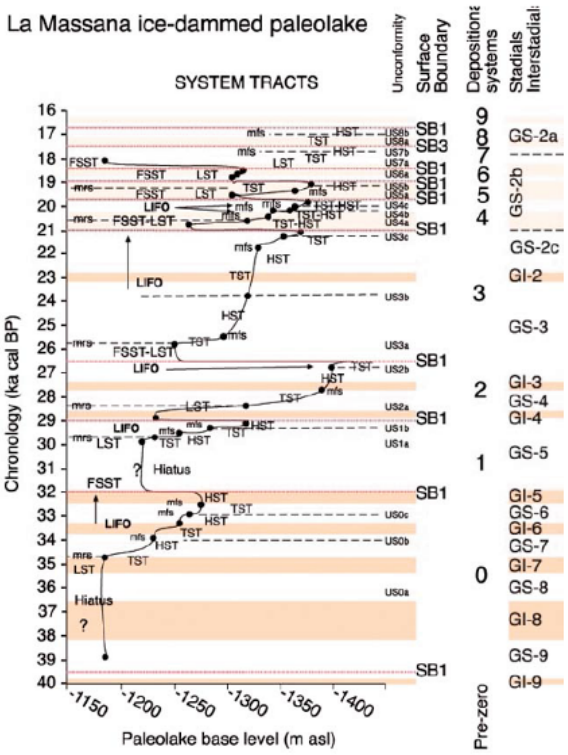

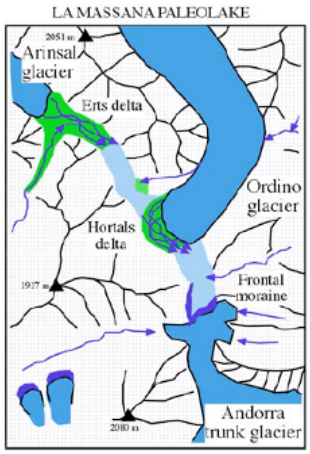

Turu and Bordonau (1997) modified

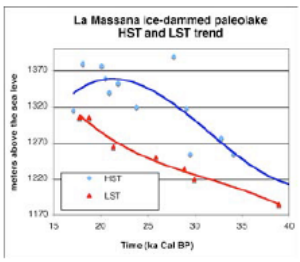

Meltwater overfed glaciers during LGM
Turu (2018

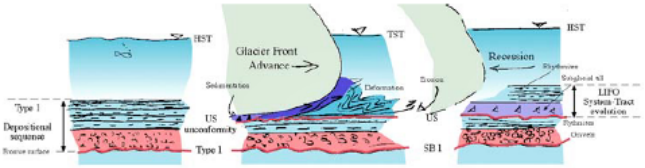

Turu et al (2018)

Sub-Milankovich cycles palaeoenvironmental signification, the P cycles

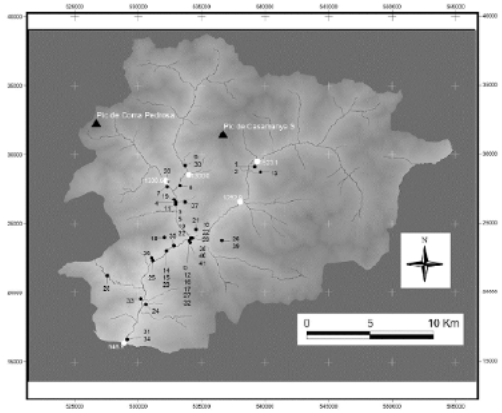

Sampled sites from Andorra

P cycles are related with low base levels falls observed in the western mediterranean shelves and the eastern Atlantic coast (Cádiz Gulf and Ria de Muros Galicia). Hernández-Molina et al. (1994)

Quick shifting of depleted δ13C to enhanced values

4.5 ± 0.5 ka to recover values of -25‰ for δ13C

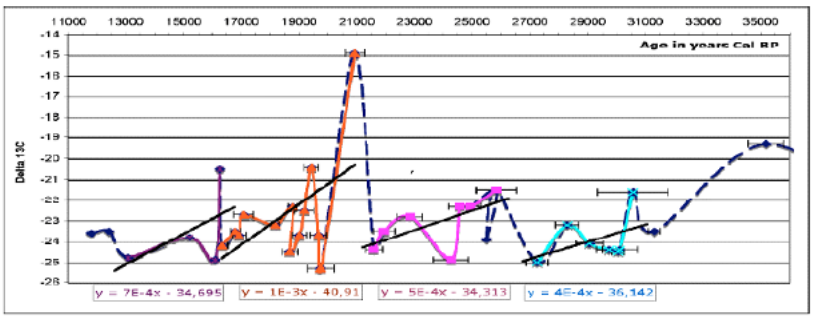

4 Engolasters lake

Different lateral moraines, deposits in the Andorra la Vella overdeepened basin.

The situation of the stop area

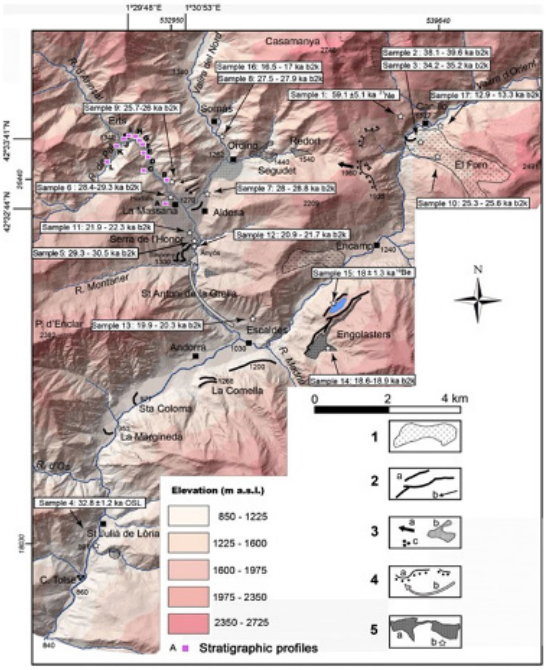

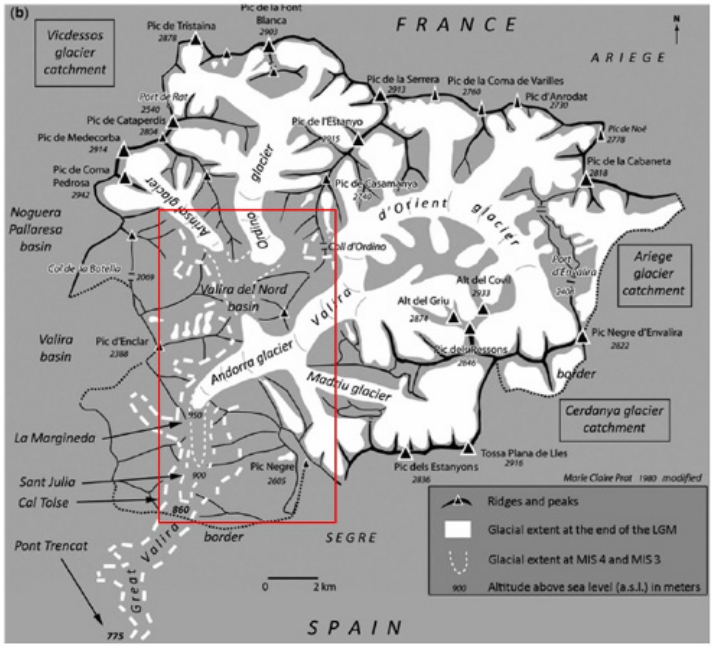

Turu et al. (2007, 2016)

The geomorphology of the main valley of Andorra

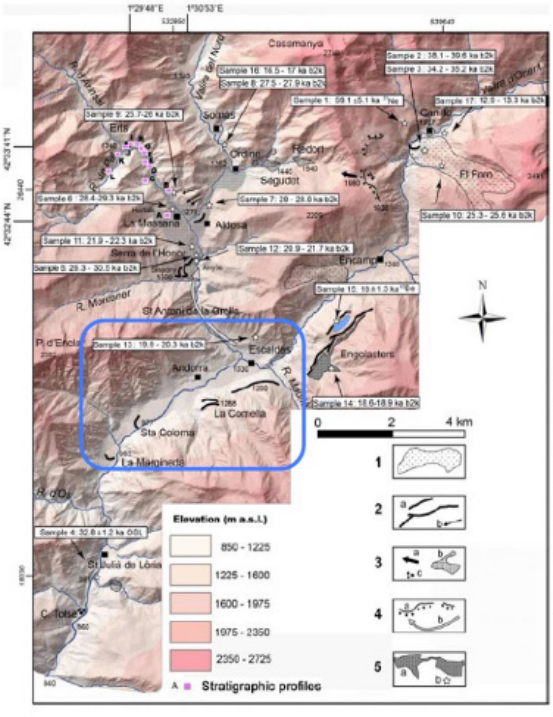

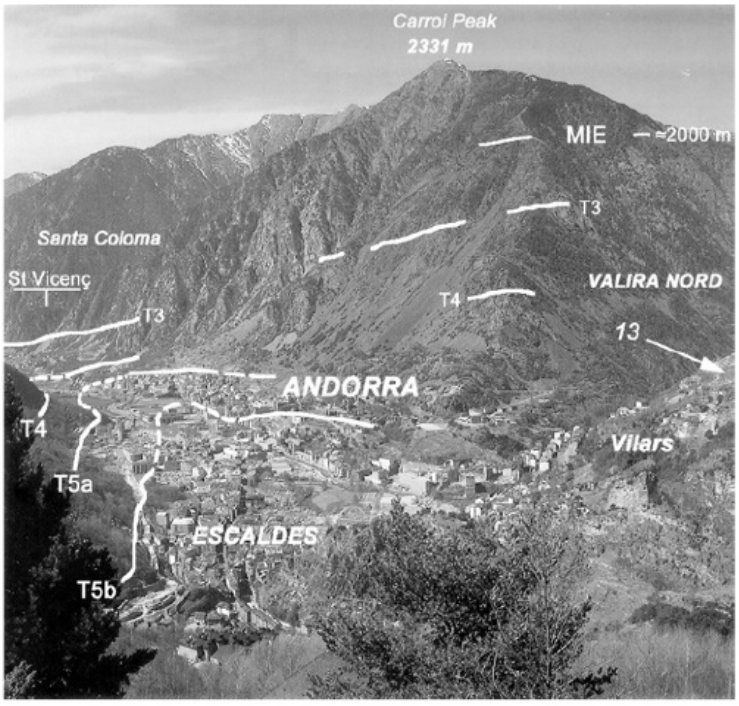

Turu et al. (2016)

The overdeepened valley of Andorra - Escaldes (Geomechanics)

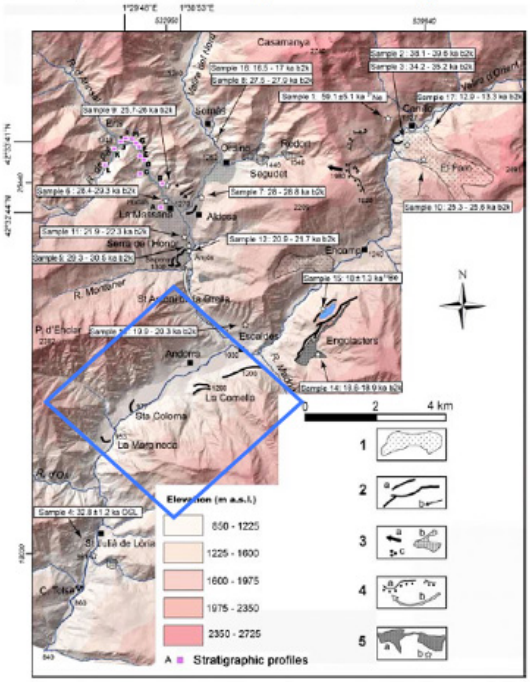

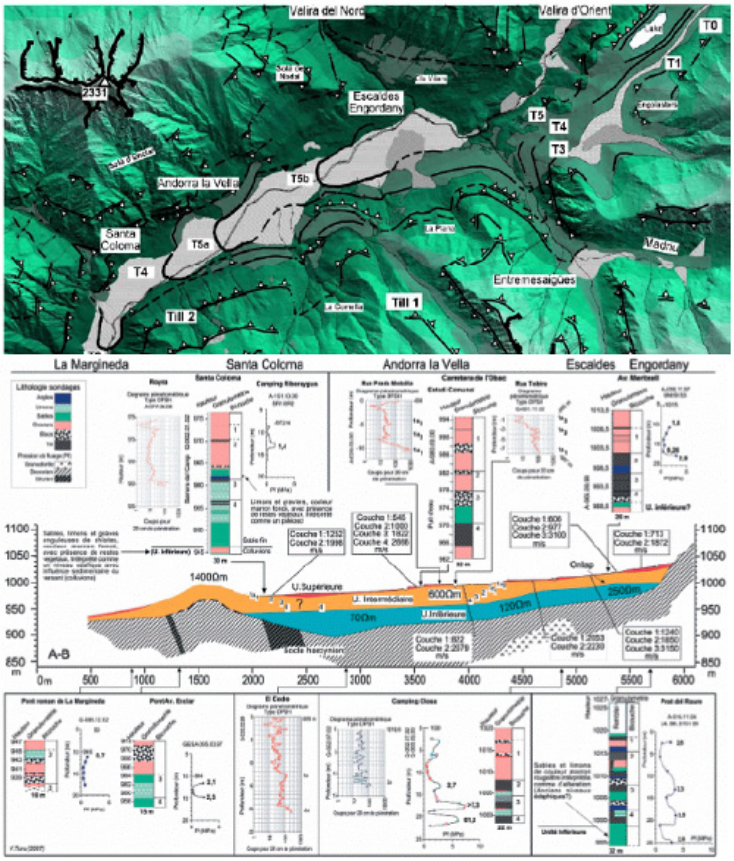

Turu et al. (2007)

Glaciotectonites and ice load pressures

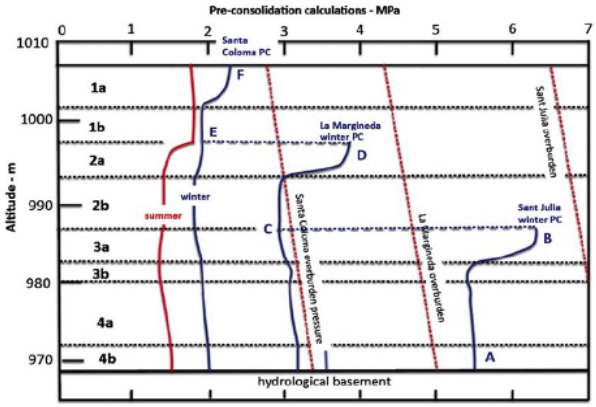

Computed overburden pressures (Turu, 2023)

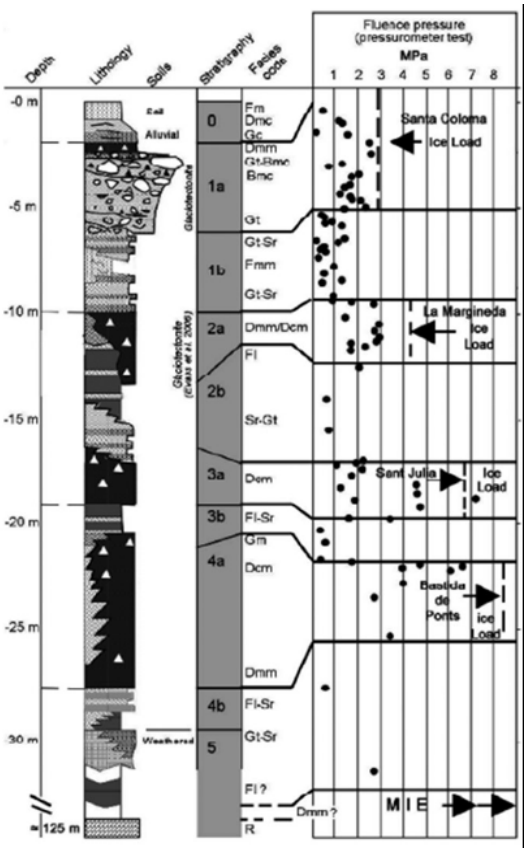

5 La Margineda.

Visit to the outcrops of the Aixovall frontal moraine (Valira Glacier).

The Santa Coloma and La Margineda end-moraines

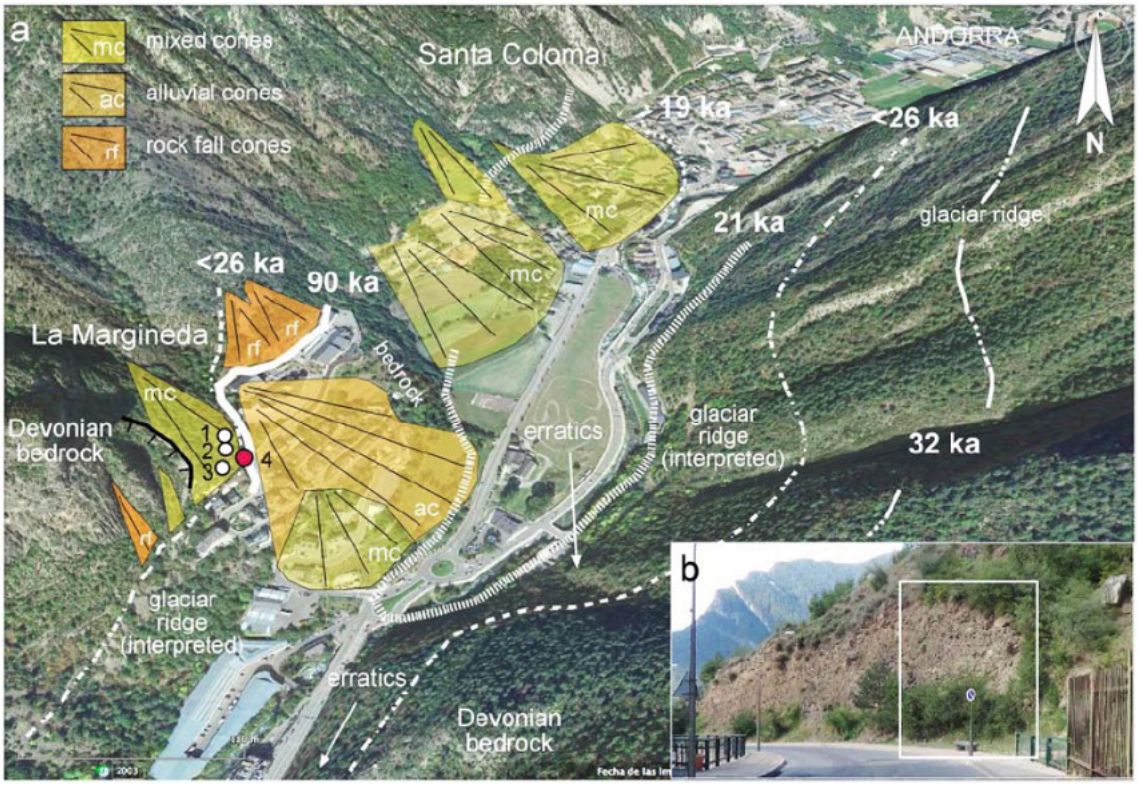

Turu et al. (2023)

Santa Coloma glaciotectonite: the impact, the subglacial drainage

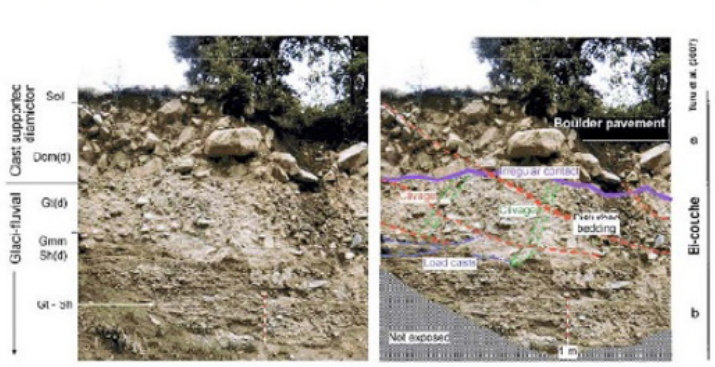

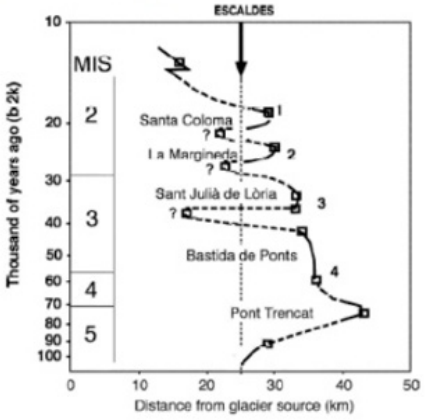

Turu & Peña-Monné (2006); Turu et al. (2023)

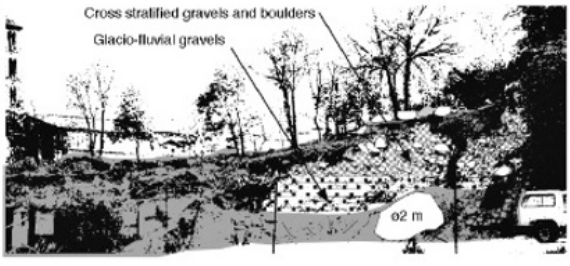

The Valira down stream - The narrower valley of Sant Julià de Lòria

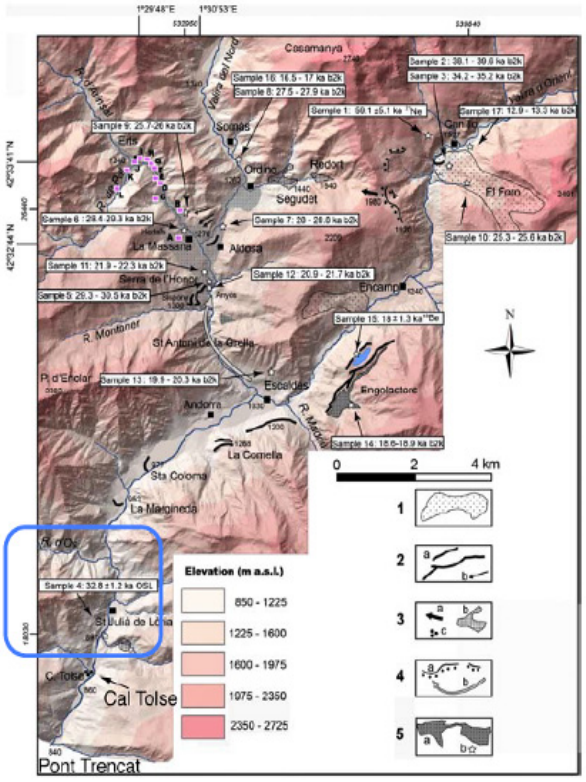

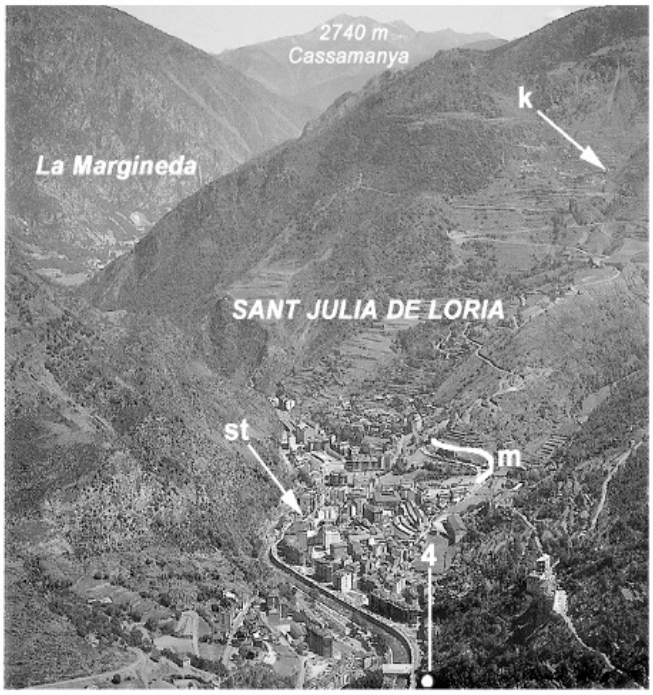

Turu et al. (2016)

The Valira down stream - The narrower valley of Sant Julià de Lòria

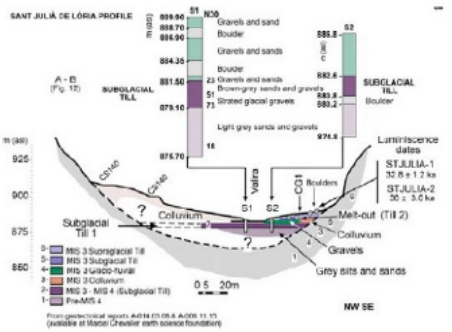

4

Cal Tolse

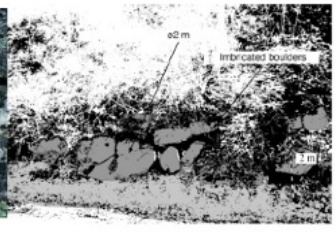

Pont Trencat

Turu & Peña-Monné (2006); Turu et al. (2023)

6

Castellciutat - La Seu d'Urgell

View of the Valira-Segre terrace system and the Tossal Bordar moraine (Valira Glacier).

Torre Solsona belvedere

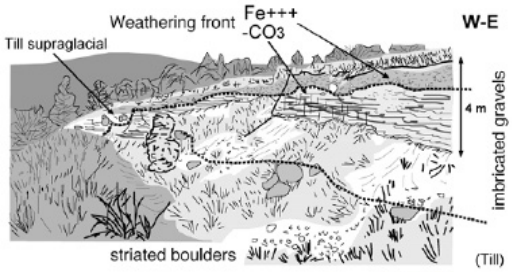

Glacio-fluvial terrace and end-moraine at Tossal Bordar

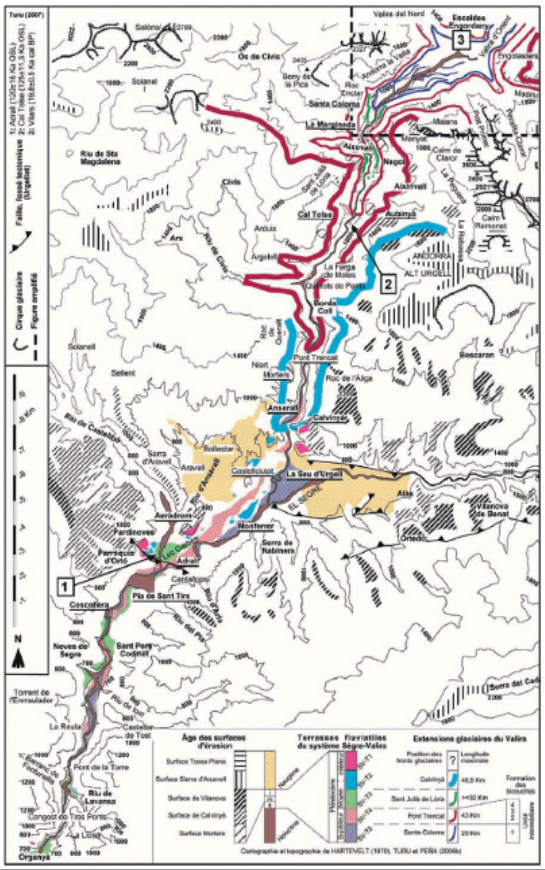

Turu and Peña-Monné (2006) – Turu et al. (2007)

The Valira end moraines

Valira glacier terminal complex (SE Pyrenees)

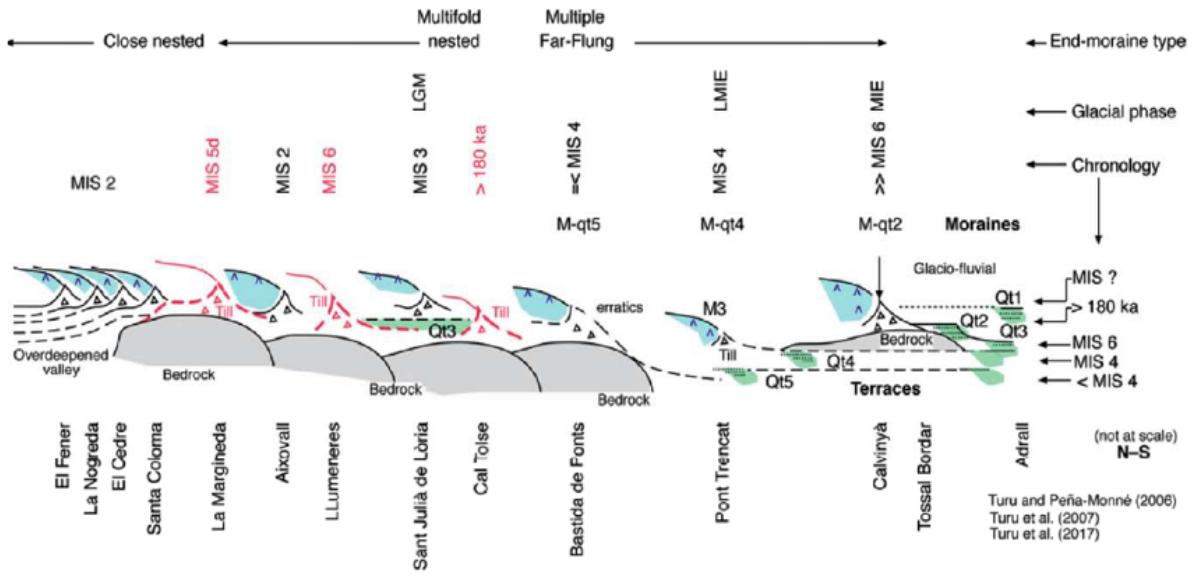

Turu et al. (2023)

REFERENCES

- BARRA, A., SOLARI, L, BÉJAR-PIZARRO, M., MONSERRAT, O., BIANCHINI, S., HERRERA, G., CROSETTO, M., SARRO, R., GONZÁLEZ-ALONSO, E., MATEOS, R.M., LIGÜERZANA, S., LÓPEZ, C., and MORETTI, S., 2017 – A Methodology to Detect and Update Active Deformation Areas Based on Sentinel-1 SAR Images. Remote Sensing, 9(10), 1002.
- BECAT, J., 1993 – Les Pyrénées méditerranéennes, mutations d'une economie montagnarde: le cas d'Andorre. Phd. Thesis from the Montpellier University III (France).
- CUSTODIO, E., LLAMAS, M.R. (1996). Hidrología subterránea. Ediciones Omega, 1157 pp.
- DEVANTHÉRY, N., CROSETTO, M., MONSERRAT, O., CUEVAS-GONZÁLEZ, M.,and CRIPPA, B., 2014 – An approach to persistent scatterer interferometry.Remote Sensing, 6(7), pp. 6662–6679.
- HERNÁNDEZ, A., SÁEZ, A., SANTOS, R.S., RODRIGUES, T., MARTINPUERTAS, C., GIL-ROMERA, G., ABBOTT, M., CARBALLEIRA, R., COSTA, P., GIRALT, S., GOMES, S.D, GRIFFORE, M., IBAÑEZ-INSA J.,
- LEIRA, M., MORENO, J., NAUGHTON, F., OLIVEIRA, D., RAPOSEIRO, P.M., TRIGO, R.M., VIEIRA, G., RAMOS, A.M., 2022 – The timing of the deglaciation in the Atlantic Iberian mountains: insights from the stratigraphic analysis of a lake sequence in Serra da Estrela (Portugal). Earth Surface Processes and Landforms. DOI: 10.1002/esp.5536
- IAEA/WMO 2008 – Global Network for Isotopes in Precipitation. The GNIP Database Consultable en: http://www-naweb.iaea.org/napc/ih/GNIP/IHS_GNIP.html
- IGEOTEST 2008 – Perímetres de protecció de la captació del Grau, Grau Roig. Parròquia d'Encamp. Expedient núm. D-020-ACE-028.09.08.
- MCCALPIN, J. AND COROMINAS, J., 2019 – Postglacial deformation history of sackungen on the northern slope of Pic d'Encampadana, Andorra;Geomorphology, 337, 134-150: https://doi.org/10.1016/j.geomorph.2019.04.007
- REIMER P.J., AUSTIN W.E.N., BARD E., BAYLISS A., BLACKWELL P.G., BRONK-RAMSEY C., BUTZIN M., EDWARDS R.L., FRIEDRICH M., GROOTES P.M., GUILDERSON T.P., HAJDAS I., HEATON T.J., HOGG A., KROMER B., MANNING S.W., MUSCHELER R., PALMER J.G., PEARSON C., VAN DER PLICHT J., REIM RICHARDS DA, SCOTT EM, SOUTHON JR, TURNEY CSM, WACKER L, ADOLPHI F., BÜNTGEN U., FAHRNI S., FOGTMANN-SCHULZ A., FRIEDRICH R., KÖHLER P., KUDSK S., MIYAKE F., OLSEN J., SAKAMOTO M., SOOKDEO A., TALAMO S., 2020. The IntCal20 Northern Hemisphere radiocarbon age calibration curve (0-55 ka cal BP); Radiocarbon, 62.: https://doi.org/10.1017/RDC.2020.41
- REIXACH T., DELMAS M, BRAUCHER R. GUNNELL, Y., MAH, C., CALVET, M. 2021 Climatic conditions between 19 and 12 ka in the eastern Pyrenees, and wider implications for atmospheric circulation patterns in Europe. Quaternary Science Reviews 260, 106923.https://doi.org/10.1016/j.quascirev.2021.106923
- TURU V., BORDONAU J.,1997 – El glacialisme de les valls de la Valira del Nord (Principat d'Andorra): Síntesi d'Afloraments. Annals 1995 de l'IEA, Barcelona (Spain), 41-104.
- URU V., PEÑA-MONNÉ J.L., 2006 - Ensayo de reconstrucción cuaternaria de los valles del Segre y Valira (Andorra - La Seu d'Urgell - Organyà, Pirineos Orientales): morrenas y terrazas fluviales. In A. Pérez-Alberti y López-Bedoya, J. (eds.), Geomorfologia y Territorio: IX Reunió Nacional de Geomorfología USC, Santiago de Compostela, (España), 129-148
- TURU V., BOULTON G. S., ROS X., PEÑA-MONNÉ J. L., MARTÍ-BONO C., BORDONAU J., SERRANO-CAÑADAS E., SANCHO-MARCÉN C., CONSTANTE-ORRIOS A., POUS J., GONZÁLEZ-TRUEBA J. J., PALOMAR J., HERRERO R., GARCÍA-RUIZ J. M. 2007 – Structure des grands bassins glaciaires dans le nord de la Péninsule Ibérique: comparaison entre les vallées d'Andorre (Pyrénées Orientales), du Gállego (Pyrénées Centrales) et du Trueba (Chaîne Cantabrique). Quaternaire, 18, 309–325. https://doi.org/10.4000/quaternaire.1167

- TURU V., CALVET M., BORDONAU J., GUNNELL Y., DELMAS M., VILAPLANA J.M., JALUT G., 2016 – Did Pyrenean glaciers dance to the beat of global climatic events? Evidence from the Würmian sequence stratigraphy of an ice-dammed palaeolake depocentre in Andorra. In Hughes, P. D. & Woodward, J. C. (eds), Quaternary Glaciation in the Mediterranean Mountains, Geological Society, London, Special Publications, 433(1), 111-136, http://doi.org/10.1144/SP433.6
- TURU V., 2018 – High resolution chronostratigraphy from an ice-dammed palaeo-lake in Andorra: MIS 2 Atlantic and Mediterranean palaeo-climate inferences over the SE Pyrenees. In Aiello, G. (Ed). New insights into the stratigraphic setting of Paleozoic to Miocene Deposits, InTechOpen, London (UK). http://doi.org/10.5772/intechopen.81395
- TURU V., PEÑA-MONNÉ J.L., CUNHA P.P., JALUT, G., BUYLAERT J-P., MURRAY A.S., BRIDGLAND, D., FAURSCHOU-KUNDSEN, M., OLIVA, M., CARRASCO, R.M., ROS-VISÚS X., TURU-FONT L., VENTURA V., 2023 – Glacial–interglacial cycles in the south–central and south-eastern Pyrenees since ~180 ka (NE Spain-Andorra-SE France). Quaternary Research. DOI: 10.1017/qua.2022.68
- VENTURA, J., TURU, V. (2021) The glaciers of the Central-Eastern Pyrenees. In: Oliva, M., Palacios, D., Fernández-Fernández, J. M. (Eds.). Iberia, Land of Glaciers: How The Mountains Were Shaped By Glaciers. Elsevier, 87-121. DOI: https://doi.org/10.1016/B978-0-12-821941-6.00006-2
- VERHAGEN, B. T., 1991 – Detailed geohydrology with environmental isotopes; A case study at Serowe, Botswana. In: Isotope techniques in water resources development, IAEA, Vienna 345-362.
- VOGEL, J.C., 1967 – Investigation of groundwater flow with radiocarbon. Isotopes in Hydrology. IAEA, Vienna, 355–36.

4 Field trip to:

Núria valley and Puigmal massif, Vall de Ribes-Ripollès

Salvador Franch, F.[1], Garcia-Oteyza, J.[1], Palet Martínez, J.M.[2]

[1]Universitat de Barcelona
[2]Institut Català d'Arqueologia Clàssica

EUROPEAN CONFERENCE ON PERMAFROST

19-23 JUNE, 2023, PUIGCERDÀ

Núria valley and Puigmal massif, Vall de Ribes-Ripollès

Salvador Franch, F.[1], Garcia-Oteyza, J.[1], Palet Martínez, J.M.[2]

[1]Universitat de Barcelona
[2]Institut Català d'Arqueologia Clàssica

INTRODUCTION

Núria valley (with a southern orientation) and the Puigmal massif are located in the easternmost glaciated mountain unit of the Pyrenees.

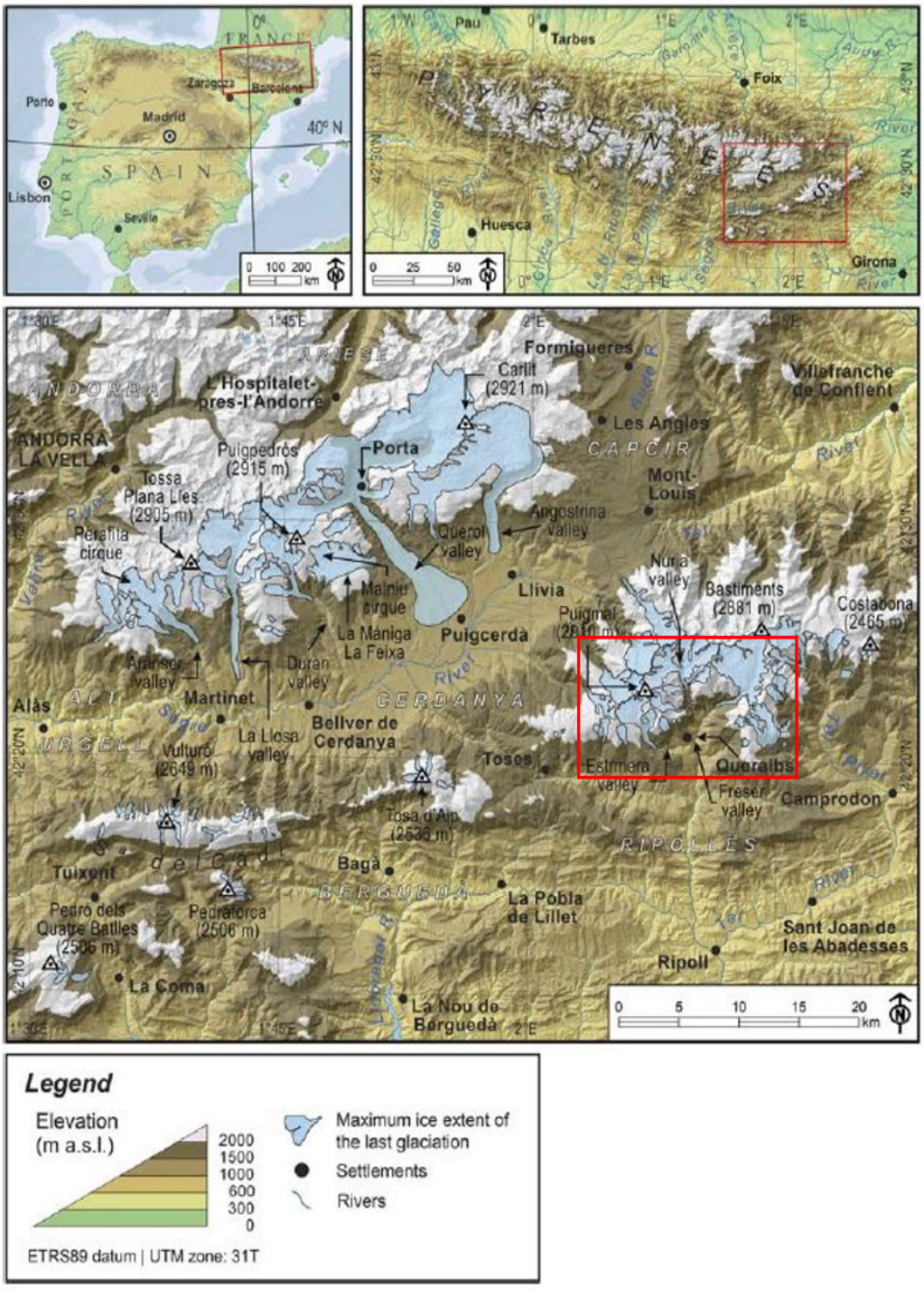

Figure 1. Location of Núria and the Puigmal massif in the Southeastern Pyrenees, and delimitation of the glaciers during their local maximum expansion (ILGM) (Salvador-Franch et al., 2022).

THE ROUTE

PRELIMINARY ROUTE

Puigcerdà - Ribes de Freser (with bus, 1 h) - Núria (with rack railway, 40 min)

Figure 2. Puigcerdà-Ribes de Freser route to access at rack railway of Núria, on ©ICGC online cartography.

Figure 3. Rack railway access to Núria.

Figure 4. Sanctuary and other facilities in the glacial valley of Núria.

FIELD TRIP AND STOPS

2 h ascent, 2 h return, plus stops.
Topics: glacial and periglacial geomorphology, deglaciation, rock glaciers, avalanches, mountain archaeology.

Figure 5 Location of stops during the field trip, on ©Google Earth image.

1 Vall de Núria 'mountain station (1970 m asl): Presentation of geographical and historical settings in the Eastern Pyrenees context.

Since the Middle Ages, Núria has been an important center of religious pilgrimage. At the beginning of the 20th century it became a pioneering ski and mountain sports center.

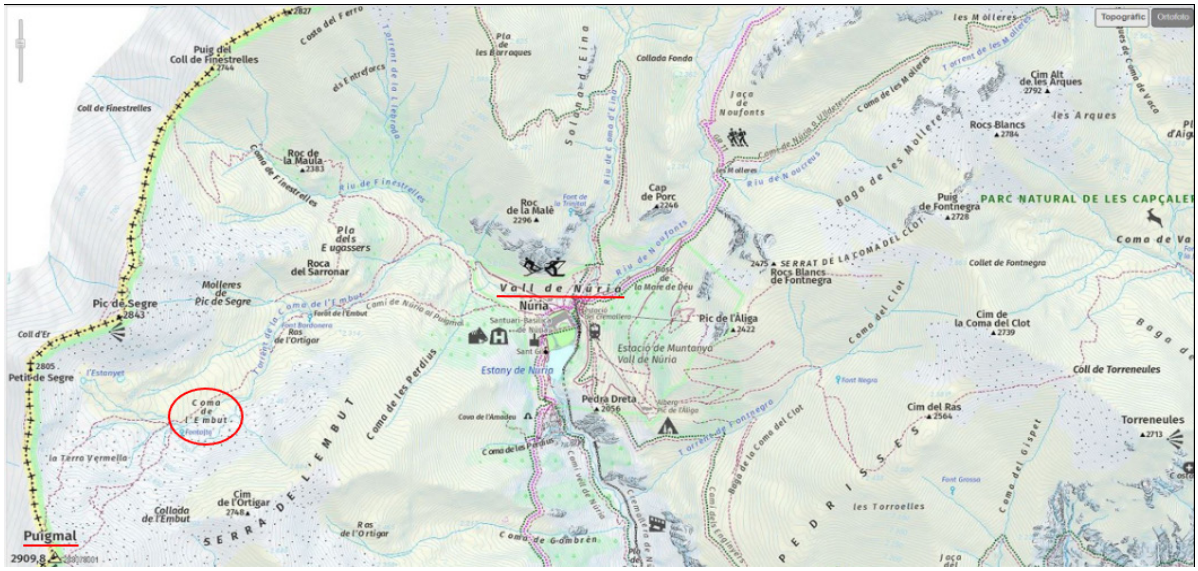

Figure 6 Topographic map of Núria valley, on ©ICGC online cartography.

2 Pic de l'Àliga' hostel lookout (2120 m asl): Presentation of the geological and geomorphological settings.

Discussion about different glacial and periglacial landforms (valley and cirque glaciers, nivation niches, avalanche channels)..

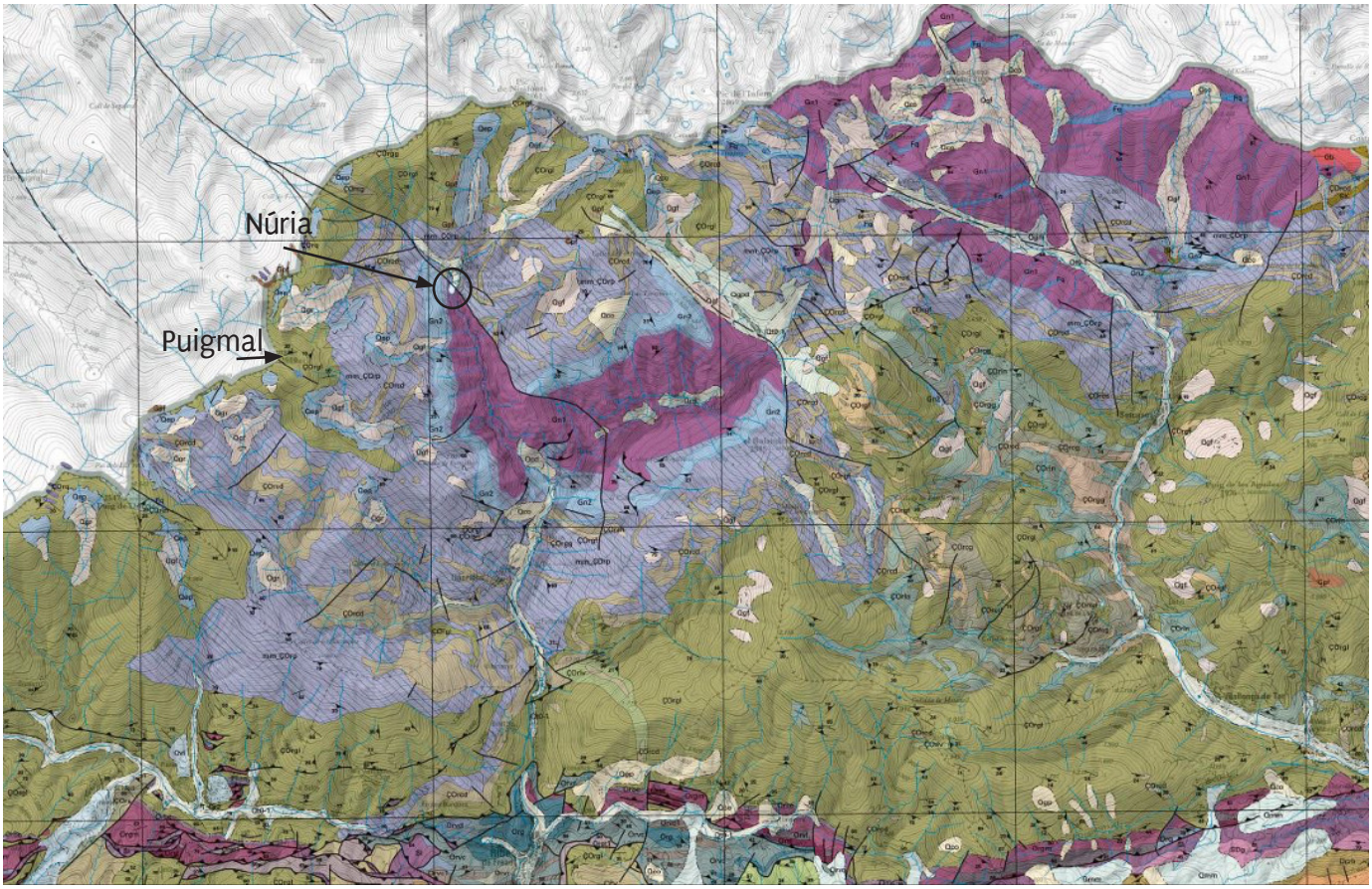

Recent and current Holocene

Qco Qep colluvial deposits and scree slopes

Pleistocene and early Holocene

Qgp Qgr glacial and periglacial deposits

Carboniferous-Permian

mm_ÇOrp Metamorphic rocks (schists, gneiss and marbles)

Gn1 Gn2 gneiss

Cambrian-Ordovician

ÇOrcd limestone, dolomite and marble

ÇOrgl sandstones and shales (Jujols Formation)

Figure 7. Fragment of the geologic map (Mapa geològic comarcal de Catalunya, 31 Ripollès). Original scale 1:50.000. ©ICGC, 2006.

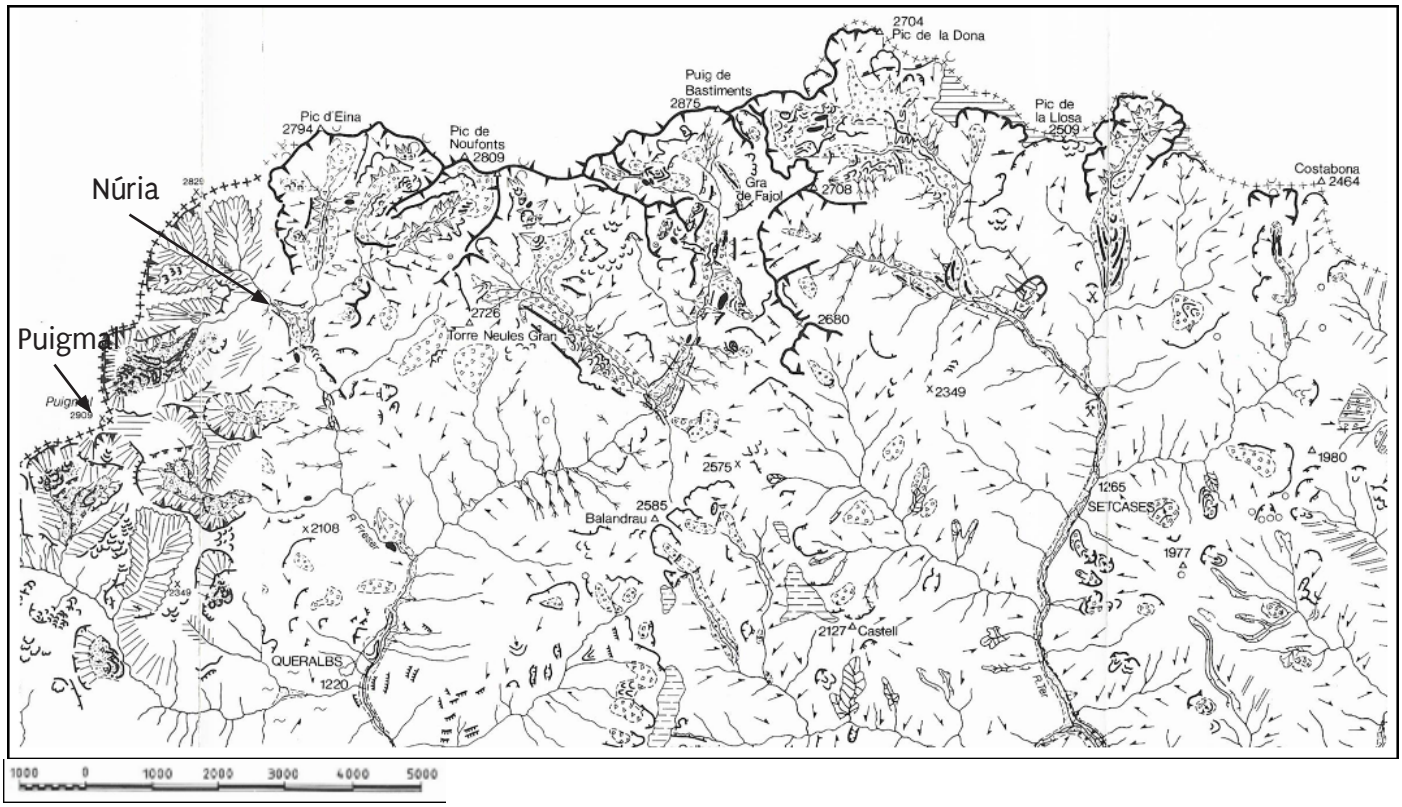

LEGEND- left part of the map

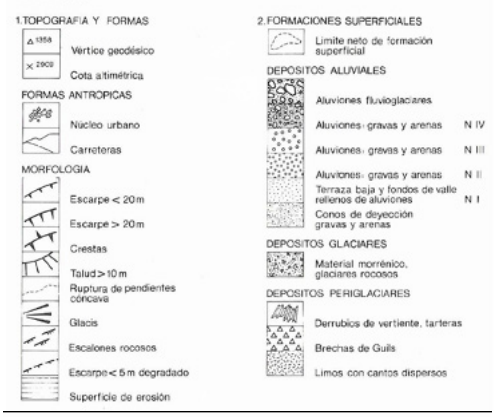

LEGEND- center-right part of the map

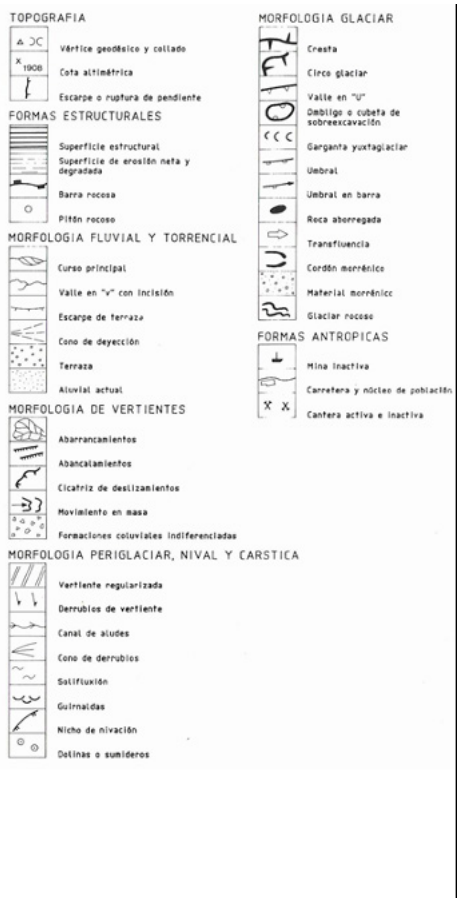

Figure 8. Geomorphological cartography of the headwaters of Freser and Ter valleys. Original scale 1:100.000. ©IGME, (Escuer; Fleta & Serrat, 1994).

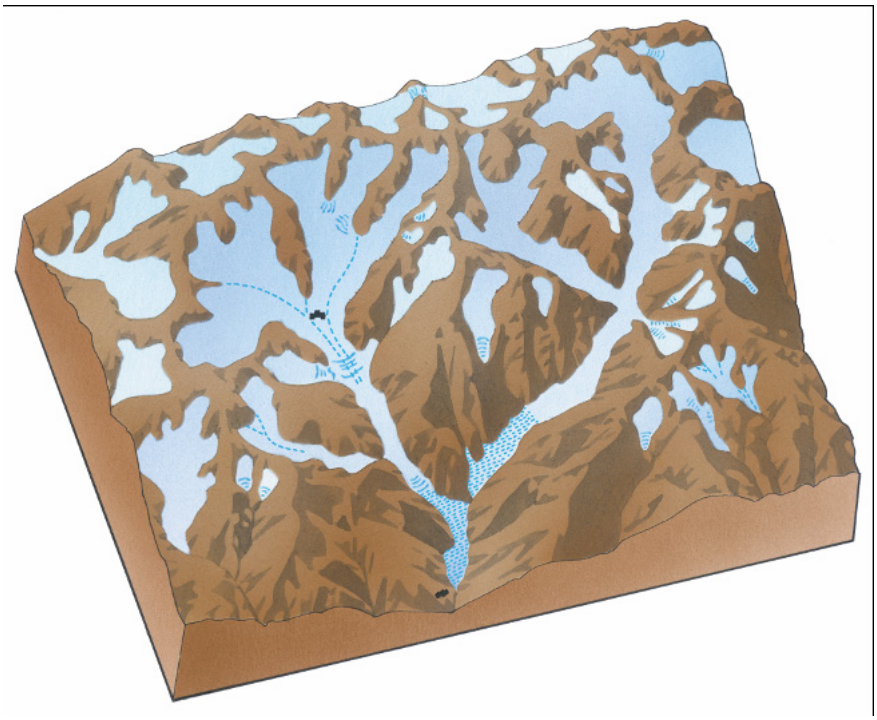

Figure 9. Maximum glacial extent reconstruction of Núria and Coma de Vaca valleys (Martí & Serrat, 1995).

During the LGM, in the valley of Núria and Coma de Vaca (Freser) complex valley glaciers were formed, with headwaters around 2,700-2,900 m a.s.l., a distance of 9 km until reaching 1,300 m near the town of Queralbs. Then there was a rapid deglaciation. Subsequent intense periglacial processes destroyed or considerably covered the glacial morphology.

3 'Forat de l'Embut' gorge (2290 m): Karstic, glacial and periglacial morphology.

In the Coma de l'Embut basin, the shallow stream that descends from Puigmal circulates underground for 1 km when it comes into contact with the marbles. In the Embut gorge, two vertical shafts access the underground river.

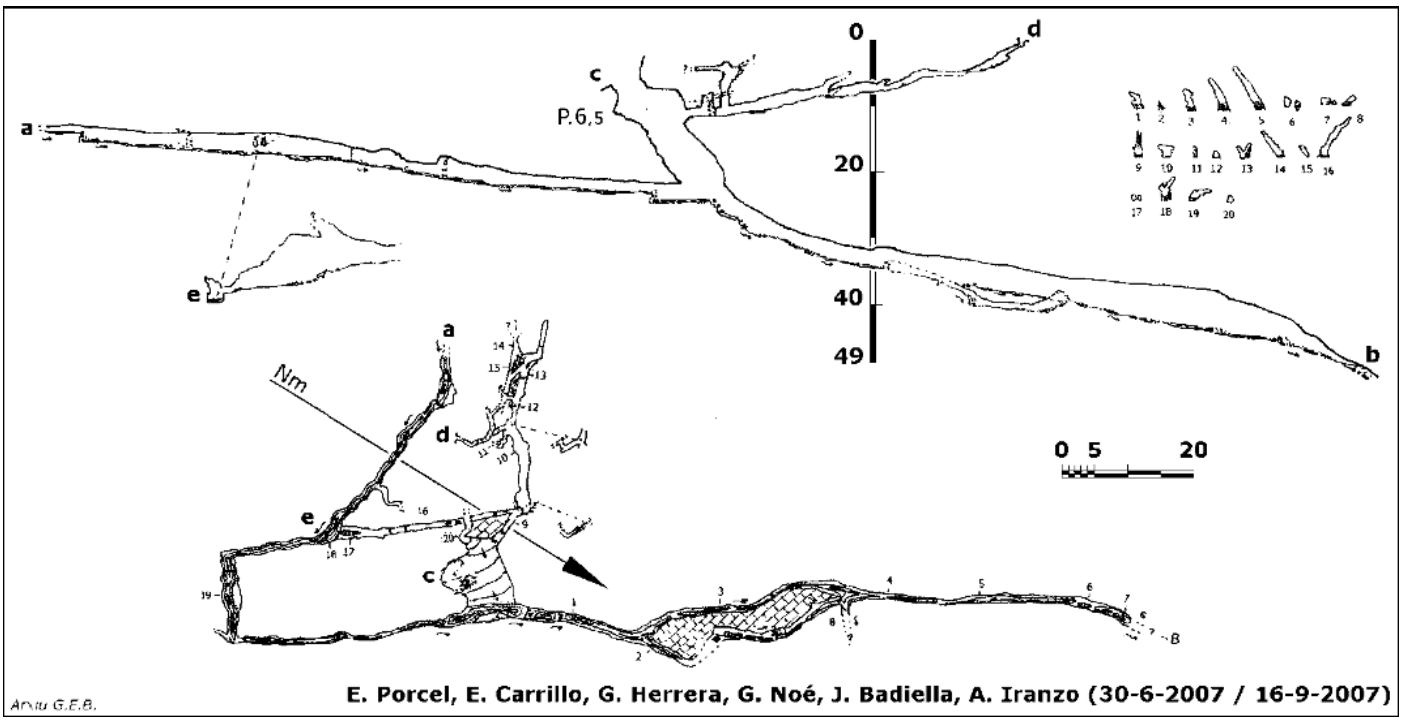

Figure 10. Forat de l'Embut karst system, in Catàleg Espeleològic de Catalunya, III (De Valles, 2009).

4 'Coma dels Eugassers 'meteorological station (2324 m asl)': Snow avalanche cartography, prevention and instrumentation. Soil thermal regime. Ancient occupation of Pyrenean high mountain, archaeological evidence of neolithic and medieval presence. Picnic lunch.

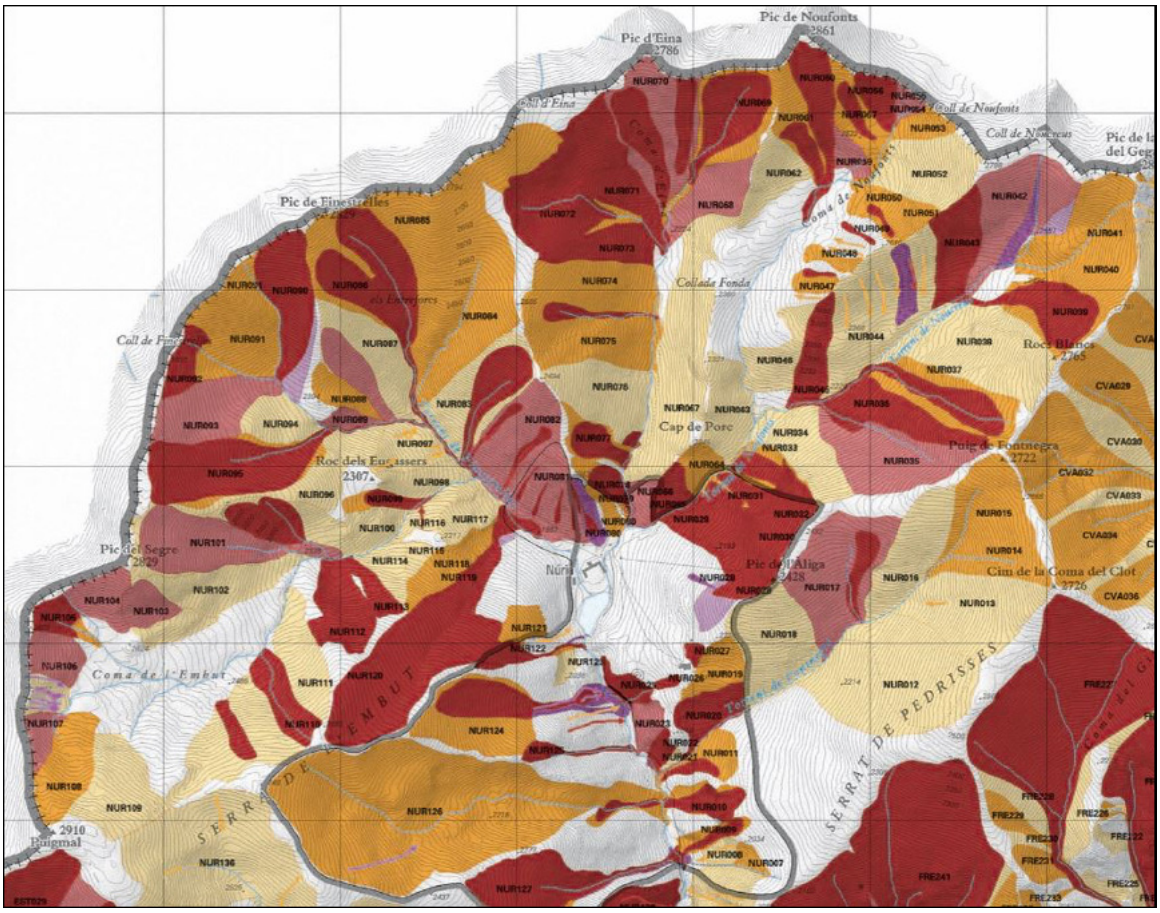

Figure 11. Fragment of avalanche zone map (Mapa de zones d'allaus de Catalunya, 13 Núria-Freser). Original scale 1:25.000. ©ICGC, 2000.

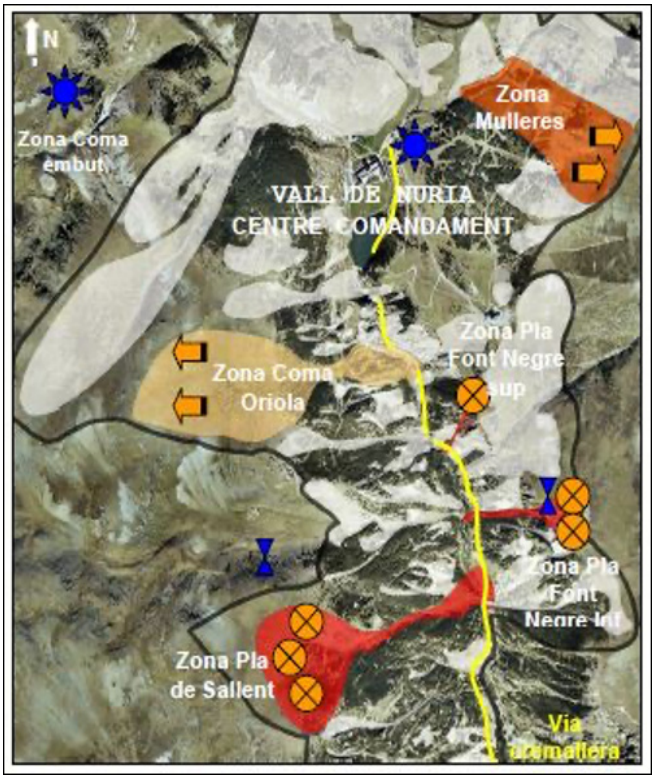

avalhex

areas covered with avalancheur canyon

flowcapts

weather station

Figure 12. Instrumentation for the preventive provocation of avalanches (Paret & Oller, 2006).

Figure 13-14. Archaeological site of 'Cova del Catau de l'Ós'. Ancient and middle Neolithic occupation (4200-3100 BC).

5 Coma de l'Embut rock glacier (2586 m asl). Rock glacier inventory, formation and chronology.

The altitude, lithology, orientation and previous morphology determine the presence and development of rock glaciers.

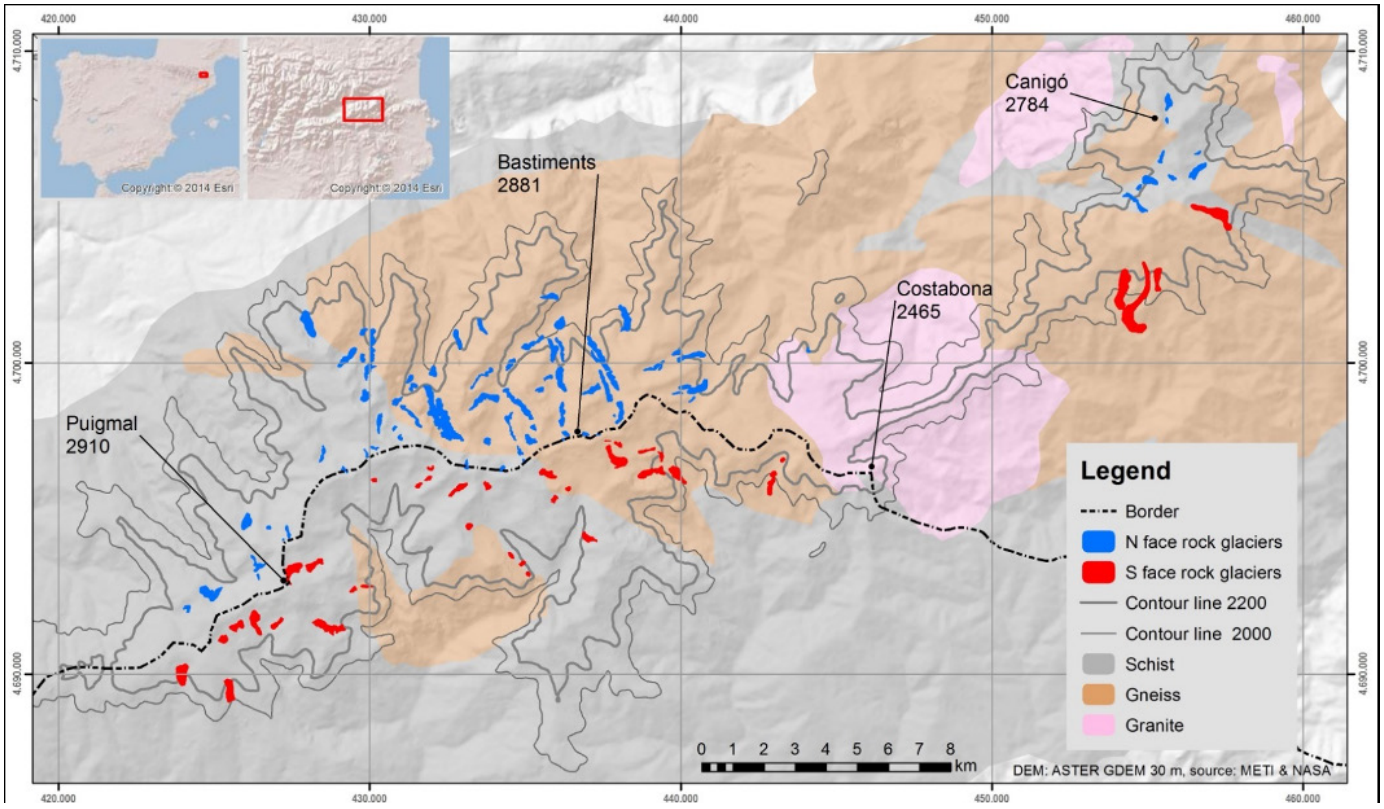

Figure 15. Spatial distribution of rock glaciers in the Puigmal-Costabona-Canigó massif (Salvador-Franch et al., 2016).

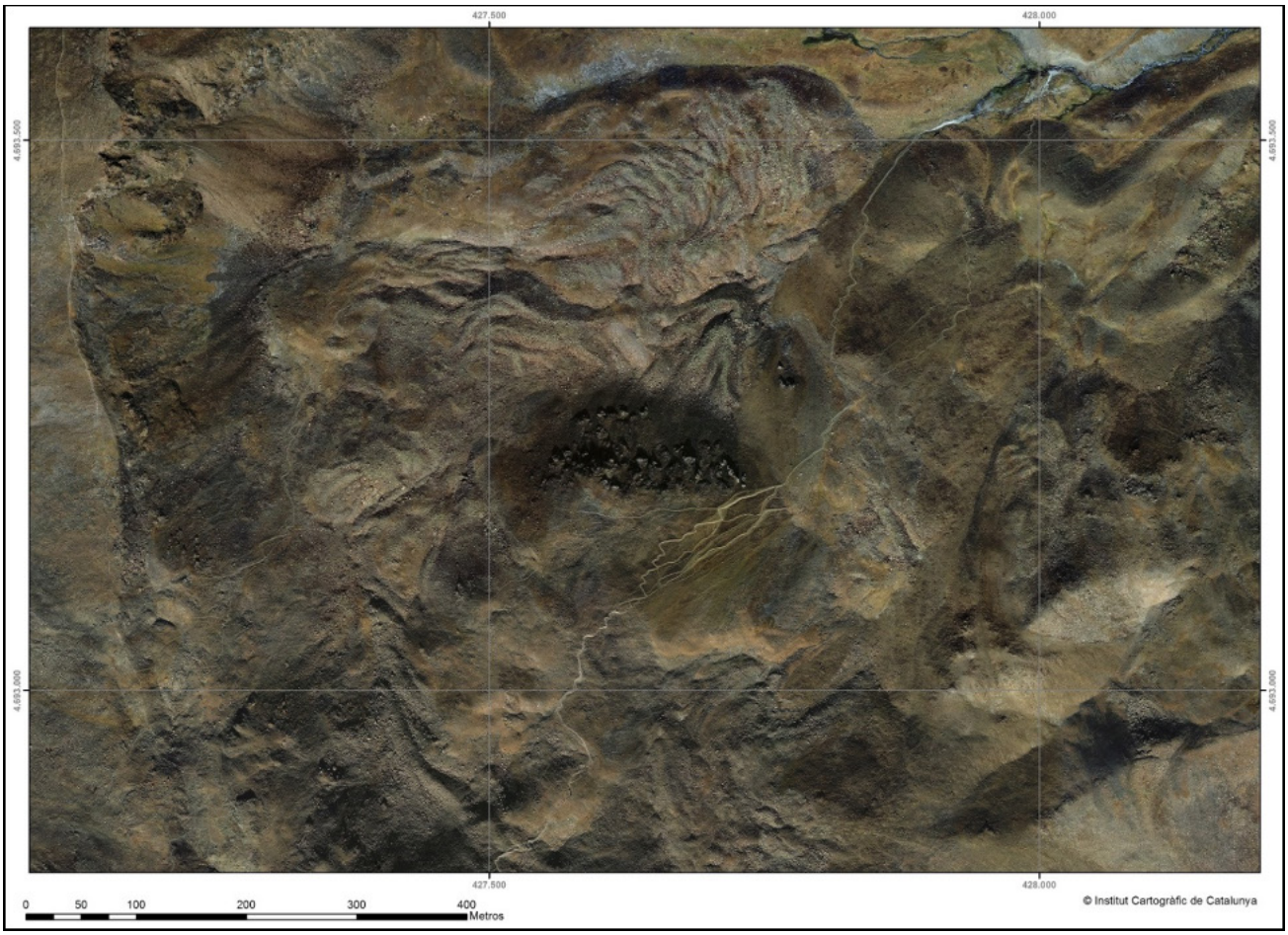

Figure 16. 'Coma de l'Embut' rock glacier. Orthoimage from ©Institut Cartogràfic i Geològic de Catalunya (ICGC).

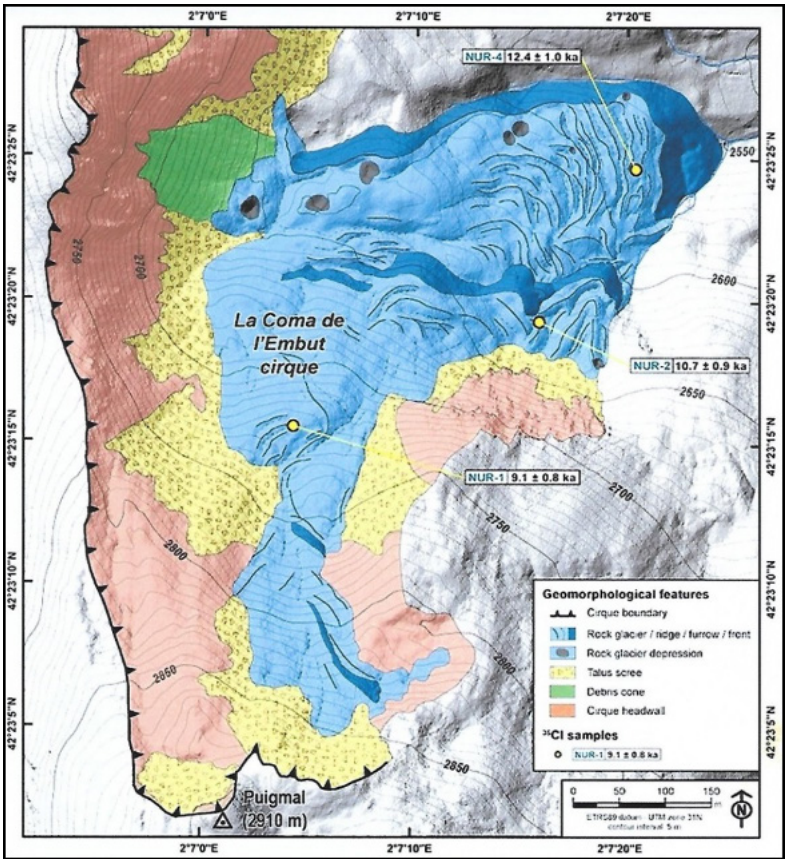

Figure 17. "Coma de l'Embut' rock glacier.

Figure 18. Geomorphological features of 'Coma de l'Embut' rock glacier (Palacios & de Andrés, 2015, unpublished).

REFERENCES

- Escuer-Solé, J. (1994). Geomorfología. Cartografía del Cuaternario. Mapa geomorfológico. In: Barnolas, A. & Cirés, J. (dir., coord.). Mapa Geológico de España. Escala 1:50.000. Hoja 217 Puigcerdà. Instituto Tecnológico y Geominero de España, Madrid. págs. 49-50, 1 mapa geomorfológico 1:100.000. ISBN: 84-7840-189-X.
- Fleta, J. & Serrat, D. (1994). Geomorfología. Cartografía del Cuaternario. Mapa geomorfológico. In: Barnolas, A.; Muñoz, J.A. (dir., coord.). Mapa Geológico de España. Escala 1:50.000. Hoja 218 Molló. Instituto Tecnológico y Geominero de España, Madrid. págs. 27-35, 1 mapa geomorfológico 1:100.000. ISBN: 84-7840-190-3.
- ICC (2000). Mapa de zones d'allaus de Catalunya 1:25.000. 13 Núria-Freser.
- ICC-IGC (2006). Mapa geològic comarcal de Catalunya 1:50.000. 31 Ripollès.
- Martí-Soler, M. & Serrat, D. (1995). Les glaceres rocalloses pirinenques. Terra. Rev. Cat. de Geogr., Cartog. i Ciències de la Terra, 25: 24-34. ICC. Barcelona.
- Palet, J.M.; Garcia, A.; Orengo, H.A. & Polonio, T. (2016). Ocupacions ramaderes altimontanes a les capçaleres del Ter (Vall de Núria i Coma de Vaca, Queralbs): resultats de les intervencions arqueològiques 2010-2015. In: Frigola, J. (ed.). Tretzenes Jornades d'Arqueologia de les comarques de Girona (Banyoles, 10-11 juny 2016). Generalitat de Catalunya. Banyoles. pp. 67-75.
- Palet, J.M.; García, A.; Orengo, H.A. & Polonio, T. (2017). Els espais altimontans pirenaics orientals a l'Antiguitat: 10 anys d'estudis en arqueologia del paisatge del GIAP-ICAC. Treballs d'Arqueologia, 21: 77-97. DOI: 10.5565/rev/tda.59.
- Palet, J.M.; Olmos, P.; García, A.; Polonio, T. & Orengo, H.A. (2019). Occupation et anthropisation des espaces de haute montagne dans les vallées de Núria et de Coma de Vaca (Gerona, Espagne) : résultats des recherches archéologiques et patrimoniales. In : La conquête de la montagne: des premières occupations humaines à l'anthropisation du milieu. Éditions du Comité des travaux historiques et scientifiques. Paris. http://books.openedition.org/cths/7007. https://doi.org/10.4000/books.cths.7007
- Pérez-Sánchez, J.; Romo-Díez, A.; Nuet-Badia, J.; Salvà-Catarineu, M. & Salvador-Franch, F. (2014). La vegetación del glaciar rocoso de la Coma de l'Embut (macizo del Puigmal, Pirineos Orientales). Datos preliminares. In: Gómez-Ortiz, A.; Salvador-Franch, F.; Oliva, M. & Salvà-Catarineu, M. (eds.). Avances, métodos y técnicas en el estudio del periglaciarismo (IV Congreso Ibérico de la International Permafrost Association. Núria, juny 2013). Publicacions i Edicions de la Universitat de Barcelona. pp. 189-201.
- Salvador-Franch, F.; Pérez-Sánchez, J.; Salvà-Catarineu, M. & Gómez-Ortiz, A. (2016). Inventory and Spatial Distribution of rock glaciers in the Eastern Pyrenees: paleoenvironmental implications. Geophysical Research Abstracts, 18: EGU2016-16284. EGU General Assembly. Viena.
- Salvador-Franch, F.; Salvà-Villoslada, G.; Vilar-Bonet, F. & García-Sellés, C. (2014). Nivometría y perfiles de innivación en Núria (1.970 m, Pirineo Oriental): 1985-2013. In: Fernández-Montes, S. & Rodrigo, F.S. (eds.). Cambio Climático y Cambio Global (IX Congreso de la AEC, Almería, 2014). AEC. pp. 729-738. http://hdl.handle.net/20.500.11765/8229.
- Salvador-Franch, F.; Andrés, N.; Gómez-Ortiz, A. & Palacios, D. (2022). The glaciers of the Southeastern Pyrenees. In: Oliva, M.; Palacios, D. & Fernández-Fernández, J.M. (eds.). Iberia, Land of Glaciers. Elsevier. Amsterdam. pp. 61-85. https://doi.org/10.1016/B978-0-12-821941-6.00028-1
- Serrat, D. (1979). Rock glacier morainic deposits in the eastern Pyrenees. In: Schlüchter, Ch. (ed.). Moraines and Varves. A.A. Balkema, Rotterdam. pp. 93-100.

Excursions book

European Conference on Permafrost

18-22 June, 2023, Puigcerdà